4. USAMP Cooperative Research

A. Automotive Composites Consortium-
US Automotive Materials Partnership

Field Technical Monitor: Khaled W. Shahwan
Chrysler Group LLC
Advanced Lightweight Systems and Active/Passive Safety
Chrysler Technology Center (CIMS: 483-05-10)
800 Chrysler Drive; Auburn Hills, MI 48326-2757
(248) 576-5609; e-mail: kws8@chrysler.com

Field Technical Monitor: Jim deVries
Ford Motor Company
2101 Village Road; Dearborn, MI 48121
(313) 322-3494; e-mail: jdevries@ford.com

Field Technical Monitor: Hamid Kia
General Motors Holdings LLC
GM Global R&D
Mail Code 480-106-2224; 30500 Mound Road; Warren, MI 48090-9055
(586) 986-1215; e-mail: hamid.g.kia@gm.com

Technology Area Development Manager: Carol Schutte
U.S. Department of Energy
1000 Independence Ave., S.W.; Washington, DC 20585
(202) 287-5371; e-mail: carol.schutte@ee.doe.gov

Field Project Officer: Joseph Renk
National Energy Technology Laboratory
626 Cochrans Mill Road; P.O. Box 10940; Pittsburgh, PA 15236
(412) 386-6406; e-mail: joseph.renk@netl.doe.gov

Contractor: U.S. Automotive Materials Partnership
Contract No.: DE-FC26-02OR22910

Executive Summary

The Automotive Composites Consortium (ACC) has three umbrella projects with each project aimed at delivering enabling technologies for future development of cost effective, high performance, fiber-reinforced, polymeric composite solutions for high-volume automotive applications that meet or exceed pre-specified functional and performance requirements.

A structural composite underbody was designed, fabricated, assembled into a steel structure, tested, and analyzed. A glass fabric sheet molding compound (SMC) material was developed and characterized for this project. A method of weld bonding the composite to the steel body-in-white (BIW) was developed and patented. The part as designed saved 11.4 kg (about 25%) of the mass of the donor steel underbody. In this fiscal year, the glass fabric SMC was further characterized for different glass layups and fabric weight and for durability after damage. The part was molded and the molded part was

assembled into a steel structure mimicking the surrounding structures of the steel BIW. A test was developed to approximate the offset deformable barrier as transmitted to the underbody structure. The part was tested and the test results compared to the predicted behavior. Results were found to reasonably match within expected variations, with discrepancies explained. A glass-reinforced, polypropylene composite seat structure was also designed and built. Successful testing of this preliminary seat design was completed using multiple load cases. The results provided some guidelines for future redesigns and validations. A 25% weight savings compared to a steel structure was achieved (at a cost increase of about 25-50%).

Energy management is a major focus and under that several studies have been carried out. The size-effects study has completed all of its experimental and computational investigation. As expected, carbon braided textiles exhibit relatively strong size-effects as was demonstrated by tests and validated by numerical models. Because they are quasi-brittle materials, their characterization requires focus on properly quantifying mechanical strength and properly accounting for the coupling between the size of the domain being studied and decrease of strength as the size of the specimen increases with respect to the physical size of the textile architecture. This is important for improving predictive methods and tools. Another study on the in-situ properties' prediction has revealed important insights into the curing process of thermosets and the relatively strong effects of exothermic reactions on the evolution of cure and thermomechanical stresses. The study has utilized advanced experimental and computational techniques to assess such effects and employed nano-indentation tests, optical techniques, and detailed 3D finite element (FE) models. The obtained results provide general guidance on how to relate curing time to material thickness and methods to quantify the evolution of the in-situ properties while the material is being cured. Finally, a third area involved the development of a modeling database (MDB) to be used for centralizing and coupling the developed modeling and analysis modules with commercial tools. The MDB is going under verification and validation studies.

The ACC developed two vinylester/polyester resin based carbon fiber SMC systems each using a unique fiber preprocessing to de-bundle or filamentize the large tow carbon fibers. One system achieved physical property performance target, the other achieved 2/3 of the target, and both exhibited high variation in properties. The work demonstrated the feasibility of producing low cost, high performance SMC materials using de-bundled or filamentized large tow carbon fibers. Five separate processing studies were completed. The studies were aimed at investigating the effect of material formulation and processing on particular composites. The team manufactured test panels from those processing studies to extract test specimens for mechanical testing. Finally, the concept of using direct compounding to process advanced composites has been validated by characterizing some of the mechanical properties of cut test specimen.

The following sections outline the specific task work conducted by the ACC in the areas outlined above.

Activity and Developments

Focal Project 4. Structural Automotive Components from Composite Materials

Principal Investigator: Libby Berger, General Motors Holdings LLC
(248) 930-5018; e-mail: libby.berger@gm.com

Principal Investigator: John Jaranson, Ford Motor Company
(313) 390-5842; e-mail: jjaranso@ford.com

Accomplishments

- Characterization of variations of the glass fabric SMC material, including heavier strand fabric and several different layups, as well as fatigue after impact testing.

- Fabricated structural composite underbodies, assembled them into a steel frame using weld bonding, and tested the composite underbodies and assemblies for modal response and stiffness, and to failure in simulated offset deformable barrier testing. Compared the test results with predictions from finite element modeling (FEM).

- Built 30 composite seat structures/assemblies.

- Completed all composite seat testing with good correlation to previous analytical results.

Future Directions

- Complete documentation of structural composite underbody.

- Document results of seat project in a technical report that includes Design, Analysis, Build, Testing and Validation, and Cost Modeling.

Introduction

ACC 007 is focused on Focal Project 4 which is divided into two parts: a structural composite underbody and a lightweight composite seat.

Approach

This project has been a collaboration between the three original equipment manufacturers (OEMs) and several suppliers. As shown in previous reports, the design of the composite underbody consolidates 16 stamped steel parts into one composite part, saving 11.4 kg out of the 44.9 kg initial steel underbody mass. The increased stiffness of the composite allows an additional 3.3 kg reduction in the mass of the steel "sled runner" rails. In the 2010 fiscal year, the team developed processing techniques and characterized material properties for the glass fabric SMC material selected, designed and analyzed the underbody structure as part of a full vehicle, tested our design and analysis technique with a model structure, developed the weld bonded joining system, designed the final test assembly, and did the initial molding of the full underbody structure. In fiscal year 2011, the team characterized other layups of the glass fabric SMC material, further investigated damage tolerance of the material via fatigue testing of impacted samples, developed preforming patterns and molding techniques, and molded testable underbodies. The team assembled those underbodies into steel frames representing the surrounding structure in the BIW. Then the teams tested both molded underbodies without the frames (UO) and assembled underbody frame units (UA) for stiffness and modal response, and to failure in a simulated Offset Deformable Barrier (ODB) test. These results were compared to predicted results from FEM.

Results and Discussion

The majority of the material property data given in previous reports was using a 7-layer, "quasi-quasi-isotropic" (QQI) layup of 45/0/-45/90/-45/0/45, using an 1854 fabric compounded with vinyl ester resin. This year, the team completed the characterization of the QQI layup at -40°C and 80°C to compare with the room temperature data and found that, as expected, the colder temperatures have higher values for tensile and compressive properties, with the properties at 80°C showing a decrease in properties. The team also characterized a number of different layups and two different fabrics, examples of which are given in Figure 1. The 1854 fabric is nominally 580 g/m^2, while the 2454 is 780 g/m^2. The layups were a (0)4 and the QQI. While the 2454 shows an overall drop in strength which could be explained by the increased out-of-plane displacement caused by the larger strands, the modulus of the 2454 is increased compared to the 1854.
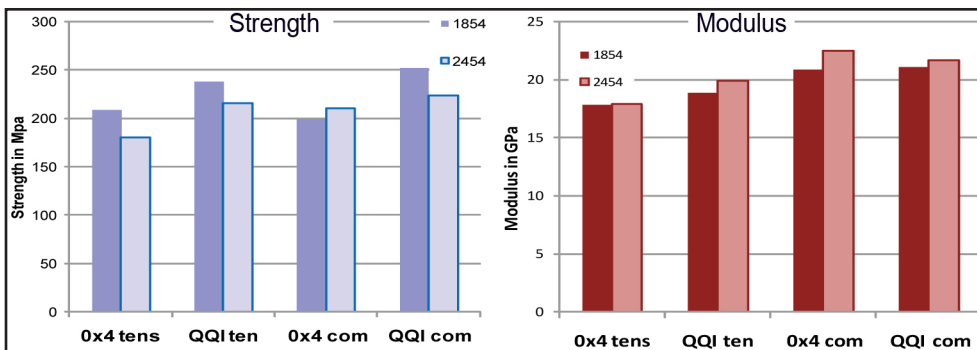
Figure 1. Effect of fabric weight on strength and modulus for tensile and compressive loading, for two different layups for both fabrics.

Tensile fatigue properties of the fabric SMC composite in the QQI layup have been measured in 0°, 90°, 45°, and -45° directions, at room temperature, -40°C, and 80°C. In addition, samples with two levels of impact damage were fatigue tested up to a maximum of 1 million cycles per specimen (referred to as "run-out") with (R = -1) load profile. Figure 2 shows the S-N curve comparing the undamaged and damaged samples. The curve shows the material life expectancy as a function of maximum stresses between 28 and 50% of the baseline ultimate strength. As expected, the number of cycles to failure increases with decreasing stress, until a run-out occurs just below 30% of the baseline ultimate strength for both the damaged and undamaged samples. While the damaged samples are slightly lower than the undamaged, the slopes are similar, indicating that low level damage does not significantly affect the material durability.
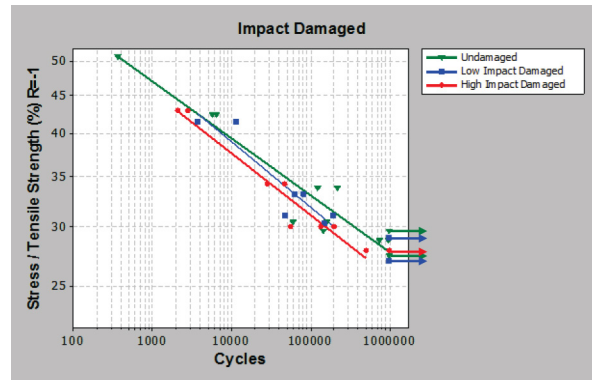
Figure 2. S-N curve showing fatigue life of undamaged fabric SMC specimens, in comparison to two levels of impact damage.

One of the most challenging parts of the project was the development of the preform pattern and charge buildup. We began with fabric deformation studies, as has been reported in previous Annual Reports. This showed the areas of the design that needed softening in the tool to avoid excessive fabric deformation or strand tensile stress and allowed us to develop patterns that fit our fabric width. We iterated these initial patterns to improve preform processing and decrease overlaps. However, making the preforms from several pieces for each of the 12 fabric plies in the optimized design geometry required overlaps, which sometimes crossed or otherwise stacked. Figure 3 shows the overlaps, with the more intensely-colored areas having the greater number of overlaps, up to four in some parts of the circled area, which may increase thickness of the part by a millimeter or more. In the final molding trial, the team molded ten parts deemed suitable for testing, although all of these were thicker and thus heavier than design. Burn off of a full part confirmed our hypothesis that the overlaps contributed to the thickness, along with wrinkling at the corners of the crossbars and build up in the trough areas.
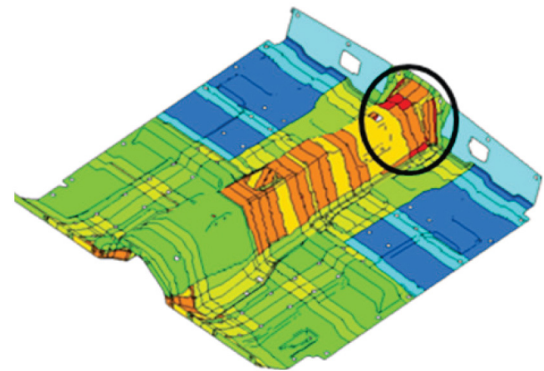
Figure 3. Overlaps in the designed preform layup. More intense shades indicate more overlaps, up to 4 in the circled area.

A particular challenge in validating the design of the composite underbody stems from the fact that the composite assembly is integral to the vehicle structure. As a result, the durability and impact load inputs are complex, so that it is difficult to conduct simple component level tests. The primary design driver for the composite structure was deemed to be the 40mph front ODB test. Because of the cost and complexity of doing full-vehicle testing for a concept component, we have elected to do our final testing with a subassembly. The proposed testing plan involved weld bond joining to a steel frame made up from the steel parts that would surround the underbody in production, then inducing loads through that frame, thus testing both the molded component and the joints. The purpose of this testing is validating the computer aided engineering (CAE) methodology used to design the structure, as well as the processing technology. Since CAE analysis shows that, even for the 40 mph ODB test, the loads are introduced to the underbody at rates close to quasi-static rates, quasi-static testing methods were used to minimize the test complexity and cost.

Several simple quasi-static non-destructive bending and torsional stiffness and modal tests were used to evaluate the basic molded component performance. After this testing, the molded underbodies were weld bonded into a subassembly consisting of the underbody and the surrounding structure from the donor vehicle, including the rockers, front rails, dash panel, and rear floor. This was then subjected to quasi-static testing to mimic the ODB. This testing consisted of longitudinal loading on the driver's side front rail and the face of the transmission housing.

Figure 4 shows the load-displacement curves for two of the underbodies assembled into steel frames and tested as per the quasi-static ODB methodology. The final failure mode was the buckling of the driver's side rail, inducing crush at the toe

pan and tunnel. This rail buckling was not fully predicted in the models, as this was rather coarsely modeled in the original vehicle model. Although there was sufficient crush to absorb and distribute the energy, there was no material separation or gaping and all of the weld bond joints were maintained. The initial agreement of the experimental results with the three predicted curves is quite good, particularly for assembly #5. The change in slope at about 18 kN in the curve for assembly #4 is attributed to an increased stiffening of the transmission crossmember and contact of the transmission housing with the tunnel.

Trial	Thickness	Tunnel	Properties
1378	Design	30% increase	Design
1385	Variable, based on #5	Based on #5	Based on #1 coupon tests & ply thickness
1386	Design	30% increase	Based on typical #1 coupon test (reduced vs. design)
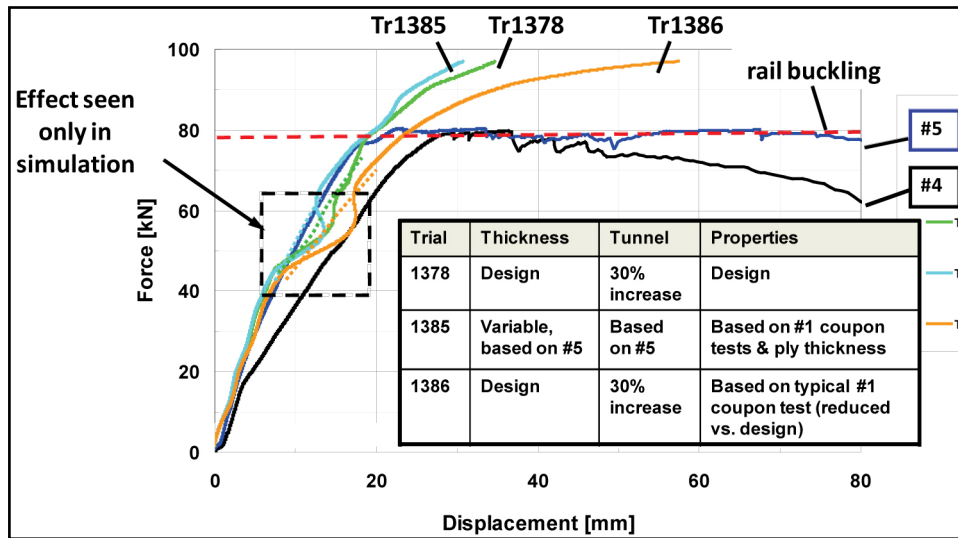
Figure 4. The force-displacement curves for two underbodies assembled into steel frames, compared to the predictions. The predictions are as modified for actually molded parts, which were heavier than the design.

Based on the preliminary seat design, thirty seat assemblies were built for testing and design validation in 2011. All completed seat-assembly tests included building pads and trim covers. The metal reinforcements and the composites panels were all bonded with acrylic adhesive. All steel parts were e-coated and the composite parts were plasma treated.

Because these are non-production seats, their preliminary design was tested for some durability, strength, and impact requirements (Figure 5). Some of the tests met the pre-specified pass criteria and all but three of the tests were unconditionally passed. The cargo retention test met the pre-specified criteria. Subsequent analyses showed that there is reasonable correlation between the test results and the CAE analysis with the as-built recliner plates. Other tests, including the front impact test, met the pre-specified criteria including no-separation of crushed components. This was also correlated reasonably well with the nonlinear finite element CAE analyses. However, other tests performed on this preliminary seat design revealed that some components of the current preliminary seat design (e.g., the surrogate recliner plates) needed redesign in order to meet the team's pre-specified pass criteria such as those for the rear impact test. Comparison of test results and CAE analyses showed that there is reasonable correlation with the updated, as-built CAE model up to the point of damage initiation and the location of the predicted high stresses was consistent with the damage crack initiation locations. The as-built weight save exceeded the predicted weight save. Final weight savings is 1.86 kg per seat which is a 25% weight savings versus the steel comparator seat.

Test	Subtest	Regulation	Environment
Seat Belt Pull	Spec	FMVSS 207/2	RT
	Limit		RT
Front Impact		Sled test	RT
Rear Impact		Sled test	RT
Headrest Loading	Spec	FMVSS 202A	RT
	Limit		RT
Child Seat Anchorage	8 configurations	FMVSS 225	RT
Knee Loading	5 configurations		RT
Cargo Retention		Sled test	RT
Modal Analysis			RT

Figure 5. Composite seat test matrix.

Conclusions

While molding in a 2 ½ minute cycle time is feasible with a 3-piece tool, preforming a complex part like an underbody requires significant automation (beyond the scope of this project). However, the composite underbody as designed saved 11.4 kg (about 25%) of the mass of the donor steel underbody. A test was developed to approximate the ODB as transmitted to the underbody structure. The part was tested and the test results compared to the predicted behavior. Results were found to reasonably match within expected variations, with discrepancies explained. A glass-reinforced, polypropylene composite seat structure was also designed and built. Successful testing of this preliminary seat design was completed using multiple load cases. The results provided some guidelines for future redesigns and validations. A 25% weight savings compared to a steel structure was achieved (at a cost increase of about 25-50%).

Predictive Technology Development & Composite Crash Energy Management

Principal Investigator : Khaled W. Shahwan, Chrysler Group LLC
(248)576-5609; email : kws8@chrysler.com

Accomplishments

Two important enabling-technology studies on improving predictive methods and computational tools have been completed. The size-effects study has completed all of its experimental and computational investigation. As expected, carbon braided textiles exhibit relatively strong size-effects as was demonstrated by tests and validated by numerical models. Another study on the in-situ properties' prediction has revealed important insights into the curing process of thermosets and the relatively strong effects of exothermic reactions on the evolution of cure and thermomechanical stresses.

Future Directions

Incorporating such findings into main-stream technologies prior to production deployment is vital for successful implementation of predictive tools for energy management. Further verification and validation are still needed in order to test these technologies under various loading and performance conditions. Incorporating high-speed dynamic effects remains a challenge and needs to be better understood. Other in-service effects need to be studied in-depth in order to be incorporated into the mechanical models used to predict long-term performance of advanced lightweight materials. Finally, the necessity of having standardized experimental procedures and methodologies to test advanced composites (e.g., carbon textiles) still exists and poses a challenge to future development of robust predictive tools.

Introduction

ACC 100 is focused on understanding the mechanical behavior of composites and its characteristics that are necessary to develop the analytical methodologies and computational tools needed to analyze and predict the mechanical response and crash-energy management of automotive structural components. Three sub-projects will be highlighted as each is focused on a different aspect of the development process.

Approach

Throughout the studies the focus has been to develop well-balanced experimental, analytical, and computational components within each study. Due to the complex nature of these studies, the experimental component has posed its own challenges due to lack of available testing standards. The analytical and computational components relied on using existing tools (albeit limited) as well as numerous newly developed ones that incorporate new knowledge and physics of polymers.

Results and Discussion

 Significant focus was placed on quantifying size effects. "Size" refers to the size of specimen/structural dimensions relative to the size of the damage zone and/or micro-structure of quasi-brittle materials such as textiles. "Effects" refer to those effects on damage characteristics, nominal strength, and post-peak regime in materials exhibiting such strength–size dependence. Figure 6a shows the four different structural (plaques) sizes that were selected for testing and modeling (all plaques had the same total thickness). Figure 6b shows schematics of the classical relationship between nominal strength vs. relative size (normalized measures). Such a relationship is typically bounded between strength criteria and linear elastic fracture mechanics (LEFM) criteria. The motivating question has been: do some of the measured non-local material properties (e.g., mechanical strength) change when different size specimens of the same textile material are tested?
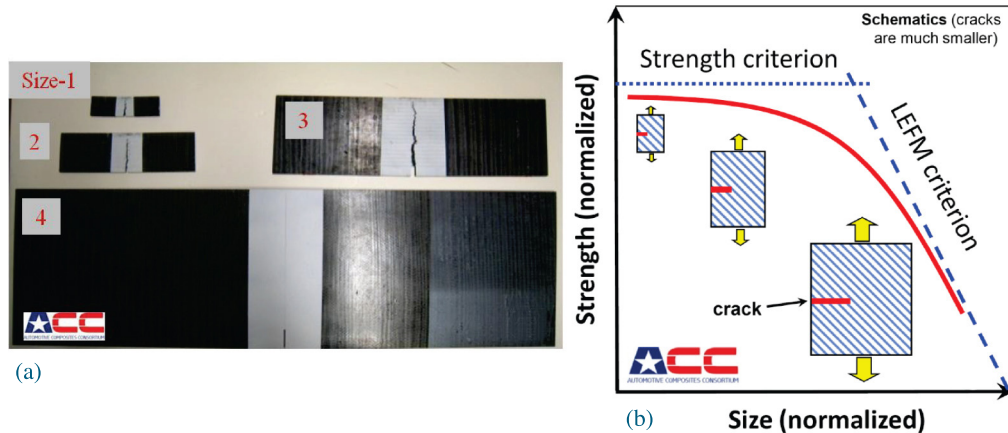
Figure 6. (a) The four different structural (plaques) sizes that were selected in order to study size effects on braided carbon composites' nominal strength. (b) Schematic showing the classical relationship between nominal strength vs. relative size (normalized measures).

Figure 7 shows the numerical results from 3-point beam bending analyses which demonstrate the converging dependence of load-deflection relationship on the number of repeating unit cells (RUCs) used. The completed experimental and computational studies demonstrated the relatively strong size-effects that are present in such quasi-brittle textiles (for the specific material system being considered). This implies that the measured strength characteristics depend not only on the material properties but also on the size of the specimen being considered. Such dependence poses an additional special challenge to modeling/analyses aimed at predicting nonlinear response including damage initiation and progression.
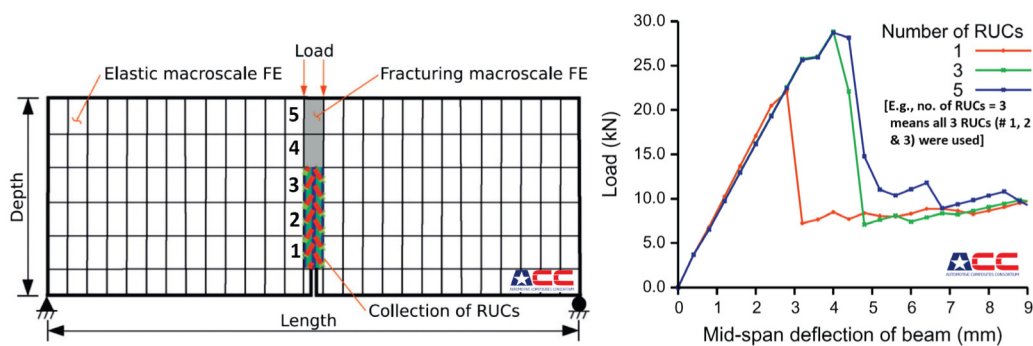
Figure 7. FEM results of 3-point bent specimen. The three curves demonstrate the converging dependence of load-deflection relationship (peak and plateau) on the number of RUCs used.

Additional work was focused on developing the knowledge needed and the computational tools necessary to make assessments and estimation of in-situ properties of textile reinforced composites (TRC). Extensive experimental and computational programs were carried out including nano-indentation testing and analysis, characterization using optical techniques (such as Brillouin and Raman Light Scattering), and advanced state-of-the-art FE modeling and analytical methodologies. The 3-D FE analyses were carried out on simplified systems in order to characterize the fundamental principles governing the mechanics and evolution of cure. Figure 8 shows one such task in which a braided carbon-fiber composite (resin/matrix not shown for clarity) is modeled (Fig. 8a). Because of the computational intensity of modeling all the fibers within a tow a representative tow is selected (Fig. 8b). Out of that a representative fiber is selected and modeled as surrounded with resin-rich cylinder (Fig. 8c). The simplified model focuses on studying the curing process of one fiber

embedded in a matrix by quantifying the degree of cure (ϕ) (Fig. 8d) and mechanical stresses (σ) as a function of time (t) and temperature (T) (Fig. 8e). Recall that in general $\phi = 0.0$ means the resin is uncured (liquid), and $\phi = 1.0$ means the resin is fully cured (hardened solid).

The analysis further reconfirmed the strong relationship between the size of the domain (in this case radius of the concentric cylinders containing the fiber and surrounding matrix) and the coupled thermal- curing effects resulting from this exothermic interaction. Figure 9 shows the computational results for T and ϕ variation with time (t) for different size 1-fiber concentric-cylinder finite element models. This highlights the important relationships between specimen/component size and the curing degree and time required for its cure. Figure 10 shows a more detailed larger model with multiple fibers embedded in a matrix and the spatial distribution of ϕ within the system at some time during the curing process.

Many of the modeling and analysis methodologies developed by the ACC100 team involved extensive generation of specialized advanced techniques and numerical procedures that are needed to accomplish certain aspects of a holistic CAE approach. Most of these advanced techniques and procedures are embedded in state-of-the-art computational modules that are not available yet in the commercial CAE codes which are commonly used in industry. In order to consolidate and centralize many of these techniques and procedures into one location and link it with commercial pre- and post-processing CAE software packages an intermediate interface was needed. Such a tool should facilitate an efficient use of these technologies in a user-friendly fashion. As a result, the MDB was conceived and has completed several development stages. It is going under verification and validation in order to ensure higher level of data-fidelity and data-exchange quality. It is important to point out that the MDB is NOT a materials database to be used for searching and looking up composites material properties (that is not its objective).
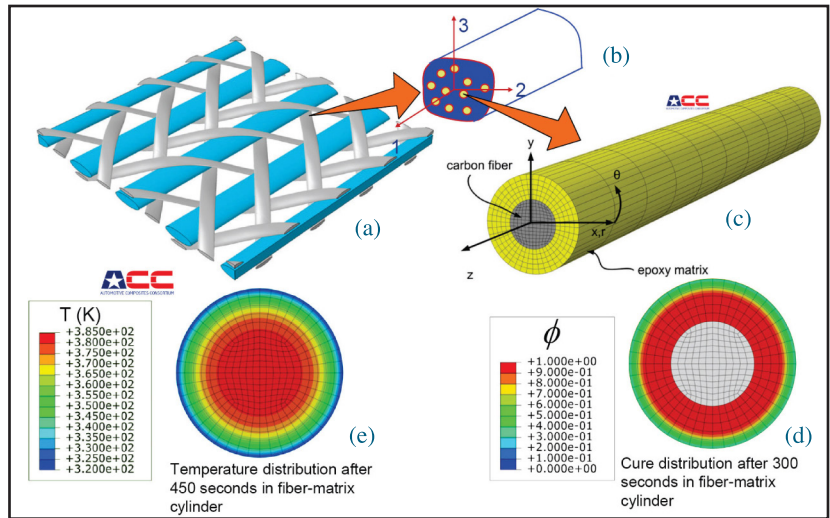
Figure 8. (a) Braided carbon-fiber composite (resin/matrix not shown for clarity). (b) A representative tow is selected. (c) A representative fiber is selected and modeled as surrounded with resin-rich cylinder. (d) Degree of cure (ϕ) variation in the matrix (the fiber is fully cured and represented as central circle with solid color). (e) Temperature (T) distribution in the fiber-resin system after a specific curing time.
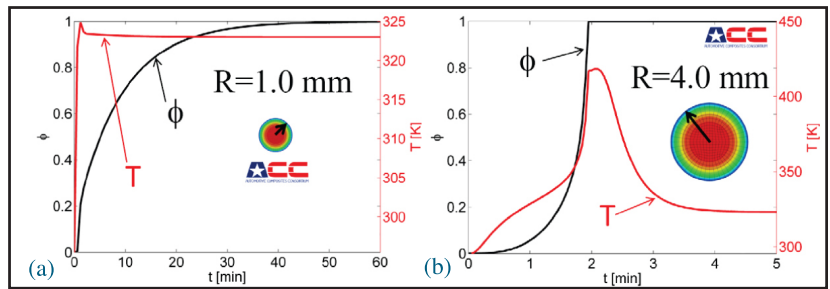
Figure 9. Computational results for T and ϕ variation with time (t) for different size 1-fiber concentric-cylinder FE models.
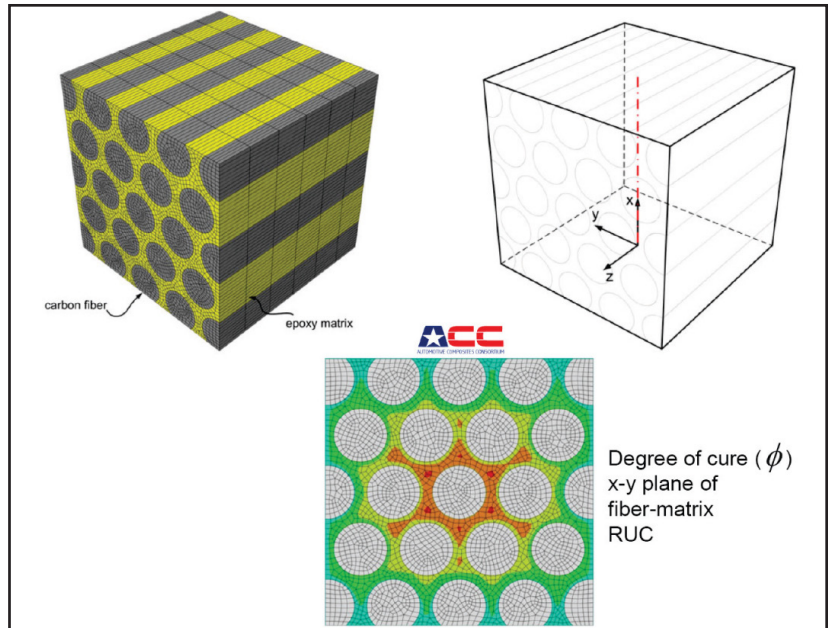
Figure 10. A more detailed larger FE model with multiple fibers embedded in a matrix and the spatial distribution of ϕ within the system at some point in time during the curing process.

Figure 11 shows an overall view of the structure of the MDB. The models referenced in this figure refer to the modeling and analysis procedures that the ACC conceived, initiated, and developed over several years of intensive development programs. The distinction between models can be attributed (but not limited) to the following: numerical incorporation of size effects in carbon textile composites; numerical techniques to quantify and predict the peak strength and post-peak response of a material region; analytical modules to model fiber-tows layout based on pre-specified local architectures; computational prediction of in-situ properties of constituents; numerical coupling between local FE size and local properties; analytical methods to introduce local imperfections, to mention a few.
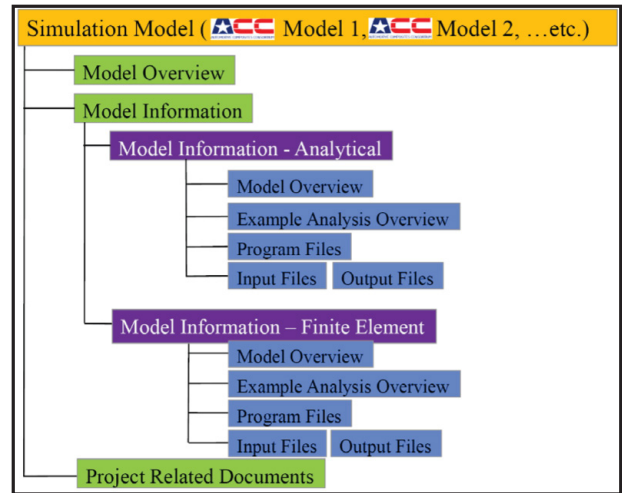
Figure 11. Overall structure of the Computer-Aided Engineering MDB.

Conclusions

While much has been learned about the physics of damage in composites, the developed computational tools are a small part of the building blocks that make up the predictive modeling capabilities needed to analyze composites under dynamic crush. Quantifying size-effects and in-situ properties are major milestones that require further development in addition to expanded validations and the incorporation of in-service effects.

Materials and Processes Technology Development

Principal Investigator: Daniel Houston, Ford Motor Company
(313)323-2879; e-mail: dhousto2@ford.com

Accomplishments

- Developed two vinylester/polyester resin based carbon fiber SMC systems each using a unique fiber preprocessing to de-bundle or filamentize the large tow carbon fibers. One system achieved physical property performance target, the other achieved 2/3 of the target, and both exhibited high variation in properties.

- The work demonstrated the feasibility to produce low cost, high performance SMC materials using de-bundled or filamentized large tow carbon fibers

- Completed five separate processing studies to investigate the effect of material formulation and processing on the composites. Manufactured test panels from those processing studies to extract test specimens for mechanical testing.

- The concept of using direct compounding to process low cost advanced composites has been validated.

Future Directions

- Additional development work on better controlling process variables would result in reduced coefficient of variation (COV) and minimal fiber orientation. Achieving good fiber wet out by understanding the appropriate control of resin viscosity, resin thickness on the carrier film, effective bundle size, and the ability to "work" the resin into the fiber bundles is a critical element for success implementation of carbon fiber SMC into the automotive industry.

- Additional process development with the nubby roller concept should allow physical property targets to be achieved.

- Final validation of the thermoplastic material formulations will require scale up of compounding and molding trials to demonstrate capabilities to mold complex three dimensional components.

Introduction

ACC 932 is focused on developing and demonstrating high-volume manufacturing (molding) processes to produce lightweight composite automotive components. This includes development of direct compounding of automotive thermoplastics polymers to reduce cost and increase performance benefits offered over conventional long fiber injection or compression molding.

Approach

*   Work with a Tier One automotive composites supplier to investigate and develop an improved carbon-fiber SMC material amenable to cost-effective high volume applications.

*   Conduct direct compounding of automotive thermoplastic polymers to reduce cost and increase performance offered over conventional long fiber injection or compression molding.

*   Program was executed to test the feasibility of direct compounding for polyamide based composites.

Results and Discussion

One part of the work was focused on using a single vinylester/polyester resin system, while varying fiber bundle breakup techniques to achieve smaller effective tow sizes during compounding. Two systems were used; both started with large 50K carbon fiber bundles. The first has been previously reported here and utilizes an air powered pretreatment to the bundle before a mechanical chopper cuts the fibers. It results in highly filamentized carbon fibers.

The other system (installed on a different compounder) had the carbon fibers pulled over flat rollers (to flatten the bundle), then going over one or more nubby rollers (Figure 12) to poke gaps into the bundle before chopping. This process resulted in transforming the bundle size to effectively a 10K tow size just before going into the compound. A US patent for this concept is pending.
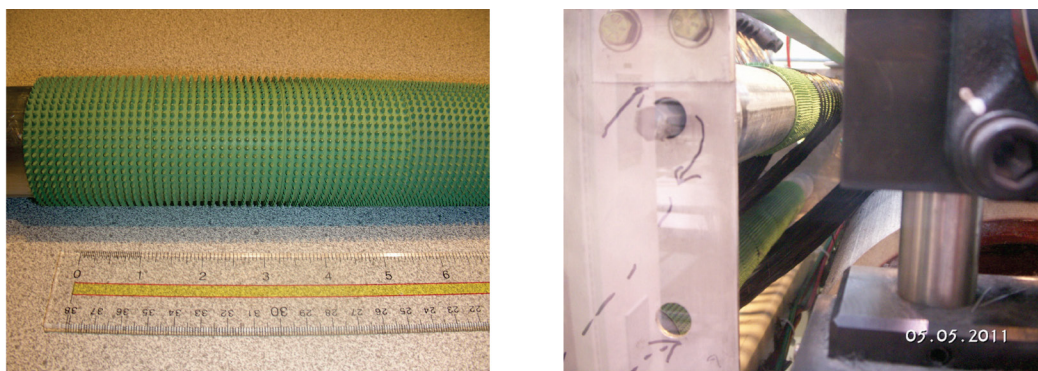
Figure 12: Nubby roller used to open gaps in large carbon fiber bundles before chopping (left). Carbon fiber bundles traveling over two nubby rollers (right).

The first system (Table 1 left) achieved many program targets values, but exhibited directional preference and had a COV over 30%. The second system (Table 1 right) generally achieved about 2/3 of its target values and also had an equally high COV.

Table 1: Best material, 1" chopped carbon fiber (left). Alternative material, ~50% by weight, 1" chopped carbon fiber (right).

Air chopper, ~50% carbon fiber by weight					Two smooth rollers and two nubby rollers			
Direction	Tensile Strength MPa	Tensile Modulus GPa	% strain		Direction	Tensile Strength MPa	Tensile Modulus GPa	% strain
0	119	31	0.52		0	117	31	0.42
90	168	38	0.50		90	75	23.6	0.37
Goal	150	30	0.50		Goal	150	30	0.50

The work demonstrated the feasibility to produce low cost, high performance SMC materials using de-bundled or filamentized large tow carbon fibers. The team is confident that additional development work on better controlling process variables would result in reduced COV and minimal fiber orientation. Achieving good fiber wet out by understanding the appropriate control of resin viscosity, resin thickness on the carrier film, effective bundle size, and the ability to "work" the resin into the fiber bundles is important. Carbon fiber SMC's close to the target tensile properties and processing characteristics were successfully made with a vinylester/polyester resin system and two fiber bundle preprocessing processes.

Another part of the work was focused on direct compounding of thermoplastic composites which has become well established within the automotive supply base. Key advantages are reduced raw materials cost and improved part properties. However, to date, the process has been limited primarily to the development of polypropylene based glass fiber composites. This prompted a new study to assess the feasibility of extending the technology to process high modulus engineering thermoplastics. Initial trials were conducted to determine the feasibility of direct compounding polyamide 66 in conjunction with injection molding. Subsequent studies were executed to determine the performance benefits of processing the same formulations through compression molding.

To establish the performance potential of direct compounding, test panels were produced using two separate laboratory facilities. Initially a 700 ton Engel unit was used to compound materials for injection molding. This facility had the capability of processing both precompounded pellets and direct compounded formulations. Rather than using ASTM or ISO standard test sample tools, a flat panel tool was used tool produce parts of dimension 800mm x 250mm. This provided a source of mechanical test samples which were excised by water jet to yield test specimens. Following injection molding trials, the flat panel tool was removed and configured for compression molding. Hence, the same molding tool was used to produce both injection and compression molded specimens.

Analysis of the designed experiment indicated that the polymer type was a significant effect (95% confidence interval) with respect to notched Izod impact strength. In this instance, the precompounded pellets yielded slightly higher impact strengths relative to the in-line compounded solution. Not surprisingly, glass content was determined to have a significant effect on the notched Izod impact strength as well. With respect to the ultimate tensile strength, glass content was the only factor determined to have a significant effect. The polymer type was significant albeit at the 90% confidence interval. Again, the pre-compounded pellets exhibited slightly higher ultimate tensile strengths. In general terms, the specified material formulations are basically equivalent in performance to the pre-compounded pelletized material types.

With respect to effects on DAM Flow Izod Impact and Ultimate Tensile Strength (UTS), experimental analysis determined that all attributes shown in Figures 13-16 (screw speed, polymer type, glass content) did affect such properties to varying degrees. Figures 15 and 16 also show that direct compounded formulations exhibit properties comparable to precompounded pelletized solution. Additionally, the interaction effect of screw speed and polymer type was determined to be significant. The pre-compounded pellets showed changes in tensile strength with varied screw speed whereas the specified formulations were insensitive to screw speed. Similarly, all three main factors had a significant effect on the notched Izod impact strength. In this case, however, the interaction effect of polymer type and glass content was significant with the pre-compounded pellets showing larger increases at higher glass content than the specified formulations.
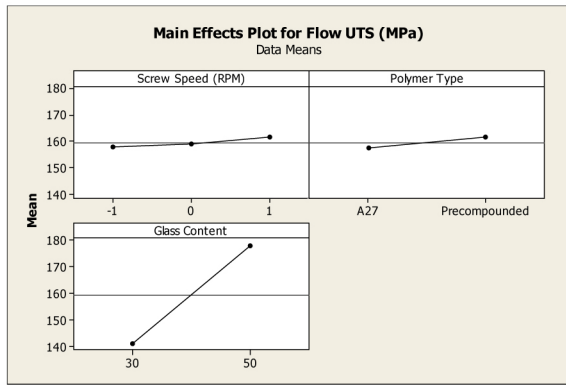
Figure 13: Attributes like screw speed and polymer type had minor effect on Ultimate Tensile Strength (UTS), while glass content had significant effects on UTS (measured in MPa).
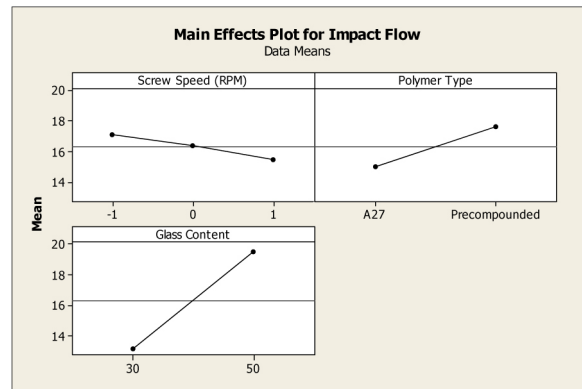
Figure 14: Attributes like screw speed, polymer type and glass content had a significant effect on Impact Flow.
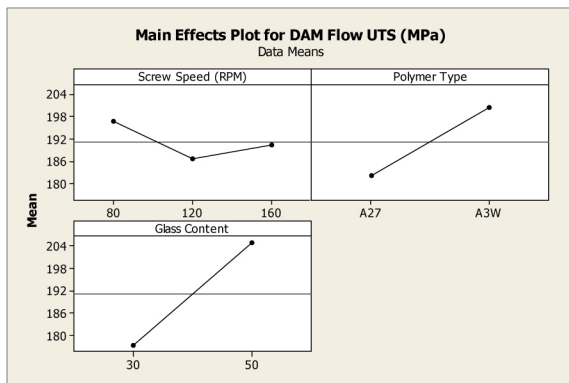
Figure 15: Data show that direct compounding formulations can exhibit tensile strength properties comparable to the pre-compounded pelletized formulations. UTS measured in MPa.
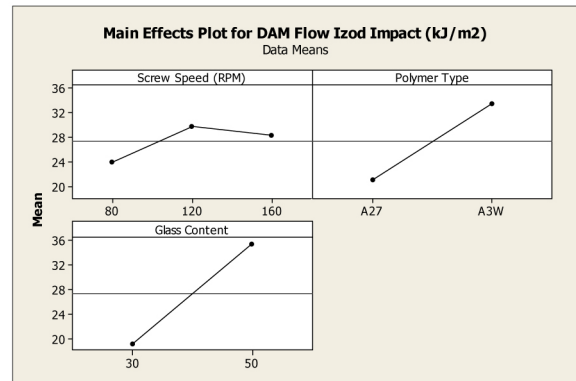
Figure 16: Data show that direct compounding formulations exhibit Izod Impact properties comparable to the pre-compounded pelletized formulations.

Conclusions

Carbon fiber SMC's close to the target tensile properties and processing characteristics were successfully made with a vinylester/polyester resin system and two fiber bundle preprocessing processes. The concept of using direct compounding to process low cost advanced composites has been validated. Mechanical test results indicate that direct compounded formulations exhibit properties comparable to precompounded pelletized solution. Further improvements in mechanical properties were achieved by adopting compression molding. With coupon level testing completed, a final validation of the material formulations will require scale up of compounding and molding trials to demonstrate capabilities to mold complex three dimensional components.

Conclusions

The ACC's three main projects carried out extensive experimental and computational development work aimed at delivering enabling technologies for future development of cost effective, high performance fiber-reinforced polymeric composite solutions for high-volume automotive applications. The studies involved rigorous methodologies and detailed data analyses focused on developing material systems for automotive applications that meet or exceed pre-specified functional and performance requirements. The underbody project developed some guidelines for future redesigns and validations after achieving a 25% weight savings compared to a steel structure (at a cost increase of about 25-50%). The predictive methods development work for energy management has yielded methods to quantify size-effects and in-situ properties which are

two of the main bottlenecks in modeling. Further development and expanded validations as well as incorporating in-service effects are still needed. Further development of carbon fiber SMC's using vinylester/polyester resin system and two fiber bundle preprocessing processes was successful. The concept of using direct compounding to process low cost advanced composites has been validated. Further improvements in mechanical properties were achieved by adopting compression molding. In summary, the ACC achieved in goals of addressing some of the technology gaps as well as technology transfer paths and in the process it has developed useful technologies and information which can be utilized in future development of composites components for vehicle applications.

Presentations/Publications/Patents

Heinrich, C., Aldridge, M., Wineman, A. S., Kieffer, J., Waas, A. M., Shahwan, K. W., "Generation of Heat and Stress During the Cure of Polymers Used in Fiber Composites," International Journal of Engineering Science, in review, to be submitted.

Heinrich, C., Aldridge, M., Wineman, A. S., Kieffer, J., Waas, A. M., Shahwan, K. W., "The influence of fiber packing on the homogenized response of cured fiber composites," Modelling and Simulation in Materials Science and Engineering, in review, to be submitted.

Caner, F. C., Bazant, Z. B., Hoover, C. G., Waas, A. M., Shahwan, K. W., "Microplane Model for Fracturing Damage of Triaxially Braided Fiber-Polymer Composites," Journal of Engineering Materials and Technology, 2011, Vol. 133, No. 2.

Smilauer, V., Hoover, C. G., Bazant, Z. B., Caner, F. C., Waas, A. M., Shahwan, K. W., "Multiscale simulation of fracture of braided composites via repetitive unit cells," 2011, Engineering Fracture Mechanics, Vol. 78, No. 6, pp 901-918.

Berger, L., "Program Summary of the ACC Automotive Composites Underbody," Society of Plastics Engineers Automotive Composites Conference and Exhibition, Troy, MI, Sept. 13-15, 2011.

Berger, L., et al., "Material Properties of a Fabric Sheet Molding Compound for a Structural Composite Underbody," Society of Plastics Engineers Automotive Composites Conference and Exhibition, Troy, MI, 9/2011.

Berger, L., "A Structural Composite Automotive Underbody," Society for the Advancement of Materials and Processing Engineering, Seattle, WA, May 17-20, 2010.

Berger, L., "Design and Fabrication of a Structural Composites Automotive Underbody," Society of Plastics Engineers Automotive Composites Consortium, Troy, MI, Sept. 15-16, 2010.

Berger, L., D. Simon, C. Dove, C. Knakal, "Properties and Molding of a Fabric SMC for a Structural Composite Underbody," Society of Plastics Engineers Automotive Composites Conference and Exhibition, Troy MI, Sept. 15-16, 2010.

Dove, C., "Shear Deformation Properties of Glass-Fabric Sheet Molding Compound," Society of Plastics Engineers Automotive Composites Conference and Exhibition, Troy MI, Sept. 15-16, 2010.

Fuchs, H., Gillund, E., "Composite Underbody Component and Assembly Structural Test-Analysis Correlation," Society of Plastics Engineers Automotive Composites Conference and Exhibition, Troy, MI, 9/2011.

Fuchs, H., B. Conrod, "Super Lap Shear Joint Structural Test-Analysis Correlation Studies," Society of Plastics Engineers Automotive Composites Conference and Exhibition, Troy MI, Sept. 15-16, 2010.

Fuchs, H., P. Deslauriers, "Double Dome Structural Test-Analysis Correleation Studies," Society of Plastics Engineers Automotive Composites Conference and Exhibition, Troy MI, Sept. 15-16, 2010.

Houston, D. Q., et al., "Fatigue Performance of SMC Composite Material under Different Environmental Damage and Temperature Conditions," Society of Plastics Engineers Automotive Composites Conference and Exhibition, Troy, MI, 9/2011.

Knakal, C., et al., "Manufacturing Scenarios and Challenges with a Fabric SMC Automotive Underbody," Society of Plastics Engineers Automotive Composites Conference and Exhibition, Troy, MI, 9/2011.

Shah, B., B. Frame, C. Dove, H. Fuchs, "Structural Performance Evaluation of Composite-to-Steel Weld Bonded Joint," Society of Plastics Engineers Automotive Composites Conference and Exhibition, Troy MI, Sept. 15-16, 2010.

Fuchs, J., Fickes, J., Banks, E., Berger, E., "Automotive Structural Joint and Method of Making Same," US Patent 7918452, Oct. 26, 2010.

.

B. Automotive Metals Division - U.S. Automotive Materials Partnerships

Field Technical Monitor: Steve Logan
Chrysler Group LLC
Materials Engineering
CIMS Code 482-00-13; 800 Chrysler Drive; Auburn Hills, MI 48326-2757
(248) 512-9485; e-mail: sl16@chrysler.com

Field Technical Monitor: Bill Charron
Ford Motor Company
Mfg. Development Center, Fairlane North 2
6100 Mercury Drive; Dearborn, MI 48126-2746
(313)805-6628; e-mail: wcharron@ford.com

Field Technical Monitor: James Quinn
General Motors Corporation
GM, R&D and Planning
Mail Code 480-106-212; 30500 Mound Road; Warren, MI 48090-9055
(586)596-4395; e-mail: james.f.quinn@gm.com

Technology Area Development Manager: William Joost
U.S. Department of Energy
1000 Independence Ave., S.W.; Washington, DC 20585
(202) 287-6020; e-mail: william.joost@ee.doe.gov

Technology Area Development Manager: Carol Schutte
U.S. Department of Energy
1000 Independence Ave., S.W.; Washington, DC 20585
(202) 287-5371; e-mail: carol.schutte@ee.doe.gov

Field Project Officer: Joseph Renk
National Energy Technology Laboratory
626 Cochrans Mill Road; P.O. Box 10940; Pittsburgh, PA 15236
(412)386-6406; e-mail: joseph.renk@netl.doe.gov

Executive Summary

The realization of significant weight savings in passenger and commercial vehicles is likely to occur through the use of a variety of advanced materials. While improvements in the properties, manufacturability, and cost of advanced materials are critical in achieving vehicle weight reduction, enabling technologies that facilitate the use of these materials in a multi-material system are equally important. Structures composed of different metals and polymer composites present difficult challenges in areas such as joining, corrosion, recycling, component/system simulation, and non-destructive evaluation.

The mission of the AMD is to facilitate the development of improved light metals and increased implementation of light metals applications by supporting advanced manufacturing technologies and enabling technologies to support integration into functional vehicle environments where they must perform in an environment including such challenges as general corrosion, galvanic corrosion, joint compatibility with other materials, etc. To achieve these goals, current AMD projects focus on technological hurdles faced in high volume application of magnesium (Mg) and aluminum (Al) in the alloys themselves

and in the manufacturing technology and infrastructure gaps in casting, sheet forming, and joining of these materials to themselves and to other materials.

Over the past year, AMD has supported projects focused on 1) Integration of Computational Materials Engineering (ICME) for Mg to enable better prediction of Mg alloy properties as a function of process conditions, 2) development of nano-ceramic coatings for steel fasteners to reduce the risk of galvanic corrosion of bolted Mg components, 3) enabling technologies required to predict behavior of a Mg vehicle front end structure and to produce the components and assemblies, 4) warm forming processes to improve formability of challenging Al sheet metal components for high volume applications, 5) development and evaluation of pre-treatment processes to accommodate coating and painting of multi-material vehicles through one process instead of having separate processes for Mg, Al, and steel, 6) collaborative benchmarking of competitive vehicles to understand best practices in body lightweighting, and 7) development and evaluation of high volume production capable ablation casting process for Al alloys.

The following sections outline specific task work conducted at AMD Project Teams in addressing the technology gaps and challenges described above.

Activity and Developments

Integrated Computational Materials Engineering for Magnesium (AMD703)

Principal Investigator: Mei Li, Ford Motor Company
(313) 206-4219; e-mail: mli9@ford.com

Principal Investigator: Alan A. Luo, General Motors Research & Development Center
(248) 912-8254; e-mail: alan.luo@gm.com

Accomplishments

First Principles Calculations – Density Functional Theory (DFT) was used to determine energetics of Mg-rare-earth (e.g. lanthanum, neodymium, etc.) compounds in such alloys, as well as diffusion of these rare-earth alloying elements in the Mg crystal structure.

Calculated Phase Diagrams – Assessment of the Extensible, Self-optimizing Phase Equilibria Infrastructure (ESPEI) has continued with "beta" site testing underway at several locations.

Precipitation Strengthening of die casting AZ91D alloy – transmission electron microscopy is being used to characterize the nature and morphology of β-phase precipitation and strengthening in this alloy system, as it relates to the yield, ultimate, and fatigue strength of such alloys.

Fatigue of two common Mg die casting alloys, AZ91D and AM60B – Completed microscopic and mechanical loading study of fatigue in AZ91D in as-cast and heat-treated forms, and AM60B in the as-cast condition. Fatigue of these alloys is largely controlled by the casting pore size and distribution.

Sheet-forming Process Modeling – Continued development of a constitutive model for sheet forming of the most common Mg sheet alloy, AZ31 incorporating twinning/de-twinning phenomena. Began studies of WE43 rare-earth strengthened Mg.

Future Directions

- USAMP's Project will conclude by January 31, 2012.

- Mg studies are expected to be a continuing part of events (e.g. topical symposia) aimed at the broader field of ICME, hosted by The Minerals, Metals, and Materials Society (TMS).

- ICME of Mg will be incorporated as a unique task within USAMP's ongoing 'MFERD' project under DOE sponsorship, including international participation from China and Canada.

Technology Assessment

- Target: Provide an initial organizational framework for ICME of Mg including cyber-infrastructure, first principles calculations, thermodynamics, diffusion, deformation, casting, and mechanical properties – e.g. fatigue.

- Gap: ICME is an ongoing "community of practice" enterprise and is expected to be continued as part of a broader, more nationalized and international framework beyond USAMP.

Introduction

ICME is a coordinated framework to develop computational approaches to materials engineering that extend over a variety of length scales from the atomic and quantum level to the scale of engineering objects. It is the broad goal of ICME to provide a computational infrastructure to generate predictive approaches to the processing-structure-properties relationships in engineering materials and objects. USAMP AMD703 was launched in 2007 as a companion project to AMD604 (MFERD-"Mg Front End Research and Development), with a focus on national and international efforts devoted to ICME of Mg alloys. USAMP principals also contribute (via USAMP AMD702) to a separate DOE-sponsored project at the Center for Advanced Vehicular Studies (CAVS) at Mississippi State University (MSST), having various linkages to ICME topics and data for Mg alloys. The MSST activities are reported separately.

Approach

USAMP ICME of Mg Project (AMD703) was structured as follows.

Task 1 – Cyber-infrastructure

Task 2 - Calculated Phase Diagrams (CALPHAD), Diffusion Infrastructures, and Database

Task 3 - Processing-Structure–Property Relationships for Extruded Mg Components

Task 4 - Processing-Structure–Property Relationships for Sheet Mg Components

Task 5 - Processing-Structure–Property Relationships for Die-cast Mg Components

Task 6 - Multi-Attribute Design Optimization

Task 7 - Multi-Stage Fatigue Modeling

Tasks #2, #3, #4, #5 and #7 received direct support from USAMP to universities or other suppliers. The others are funded chiefly through MSST's project, albeit with common reviews and interactions with the USAMP partners and suppliers. DOE Laboratories (Pacific Northwest National Laboratory and Oak Ridge National Laboratory) also participate in Mg ICME; these efforts are reported separately. Results from the various tasks are reported in committee format and also incorporated as data into the "cyber-infrastructure," maintained as an internet resource by MSST. The cyber-infrastructure is apportioned into two different types of representation, 1.) a SharePoint® web site which permits file placement and exchange and 2.) a more recent "wiki" site. Participants are encouraged to format and deposit data on the web site for use by other researchers in the field.

Results and Discussion

Task 1 - Cyber-infrastructure.

Buildup of this database continues as an ongoing effort overseen by principals at MSST. ICME Participants are encouraged to provide data to this site as a repository.

Task 2 - Phase Diagrams (CALPHAD, Diffusion Infrastructures, and Database.) Materials Informatics.

This project developed and is testing a user-friendly, extensible, self-optimizing phase equilibrium software package (ESPEI) for Mg alloys. It integrates databases of input and derived data including crystallographic, phase equilibrium, thermochemical, and Gibbs energy functions with the automation of database development functionality. ESPEI was made more flexible for the automation of thermodynamic modeling, the key being the complete thermochemical data of stable, metastable, and unstable phases (endmembers). The updated features of ESPEI were tested for the Mg-Ni, Mg-Zn and Mg-Al systems. These include: (i) Excel templates for massive data inputs have been improved, making each data sheet more clear; (ii) the strategy of automation has been updated with the keys being the thermochemical data from first-principles and the modeling of each single phase (endmember);(iii) first-principles predicted Gibbs energy data for each phase endmember have been stored;(iv) automation of each phase/endmember and interactions between different endmembers have been implemented, with the main inputs being the thermochemical data from first-principles calculations;(v)the graphical user interface windows of ESPEI were improved (vi) the Al-Zn binary system and the Mg-Al-Zn ternary system will be evaluated.

Northwestern University - The role of rare earths (RE) in Mg alloys is being investigated by calculating, with density functional theory critical thermodynamic properties that govern experimentally observed improvements in mechanical properties. Unique precipitate morphologies in Mg-RE alloys are considered the cause of the improved properties, particularly the formation of β"-D019 Mg3RE precipitates. Thermodynamic stability, coherency strain, interfacial energies and mechanical properties of D019 are being predicted. Energetic stability is analyzed in terms of a structure competition between the stable and metastable phases. The elastic constants of these precipitates and of the pure constituent elements are tabulated. Coherency strain energies between the precipitate and the Mg matrix are calculated as a function of different directions. The coherency strain energies are then correlated with the size and stiffness of the RE dopants. Coherency strain calculations indicate Mg3RE D019 precipitates prefer non-basal habit planes, a necessary condition for effective impedance of basal slip and strengthening of the Mg matrix. Interfacial energy between precipitate and matrix is also calculated in the basal and prismatic planes. The diffusion of the RE atoms in Mg has been explored, by calculating the solute-vacancy binding energies for all the lanthanides in HCP Mg. The binding between a vacancy and a RE solute continuously changes from favorable to unfavorable down the lanthanide series. Early lanthanides (La, Ce, Pr, and Nd) in the form of mischmetal are typically added to improve Mg's mechanical properties, suggesting favorable binding is a desirable property.

Task 3 - Processing-Structure, Property Relationships for Extruded Mg Components.

Updates reported through MSST's project.

Task 4 - Processing-Structure, Property Relationships for Sheet Mg Components - University of Virginia.

The development of a constitutive model for sheet forming of AZ31 incorporating twinning/de-twinning phenomena was continued. Studies of WE43 rare-earth strengthened Mg deformation were initiated including in-situ neutron diffraction.

Task 5 - Processing-Structure, Property Relationships for Die-cast Mg Components - University of Michigan.

Techniques were developed to quantify evolution of precipitation microstructure in Mg alloys under different heat treatment processes. This information will be used to calibrate phase field/DFT models for precipitate evolution. Quantitative TEM analysis of precipitation microstructure in AZ91D used in super-vacuum die casting is ongoing. Continuous beta phase precipitates and coarser discontinuous precipitation have been observed near grain boundaries. The wide spacing between discontinuous beta precipitates suggests that this constituent does not contribute to strengthening – thus alternate heat treatments are under exploration to eliminate or minimize this constituent.

University of Michigan - The influence of microstructure and artificial aging response (T6) on low-cycle fatigue behavior of super vacuum die-cast (SVDC) AZ91 and AM60 was investigated. Fatigue lifetimes were determined from total strain-controlled fatigue tests under fully reversed loading. Cyclic stress-strain behavior using an incremental step test (IST) was compared with the constant amplitude test. Two locations in a prototype casting were investigated to examine the role of microstructure and porosity on fatigue behavior. At all total strain amplitudes, microstructure refinement had a negligible impact on fatigue-life due to significant levels of porosity. At higher strain amplitudes, AM60 showed improved fatigue-life over AZ91, because of higher ductility. T6 heat treatment had no impact on fatigue-life. Cyclic stress-strain behavior obtained via the incremental step test varied from constant amplitude test results due to load history effects. Larger initiation pores led to shorter fatigue-life. The fatigue-life of AZ91 was more sensitive to initiation pore size and pore location than AM60 at the lowest tested strain amplitude. Fatigue crack paths did not favor any specific phase, interdentritic or eutectic structure. A Multistage Fatigue (MSF) model showed good correlation to the experimental results. The MSF model reinforced the dominant role of inclusion (pore) size on the scatter in fatigue-life.

Task 7 - Multi-Stage Fatigue Model. Work reported through MSST. (See above report from the University of Michigan).

Technology Transfer Path

ICME of Mg is an ongoing and emerging "community" of researchers. It is expected that formal organization of continuing efforts will shift from USAMP to more appropriate organizations.

Conclusions

ICME of Mg has concluded 4+ year tenure with USAMP support and has generated a cyber-infrastructure and working committees focused on specific technical tasks to advance this field.

Development of Steel Fastener Nano-Ceramic Coatings for Corrosion Protection of Magnesium Parts (AMD-704)

Principal Investigator: Richard Osborne, General Motors Corporation
(248) 202-6963; e-mail: richard.osborne@gm.com

Accomplishments

The concept feasibility of using nano-ceramic coatings to mitigate galvanic corrosion between steel and Mg has been successfully demonstrated.

- Nano-ceramic coated flat 1050 steel substrates coated with a nano-ceramic coating had less than half the galvanic current (0.55 mA/cm^2) as Al (1.26 mA/cm^2) when placed in a 5% salt bath with Mg.

- When placed against Mg, nano-ceramic coated steel fasteners induced less mass loss (0.08%) than Al (0.65%) after three days of salt spray testing.

Future Directions

- Process refinement to improve general corrosion performance and effects of geometry on coating thickness and integrity.

- Comprehensive testing of nano-ceramic coatings for automotive applications per industry standards, i.e. SAE/USCAR 32 (SAE, 2007).

Technology Assessment

- Target: Demonstrate that nano-ceramic coatings are an electrical insulator thereby preventing galvanic corrosion between steel and Mg. This objective was achieved where coated steel fasteners outperformed Al in mitigating galvanic corrosion with Mg.

- Gap: The project did not achieve the Phase 1 objective of demonstrating that the nano-ceramic coatings met automotive industry requirements for fastener finishes, had sufficient durability for automotive applications and could be provided cost effectively for high volume applications. Although nano-ceramic coated bolts were effective in reducing galvanic corrosion to 1/6 that of aluminum, thereby establishing the concept feasibility of reducing galvanic corrosion (0.08 % mass loss versus 0.65% mass loss in VDA testing), additional tests are need to qualify the coatings as fastener finishes per automotive OEM requirements, i.e. drop testing, conductivity, resistance to exposure to standard automotive fluids, etc.

Introduction

Despite its lightweighting potential, automakers are slow to use Mg in automotive applications for a number of reasons as discussed in "Magnesium Vision 2020" (USAMP 2006). One specific barrier to Mg usage cited was the technical challenges in fastening Mg and preventing corrosion. The key challenge when lightweighting with Mg components are cost efficient mitigation solutions for galvanic corrosion at Mg/steel (fastener) interfaces, which can impact long-term vehicle durability. The goal of this project was to develop cost-effective durable technologies to solve the notoriously difficult galvanic corrosion problems for fasteners of Mg parts by developing nano-ceramic coatings that provide an electrical insulation barrier to stop or substantially mitigate galvanic electric current between the cathode (e.g. the steel, Al) and Mg parts. The purpose of this project is to facilitate the use of light weight Mg in automotive applications by developing and validating nano-ceramic coatings for steel fasteners that will inhibit galvanic corrosion between the fasteners and Mg components.

Mg has been identified as a structural automotive material that would enable automakers to meet fuel economy and emission requirements through light-weighting. As discussed in Magnesium Vision 2020 (USAMP, 2006), galvanic corrosion is a significant barrier to the use of Mg in automotive applications, with the most common source of galvanic corrosion originating from fastening. In theory, ceramic coatings can electrically insulate the steel from Mg and, due to improved mechanical properties and adhesion from the nano-sized cellular structure; the nano-ceramic coated fastener will be able to withstand the harsh handling, assembly, application, and environment of automotive fasteners. This project has been exploring the concept feasibility of applying nano-ceramic coatings to steel fasteners to enable the joining of Mg to steel thereby reducing joint complexity, improving joint robustness, and reducing cost through elimination of Al isolation, which is typically used to mitigate the potential for galvanic corrosion between steel and Mg.

Approach

Phase 1 of the project, which ended on July, 2010, had the following intended approach.

- Thin film single layer nano-ceramic coatings were applied to electrically and effectively isolate steel bolts, nuts and washers from Mg parts to stop the galvanic electric current to protect these Mg parts from galvanic corrosion.

- A Design of Experiments was to be performed to select the ceramic materials and film thickness for the thin nano-ceramic coatings.

- Coatings were evaluated using comprehensive corrosion testing, mechanical properties characterization, microstructural analysis, and multi-scale simulations at the atomic, nano-scale and micron scale.

- Transfer knowledge and technology to industry for high volume process.

The results from Phase 1 were promising but did not achieve the original objectives. The project discovered that different ceramic materials varied in their ability to adhere to steel, electrically insulate the steel and prevent corrosion products from penetrating the coating (Qu *et al*. 2010). A multilayer approach was needed to combine the adhesion, insulation and corrosion isolation properties of the individual ceramic coating materials and produce a durable coating with good galvanic and general corrosion performance. Phase 2 was initiated in August, 2010 with two tasks, described as follows.

1. A Design of Experiments was performed to determine the optimum multi-layer coatings approach to producing a durable and insulating barrier coating. Flat steel coupons would be coated with the most promising coating combination and tested using a galvanic corrosion test, which would measure the galvanic current between the coated steel sample and Mg when suspended in a 5% salt water solution. The coated steel sample had to achieve equal or less current than Al. The purpose of this task was to establish concept feasibility of the coatings to electrically isolate steel and justify continued investigation.

2. Assuming success in Task 1, Task 2 would establish the technical feasibility of using the successful coating from Task 1 on fasteners, which are complex three dimensional surfaces. Coated steel fasteners would be tested using a modified VDA corrosion test, which will assess the ability of the coatings to isolate steel fasteners from Mg. Successful conclusion of this task requires the multi-layer, nano-ceramic coated fastener induce less galvanic corrosion than Al fasteners when corrosion tested against Mg plates with respect to mass loss of the Mg plate.

Results and Discussion

A Design of Experiments revealed that a multilayer coating consisting of silicon nitride as a base coat, Al oxide as a second coat, and a UV curable Al oxide top coat was the optimum coating combination. The silicon nitride, in thicknesses of 60 to 850 nm, showed superior adhesion to steel and therefore was the best base coat. Based on morphology, the Al oxide coating was suggested as the middle coat to effectively seal the silicon nitride layer. Finally, the UV curable top coat was added to provide enhanced general corrosion protection. This multi-layer coating was applied to 1050 steel substrates, tested using a Galvanic Current Measurement Test and found to produce less than half the galvanic current (0.55 mA/cm^2) than Al (1.26 mA/cm^2) using the same test, see Table 1. This successful test established the concept feasibility of the multi-layer coating; the nano-ceramic coating is a more effective barrier to galvanic current between steel and Mg than Al (Lin *et al*, 2011).

Table 1. Condensed Galvanic Current Measurement Test Results

Sample #	Sample	Average Corrosion Current (mA/cm^2)
1	Control (1050 steel/no coating)	8.83
2	SiN-AlO-UVAlO (Multilayer Coating)	0.55
3	Baseline (Al)	1.26

Task 2 of the project evaluated galvanic corrosion between steel, nano-ceramic coated steel and Al fasteners placed against AZ31 Mg sheet and tested using a modified VDA test, a cyclical salt spray test. After three days of salt spray testing, the nano-ceramic coated steel bolts induced less mass loss in the Mg than Al bolts by an order of magnitude (See Table 2). This successful test established the concept feasibility of multi-layer coated fasteners; the nano-ceramic coated fastener is a more effective barrier than Al for preventing galvanic corrosion between steel and Mg.

Table 2. Selected 3-Day Modified VDA Test Results

Day 0, Uncoated fastener on AZ31	Uncoated fastener removed, sand blasted	Al fastener removed, sand blasted	Nano-ceramic coated fastener removed, sand blasted
	Mass Loss = 3.32%	Mass Loss = 0.65 %	Mass Loss = 0.08 %

Technology Transfer Path

Before this technology can be implemented by the automotive industry, the nano-ceramic coatings must first show that they meet automotive requirements for a fastener finish and have sufficient durability for automotive applications. The USCAR Fastening Team suggested a research study based upon SAE/USCAR-32 "New Finish Development", which would then enable application based studies.

Conclusions

The project has concluded that multi-layer nano-ceramic coatings can be used to mitigate galvanic corrosion between steel and Mg.

Magnesium Front End Research and Development (Phase II - AMD904)

Principal Investigator: Alan A. Luo, General Motors Research & Development Center
(248) 912-8254; e-mail: alan.luo@gm.com

Principal Investigator: Mei Li, Ford Motor Company
 (313) 206-4219; e-mail: mli9@ford.com

Principal Investigator: Stephen D. Logan, Chrysler Group LLC
(248) 512-9485; e-mail: sl16@chrysler.com

Accomplishments

- Developed piece-part manufacturing of constituent components (i.e. extrusions and sheet-formed parts) and joined them with existing vacuum die-cast parts for the "demonstration" (demo) Mg-intensive, front-end vehicle substructure emulating features anticipated in lightweight unibody construction. Produced sufficient parts and assembled over 200 demo structures, available for a variety of mechanical and corrosion tests by U.S. and international partners.

- Developed friction-stir linear welding (FSLW) and laser-assisted, self-piercing riveting (LSPR) technologies for joining of Mg component pieces into articulated structures. Incorporated relevant metal finishing technologies for corrosion protection. Produced demo structures employing these assembly methods with various corrosion protection coating processes.

- Developed material models unique to die-cast AM60B Mg for use in the LS-DYNA® computer code for prediction of high strain-rate deformation of 3-D structures.

Future Directions

- This project will conclude by January 31, 2012.

- The international 3-country project is expected to continue with an alternative funding model for the USAMP portion of the collaboration. The focus will be on advanced Mg alloys, corrosion, joining, finishing, testing, and analysis including ICME.

Technology Assessment

- Target: Achieve a 60% weight reduction compared to a steel baseline structure, with comparable performance criteria including mechanical stiffness, crashworthiness, and durability.

- Gap: The current approach has been shown in prior studies to achieve an approximate 45% weight reduction over the steel comparator structure under the design/packaging constrains of current production vehicle architectures. Such design constraints and the limited crash performance of existing Mg extrusion alloys contributed to the differential. It is believed that entirely new structural designs and more advanced Mg alloys will be required to meet the target objective.

Introduction

The Magnesium Front End Research and Development (MFERD) Project (Phase II -AMD904) incorporates ongoing technical discussions and collaborative research with counterpart organizations in the U.S., Canada and the People's Republic of China. These interactions were initiated in late 2006 under the initial project (Phase I - AMD604). The technical objective is the development of engineering expertise and manufacturing capabilities permitting the realization of integrated, Mg-intensive, automotive front-end substructures having substantial weight reduction (target: 60%) and comparable performance to steel comparators. The current project succeeded AMD604, as a second phase, aimed specifically at design, construction, and testing of demo structures employing the enabling technologies identified in Phase I. AMD904 was launched on April 1, 2010, as a 36 month project. In October, 2010, the project was reconfigured and shortened to conclude by September 30, 2011. (In September, 2011, the project received a no-cost extension to permit technical work through January 31, 2012). This report details the current status of the project and highlights certain key results and deliverables.

Approach

In 2009, the international project participants conducted an engineering gateway appraisal of technical status of Phase I and subsequently agreed to develop a Phase II project continuation with the express goal of developing, producing, and testing demo structures that exercised the various knowledge and technology-based features identified in Phase I. A sufficient number of structures would be fabricated in the U.S. to permit evaluation by the partner organizations. Additionally, kits consisting of piece parts would be provided to China and Canada for their own studies in joining, finishing, and testing, with results being reported to the partner organizations. This project was originally intended to be three years in duration, but was shortened to an 18 month project in October, 2010.

Due to the shorter time frame, a specially-engineered idealized demo structure was forgone in favor of a design that employed the shock tower die casting, which had been the subject of a super-vacuum die casting effort in Phase I (AMD604), and, for which, several hundred castings were already produced and available. Subsidiary components including an upper-rail structure comprised of two symmetric sheet-formed parts, joined to form a box section, and a lower rail consisting of an extruded Mg tubular structure (Figure 1) were designed and fabricated. The structure included fixture attachments on the shock tower top surface for introduction of alternate material couples (e.g. galvanized steel) or attachment to actuators used in mechanical testing and fatigue studies.
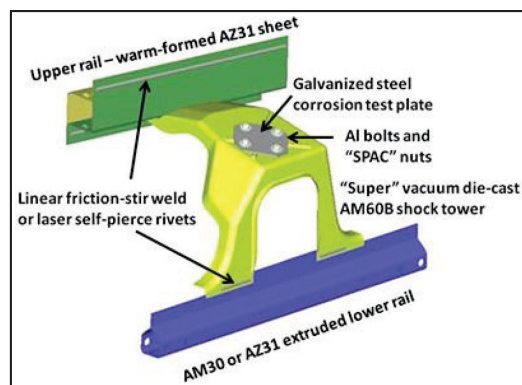
Figure 1. Final version of Mg front-end "demonstration" structure.

USAMP selected two joining technologies: FSLW and LSPR (both with and without application of structural adhesives). Additionally, three pretreatment and finishing options were identified: Alodine® 5200 (Henkel) required for LSPR followed by cathodic electrocoat (590-534 PPG), XBond® 4000 (PPG) followed by cathodic epoxy electrocoat (P-6000 CX), and AHC MagPass® followed by PPG cathodic epoxy. A regimen of mechanical strength testing of entire assemblies was developed by the general contractor, Cosma Engineering of Troy, MI., as well as a schedule of constant and variable-amplitude fatigue testing.

Results and Discussion

Task 2.0 - Design, Analysis, Build, Test, and Logistics.

Cosma Engineering was selected as the general contractor to manage this particular task, which included final design of the demo structure, (including both CAD and CAE renderings), analysis of static and dynamic (fatigue) loading, development and manufacture of assembly tooling for both FSW and self-piercing rivets, all mechanical testing and all logistics including packaging, shipping, handling, and labeling of structures and components. A subcontractor (Exova) was enlisted specifically to provide fatigue testing.

Task 2.1 - Crashworthiness.

Ongoing efforts sought to improve the crashworthiness modeling robustness for Mg. The focus within AMD904 was on the modeling of super-vacuum, die-cast AM60B Mg within the commercial code LS-DYNA®. Two projects were devised: one assessing available material models for LS-DYNA® and, a second to develop a new material model. A team at Wayne State University, led by Dr. King H. Yang, investigated five currently-available LS-DYNA® material models. The team then chose parameters for the material models from the material coupon test data and compared the predicted component response to the tested component response in the four-point bending, slow axial crush, and fast axial crush of super-vacuum, die-cast AM60B Mg beams (as determined in AMD604). The second approach from Forming Solution Technologies, led by Drs. Paul DuBois and Jeanne He, developed a new material model for LS-DYNA®, designated "MAT_233 (CAZACU_ BARLAT_MAGNESIUM)" based on the available and selected new material coupon tests performed on super-vacuum die-cast AM60B Mg. Beam component predictions using this material model showed excellent correlation to the previously-tested component test data. This latter model will be provided by LS-DYNA® as a built-in subroutine, thereby simplifying its use by participating OEM's in predicting crash performance of AM60B Mg structures.

Task 2.2 - NVH.

No active USAMP work on NVH was commissioned in this project, although studies continued in both Canada and China. The USAMP team provided front-of-dash panels from the Dodge Viper (Mg die castings) to China and Canada for NVH analysis.

Task 2.3 - Durability and Fatigue.

The strength and fatigue resistance of joints produced between component pieces of the structure using FSW and self-piercing rivets were the focus of this task. Coupon tests were conducted for strength and fatigue lifetimes by AET Integration (Wixom, MI) for all material stack-up combinations (e.g. AZ31 sheet to AM60B casting, etc.). These results were then used by the University of Michigan (Dearborn) for generating adaptive models that permit assessment of fatigue likelihood in 3-D structures using FE codes for assessment. Cosma Engineering will ultimately generate predictive models for fatigue of joints in the demonstration structures.

Task 2.4 - Corrosion and Surface Treatment.

Pilot surface-processing capabilities for the demo structures were developed at B.L. Downey Co., Broadview, IL, using Henkel Alodine® 5200 pretreatment and PPG 590-534 cathodic epoxy topcoat. Additional pilot capability was established at PPG Industrial Products Division in Euclid, OH, providing XBond 4000® pretreatment with P-6000 CX cathodic epoxy topcoat. Capability for AHC MagPass® was established at Luke Engineering, Wadworth, OH. LSPR and adhesive bonding require Mg to be surface pretreated before joining. North Dakota State University conducted AC/DC/AC electrochemical testing and conventional scribe creepback measurements of coupon samples, including all of the various pilot lab combinations, as well as experimental pretreatments and topcoatings to establish the utility of this method as a rapid comparison technique for coating systems.

Task 2.5 - Extrusion.

Lower rail extrusions for the demo structures were produced in AZ31 and AM30 alloys by Applied Magnesium. Unfortunately, the U.S. division of the company filed for bankruptcy protection in 2011, leaving a challenge in procurement of test parts and also for any follow-on projects. Lehigh University conducted Gleeble® (thermomechanical) testing of ZE40 and ZE60 zinc-rare earth alloys, determining temperature limits for hot extrusion of these materials.

Task 2.6 - Sheet Forming.

This task was coordinated with USAMP Project AMD602 (Warm Forming of Mg Sheet). Over 500 upper rail sheet parts were produced for the demonstration structures by Troy Tooling Co., Roseville, MI., using methods and parameters established via AMD602. Mechanical assessment of novel AZ31 sheet materials and new twin-roll cast materials (Mg-Zn-Y alloys) from CANMET (Canada) were evaluated by Missouri University of Science and Technology.

Task 2.7 - High-integrity Body Castings.

Super-vacuum die-cast shock towers of AM60B alloy produced by the Contech Company in MFERD Phase I (AMD604) were provided for use in demo structure assemblies. Contech has since entered bankruptcy and a new supplier for large, vacuum die castings of Mg has not yet been identified. It is expected that future work will exploit capabilities currently being developed at CANMET (Canada).

Task 2.8 - Welding and Joining.

Activities focused on continued development of FSLW, self-piercing rivet and mechanical fastener technology, with emphasis on a laser thermally-assisted process to facilitate self-piercing riveting of Mg (LSPR)(Durandet *et al*. 2007). In conjunction with Henrob Corp. (Livonia, MI) and Cooperative Research Center for Alloy and Solidification Technology (Swinburne University of Technology, Melbourne, Australia), the team tested and further developed the laser preheating method and process parameters for self-pierce riveting of Mg in sheet, cast, and extruded form, for joints with and without adhesives. Tooling and process parameters for FSLW of the dissimilar Mg alloys were also developed. Coupons for fatigue testing of

FSLW and LSPR joints were produced and roughly 80 riveted and 100 FSLW assemblies for durability and corrosion testing were manufactured. The team also specified and developed Al SPAC® (Self Pierce and Clinch) nuts for use in securing test plates to Mg cast components.

Technology Transfer Path

- Material cards for LS-DYNA® - Outcomes of Task 2.1 (Crashworthiness) will have immediate application in computer code for high strain-rate deformation for die cast AM60B by OEM and supplier organizations. This will be implemented as soon as practicable.

- Joining – Both FSLW and LSPR are validated for assembly of Mg components. LSPR is a patented technology from Henrob Corporation and is available in the marketplace.

- Corrosion Protection – Prototype production is available through at least one supplier (Downey) and alternative approaches are in development through PPG Industries and Luke Engineering. Selected processes are all commercially available from these suppliers.

- Validation of Structural Performance – Methodologies were developed to permit assembly-scale assessment of fatigue of joint structures in Mg-intensive assemblies.

Conclusions

AMD904 has achieved its intended outcomes (i.e. the production and evaluation of demo Mg-intensive front-end example structures) in a foreshortened time period (18 months). Work is expected to continue in a new project insofar as exploration of novel alloys, improved joining and finishing processes, and improved analytic methods of engineering ultimately employable vehicle substructures.

Optimization of High-Volume Warm Forming for Lightweight Sheet Alloys (AMD 905)

Principle Investigator: Nia Harrison, Ford Motor Company
(313)805-7426; e-mail: nharri31@ford.com

Principle Investigator: Peter Friedman, Ford Motor Company
(313)248-3362; e-mail: pfriedma@ford.com

Principle Investigator: Jugraj Singh, Chrysler Group LLC
(248)512-0029; e-mail: js329@chrysler.com

Principle Investigator: Ravi Verma, General Motors Corporation
(248)807-4188; e-mail: ravi.verma@gm.com

Accomplishments

- Engineered the door inner die using traditional die construction practices optimized for Al sheet, enabling a weight savings of 5.1 lbs. which is approximately 40%.

- Established a low-cost warm forming process which requires minimal die heating based on thermal simulation analysis recommendations.

- Minimized wrinkling and cracks through radii and draw bead modifications while preserving the part complexity by utilizing FE analysis recommendations.

- Identified Cosma as the production supplier partner.

Future Directions

- Demonstrate a full-scale run-at-rate production cell of the low cost warm forming process of the door inner panel at a supplier partner facility.

Technology Assessment

- Target: Attain craftsmanship levels in Al similar to steel.

- Gap: No established coupled thermo-mechanical simulation model for formability studies.

- Target: Manage die heat-up during start-up and production.

- Gap: Run-at-rate production cell has not been established to verify thermal simulation predictions.

Introduction

Successful completion of two projects on warm forming (ADM307 and AMD602) have shown that warm forming can be used as a cost-effective method of manufacturing complex 3-dimensional panels from both Al and Mg sheet alloys. This current project is aimed at investigating non-isothermal methods of warm forming to further optimize the process in terms of production robustness and total cost. By controlling temperature locally on different elements of the die as well as the blank, the formability of these alloys can be significantly improved while also reducing process complexity and cost. This could include, as a technical stretch, complete elimination of heating of the forming tool.

Approach

In Phase 1 of AMD905, the AMD602 warm forming die was modified with a feature that added a secondary forming operation to simulate the in-plane stretch which is seen in typical automotive components. The demonstration showed that optimal formability occurred during the non-isothermal condition in which there was a pairing between a warm blank and a cold die. Designing a non-isothermal warm forming process, which only requires a warm sheet, results in significantly lower cost when compared to the isothermal condition. Phase 2 of the AMD905 project has scaled the non-isothermal process to produce a full-scale door inner. A series of thermal and forming analyses have been performed such that the aggressive nature of the door inner die has been maintained. The steel intent die design was modified based on the recommendation of the simulation studies to improve formability. The die performance will be validated through forming trial work to be conducted at the production supplier partner.

Results and Discussion

Thermal Simulation

The objectives of conducting thermal simulation analysis were to: (1) establish steady-state die temperature, (2) minimize distortion within the die, (3) minimize the time to steady-state production, and (4) reduce the number of defective panels during forming start-up.

After analyzing each of the die components (ring, punch, etc.) it was determined that the ring on the lower die assembly would require the most consideration when designing for run-at-rate production. At production rates, the ring will continue to absorb heat until a natural steady-state state of the system is achieved. For this reason, heating/cooling channels were incorporated in the ring in which fluid is able to be passed to assist with regulating the system.

During start-up the fluid was set to 65°C. Preheating the die prior to production reduces the time to reach steady-state, ~400
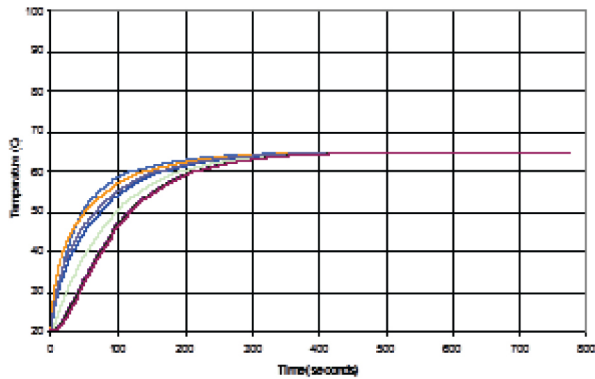
Figure 2. Start-up TC readings at various depths within the ring when preheating with water at 65°C.
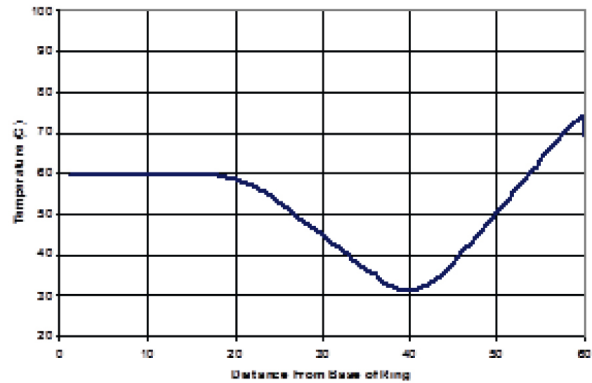
Figure 3. Steady-state TC readings when cooling with water at 15°C.

seconds (Figure 2). During steady-state, the fluid temperature was reduced to 15°C. By incorporating channels at 50mm from the bottom and the top surfaces of the ring, the temperature differential was minimized to ~15°C from the tool surface to base (Figure 3). Additionally, by cooling the ring during steady-state, the ring surface temperature was maintained at 70°C; this balances base and surface temperatures and minimizes die distortion.

FE Simulation

The objectives of the FE analysis were as follows: (1) assess formability at room temperature and at elevated temperatures, (2) guide the die design and modification process to reduce the probability of cracking, (3) optimize the draw bead design and location, and (4) optimize the blank size and relief windows configuration.

The numerical analysis was performed in a commercial FE software package: LS-DYNA. Altair Hypermesh and LS-PrePost were utilized for pre- and post-processing respectively. The process was subdivided into 3 steps: gravity, binder closing, and drawing. The implicit solver was used to simulate the first step whereas explicit solver was used to simulate the other two steps. The blank was simulated with fully integrated shell elements with 5 integration points through the thickness and all the tools were simulated with rigid elements. The process was assumed to be quasi-static, therefore, no strain rate effects were considered. An anisotropic elastic-plastic material model with Barlat'89 yield function was used to model the blank behavior. A piecewise linear approximation of the experimentally determined stress-strain curves in the rolling direction was used as the reference direction flow curve in the model. All simulations were performed in the isothermal conditions. Additionally, an
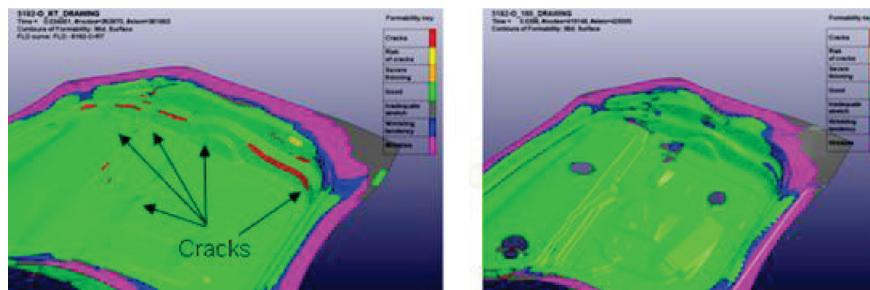
Figure 4. Simulation results for the initial die geometry at 20° C (left) and the final die geometry at 180° C (right).

AA5754-O forming limit diagram was substituted for AA5182-O at elevated temperatures.

Figure 4 shows an FLD plot for the initial die geometry and blank configuration at room temperature and the modified die geometry blank condition at 180°C. The probability of cracking is substantially reduced in the elevated temperature condition. The additions of relief "windows", or holes, have been included in the sheet to further support material flow and minimize cracking; adding windows is a common practice in the forming of steel sheet.

Technology Transfer Path

The optimized warm forming process is more cost competitive with traditional stamping due to the removal of heaters and controls and likely more attractive for components like the door inner by OEMs. A part made by this process with Al in comparison to steel could have a weight savings of 40%. An additional benefit of this process is the reduction of forming operations from five to four given that a part like the door inner can be produced in a single draw; this implies capital equipment savings. For these reasons, there is a high probability that the optimized warm forming process would be adopted by OEMs and suppliers for the forming of various Al components in an effort to achieve mass savings.

Conclusion

A majority for the work accomplished this year was focused on the engineering of the door inner die. The die was crafted for optimum material flow and designed to achieve a steady-state production process. Given the results of AMD905 Phase 1, which demonstrated the in-plane stretch capability of the non-isothermal process, there is a high level of confidence that the forming trials, to be concluded in the forthcoming months, will be successful. The objective of the forming trials will be to verify performance and cycle time of the optimized warm forming process.

Development of Corrosion Inhibiting E-coat System for Body-in-White Assemblies (AMD 1001)

Principal Investigator: Matthew J. O'Keefe, Missouri University of Science and Technology
(573) 341-6764; e-mail: mjokeefe@mst.edu

Principal Investigator: Surender Maddela, Missouri University of Science and Technology
(573) 341-4358; e-mail: maddelas@mst.edu

Principal Investigator: Thor Lingenfelter, PPG Industries
(412)492-5341 e-mail: lingenfelter@ppg.com

Project Lead: Yar-Ming Wang, General Motors Research & Development Center
(586) 986-0762; e-mail: yar-ming.wang@gmail.com

Project Lead: Adam Stals, Chrysler Group LLC
(248) 576-7423; e-mail: as926@chrysler.com

Accomplishments

A corrosion protection system consisting of a cerium-based conversion coating (CeCC) or a zirconium (Zr) - based pretreatment and a commercial E-coat layer have been successfully deposited on individual, bi-metallic, and tri-metallic couples that have performed well during corrosion testing and are compatible with vehicle assembly processes.

- A single layer of CeCC or Zr pretreatment significantly enhanced the corrosion resistance of individual alloys, bi-metallic couples, and tri-metallic couples.

- An E-coat layer over CeCC on bi-metallic and tri-metallic couples was compatible with existing processes, had excellent adhesion strength, and performed well during electrochemical, salt spray, and cyclic corrosion testing.

- E-coat over Zr pretreatment deposited on bi- and tri-metallic couples had strong adhesion strength and corrosion resistance in both salt spray and cyclic testing compared to the current commercial control surface treatment.

Future Directions

Further development of a CeCC or a Zr-based pretreatment and a commercial E-coat will be carried out on a demo structure within a new Mg front-end project recently awarded by the DOE.

Technology Assessment

- Target : Develop in-line corrosion coating process capable of protecting body-in-white (BIW) assemblies containing Mg.

- Gap: The ability to assemble Mg-Al-steel components prior to corrosion coating application will eliminate off-line assemble processes and allow for integration of BIW into existing production lines while improving lifetime corrosion protection.

Introduction

Mg has a very negative standard electrode potential resulting in poor corrosion resistance in aqueous solution. The use of Mg alloys in the automobile industry has been limited due to galvanic corrosion with other structural components (Kulekci, 2008). Moreover, the development of a robust paint-line compatible pretreatment process for Mg intensive vehicles is critical to its expanded use in automotive body and chassis assemblies. Current phosphate electrolyte baths are formulated to treat steel BIW assemblies with limited Al applications. However, because of high solubility of Mg in the phosphate baths, Mg alloys are not compatible with existing phosphate processes used in automotive manufacturing. In order to treat a mixed-metal BIW assembly, including Mg alloy parts, a new conversion coating process needs to be developed. Chromium-based conversion coatings are one of the most effective ways of preventing corrosion of base metals (Gray and Luam, 2002). However, the carcinogenic nature of chromates restricts the use of chromate baths and extensive effort is being done to find a suitable replacement (Costa & Klein, 2006). Several researchers have reported alternative chromate replacement coatings (Pine et al., 2009; Maddela et al., 2010; Zheng and Liang, 2007). Among the alternatives, CeCCs are promising as they offer significant corrosion protection and are environmentally benign.

This project also evaluated a Zr-based pretreatment for adhesion and corrosion resistance with electrocoat technology. The Zr pretreatment utilizes the commercially available Zircobond® technology, which has shown strong corrosion resistance over ferrous, zinc, and Al substrates. Zircobond® is currently used in eight assembly plants in North America and Europe.

Approach

CeCCs and Zr pretreatments were deposited on individual alloys (Mg AZ91, Mg AZ31, Al 6016, Electrogalvanized Steel EGS), bi-metallic couples (AZ91-6016/EGS, AZ31-6016/EGS, and 6016-EGS) and tri-metallic couples (AZ91-6016-EGS, AZ31-6016-EGS). The corrosion protection of CeCCs on individual alloys, bi-metallic couples, and tri-metallic couples have been studied using potentiodynamic polarization measurements, electrochemical impedance spectroscopy (EIS), ASTM B117 neutral salt spray testing, and PATTI adhesion test. Similarly, the Zr pretreatment was applied over the individual alloys, as well as bi- and tri-metallic couples listed above. The corrosion resistance was evaluated in both ASTM B117 neutral salt spray and GMW 14872 cyclic testing, while the adhesion was tested using pneumatic adhesion tensile testing instrument (PATTI).

The project "Development of Corrosion Inhibiting E-coat System for Body-in-White Assemblies - AMD 1001), started in September 2010. This project is divided into three major tasks:

- Task I: Conversion coating development

- Task II: E-coating on conversion coating development

- Task III: Corrosion inhibiting E-coat formulation (extended to next project)

These tasks assess the viability of developing a new pretreatment process for high volume production of BIW automotive structures containing Mg alloy parts. The stretch goal of the program is to incorporate corrosion inhibiting compounds into an E-coat formulation. This would provide a single coating process that has active corrosion protection of the BIW assembly. Due to time constraints, incorporation of corrosion inhibitors into the E-coat was not attempted.

Results and Discussions

Task I (conversion coating development): CeCCs have been successfully deposited on individual alloys, bi-metallic couples, and tri-metallic couples. It was demonstrated that CeCCs can be deposited multiple times on bi-metallic couples and tri-metallic couples by a single coating solution (i.e. no poisoning of the deposition solution). The corrosion results show that CeCCs enhance the corrosion resistance of individual alloys, bi-metallic couples, and tri-metallic couples.

Task II (E-coat on conversion coatings): E-coat deposition on cerium coated individual alloys, bi-metallic couples, and tri-metallic couples has been successfully accomplished. The use of CeCCs significantly improved the corrosion resistance of bi-metallic and tri-metallic couples. A uniform coating without any blisters/pinholes was observed for E-coat layers on cerium coated tri-metallic couples but blisters were present on samples without CeCCs. It was also observed that the E-coat on CeCCs significantly enhances the corrosion resistance of bi-metallic and tri-metallic couples after 336 hours of corrosion testing.

Electrochemical polarization studies have also demonstrated that the CeCCs improve the corrosion resistance of individual alloys and bi-metallic couples. Cerium coated individual alloys have shown passive behavior with a lower corrosion current density. The galvanic current measured between Mg-Al, Mg-galvanized steel, and Al-galvanized steel couples correlated with significant changes in coating morphology and deposition rate. Panels with a CeCC had lower galvanic corrosion current compared to bare panels. The effect of galvanic current between different couples with cerium in the test solution was lower than when panels were tested in a sodium chloride solution. Galvanic current not only assisted the cerium deposition mechanism and deposition rate, it also improved the overall corrosion resistance of bi-metallic and tri-metallic couples.

The PATTI adhesion strength of E-coat on CeCCs was found to be as good, or better, than the adhesion of E-coat on an Alodine 5200 pretreatment used as a standard.

Electrocoat was successfully applied over Zr-treated individual substrates, as well as bi- and tri-metallic couples. The resulting E-coat films were uniform and defect-free while the deposition characteristics of the Zr treated Mg alloys were consistent with similarly treated EGS and Aluminum 6016. The corrosion resistance of the Zr treated single alloy panels were compared to two commercially available conversion coats, chromated Alodine™ 1200s and chrome-free Alodine™ 5200, and a commercial available zinc phosphate (Chemfos 700) using GMW14872 cyclic corrosion testing. The use of Zr pretreatment significantly improved the corrosion resistance of the three Mg alloys compared to the chrome-free commercial control and equaled the performance of the chromated conversion coat.

Corrosion testing of the tri-metallic panels are in test as of Oct 2011. Preliminary results after 20 cycles of GMW14872 show that both the Zr pretreatment and the CeCC are significantly better than Alodine 5200, the commercial control. Both the Zr pretreatment and CeCC show very little blistering on the AZ31 alloy, while the control shows blistering along the scribe. PATTI adhesion of the E-coated Zr pretreated panels were found to be equal to, or better than, the commercial chromated conversion coat, Alodine 1200s.

Technology Transfer Path

PPG is working with Missouri S&T to develop manufacturing processes and prototype coating capabilities to demonstrate the technology and evaluate production volume fabrication.

Conclusions

- CeCCs and Zr pretreatments were successfully deposited on individual alloys, bi-metallic couples, and tri-metallic couples without contaminating the deposition bath.

- CeCCs and Zr pretreatments significantly improve the corrosion resistance of E-coated bi-metallic and tri-metallic couples.

- Galvanic current influences the conversion coatings on bi-metallic couples; cerium coated bi-metallic couples showed better salt spray performance compared to bare couples.

- The adhesion strength of E-coat over CeCC was as good as, or better, than over Alodine 5200. The adhesion strength of E-coat over Zr pretreatment was equal to, or better than, Alodine 1200s.

Global Vehicle Assessment (AMD-1003)

Principal Investigator: Shawn Morgans, Ford Motor Company
(313) 805-3596; e-mail: smorgans@ford.com

Principal Investigator: Bruce Mattarella, Chrysler Group LLC
(248)576-6585; e-mail: bpm3@chrysler.com

Principal Investigator: Joe Polewarczyk, General Motors Company (248)907-2872;
e-mail: joseph.m.polewarczyk@gm.com

Accomplishments

- Developed a common strategy for conducting vehicle teardowns and summarizing teardown results.

- Identified twelve vehicles for teardown based on agreed upon vehicle selection criteria

- Completed ten of twelve vehicle teardowns

Future Directions

- Complete remaining two vehicle teardowns

- Analyze vehicle teardown results and summarize results in vehicle teardown reports

Technology Assessment

The objective of this project was to facilitate lightweighting through competitive teardown analysis.

- Target: Key to the teardown analysis is compilation of the individual teardown results into a useable database. Vehicle teardowns are nearing completion and data entry and analysis will soon follow. However, as of the writing of this report, insufficient data is available for analysis or conclusions.

- Gap: A2Mac1 and each of the Original Equipment Manufacturer (OEMs) have different teardown procedures, which inhibit the ability to create a common database. Individual vehicle analysis will not be affected but the lack of a common database will limit the project's ability to directly contrast and compare all attributes of the twelve vehicles studied.

Introduction

Prior to this program, strategic full body vehicle teardown assessment data was not directly available to USAMP, which impaired the ability of USAMP to identify vehicle level opportunities for inclusion in a unified strategic roadmap for developing high value projects that addressed agreed upon technical gaps to achieving lightweighting goals. This program provides USAMP with the ability to develop a common vehicle benchmarking strategy that not only increases the breadth of available benchmarking data, but also reduces the time needed to develop a strategic roadmap of lightweighting opportunities by virtue of drawing from a collective and agreed upon source of data.

Without a unified strategic approach, vehicle benchmarking data available to each of the OEMs is limited and often duplicated. Existing commercial benchmarking databases are available, but are limited as well, dated, expensive, and lacking a strategic focus (and much of it is a duplicate of OEM data). As a result, strategic plans and roadmaps are not as robust as they should be and opportunities are missed. Consequently, a gap in USAMP lightweighting efforts is created between "what could be" and "what is" implemented. A strong leveraged full vehicle teardown assessment process would significantly reduce this gap and improve the efficiency of the available resources to maximize implementation of proven lightweighting technologies. This project proposes to implement a full body materials and structures teardown assessment process as well as identifying lightweighting opportunities based on implemented solutions.

Approach

Each USAMP OEM will tear down and contribute data for two vehicles and USAMP will provide resources for teardown of two additional vehicles per USAMP OEM per year. This process will provide shared data from twelve vehicles versus none today.

The approach will begin with agreement on common teardown practices, component displays, analyses procedures, data reporting, and final report formatting. The teardown components, which may be included in the vehicle reports, are listed in Table 3.

Table 3. Teardown Analysis Components

Static stiffness (bend/torsion)	Material data on critical parts	Joining practices
Dynamic stiffness	Tensile strength	Corrosion mitigation
Body in white weight	Material composition	Design for Disassembly
Weld counts (Type, use, application, length)	Component sectioning	Impact on recyclability
Overall BIW and individual part weights	Assembly sequences	

A list of non-domestic, first year in service, vehicles will be selected. Two of the selected vehicles will be assigned to each domestic OEM for teardown, while the remainder of the vehicles will be torn down at an independent supplier. USAMP will be provided individual vehicle reports that summarize the displays and data. A final report will be provided that summarizes the vehicle reports upon an agreed upon reporting structure. A full final report of all data will be prepared for each vehicle benchmarked and distributed to each OEM for individual analysis.

Results and Discussion

The group identified twelve vehicles for teardown as shown in Figure 5, grouped by the company conducting the teardown. The selected vehicles were new vehicles structures with above average performance and/or fuel economy for their class.

The project has completed ten of twelve vehicle teardowns. The 2011 Audi A8 and the Toyota Sienna teardowns are expected to be complete by December. Vehicle reports are expected by December 16, 2011 and a Final Report by December 31, 2011.
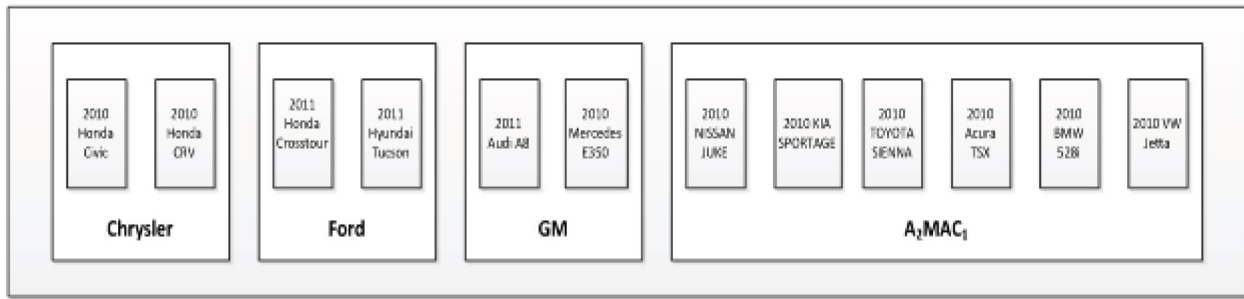
Figure 5. Selected Vehicles

The development of vehicle reports has begun using a format developed by Ford. The 2011 Honda Crosstour (Figure 6) and 2011 Hyundai Tuscon (Figure 7) vehicle reports have been drafted with example observations provided below.

Figure 6. 2011 Honda Crosstour

Figure 7. 2011 Hyundai Tuscon

- 2011 Honda Crosstour: Increased use of dual phase steels, but a surprising lack of UHSS steels (boron or martensitic). The typical range of the dual phase steels used in the body structure is DP600. The front & rear bumper beams employ DP980. This material implementation strategy confirms why the roof strength of the Crosstour does not meet the new 2012 4x roof strength requirement, and a weight penalty of ~5-10kg is expected in the future for this.

- 2011 Hyundai Tuscon: Increased use of dual phase steels, and some use of UHSS steels (boron). The typical range of the dual phase steels used in the body structure is DP590-780. There is significant use of HSLA340 and HSLA 500 in the front header. The front bumper beams employ hot stamped boron steel. Coatings are strategically used with the predominance in the lower structure. Hyundai favors HDGA over GI coatings for this vehicle

Technology Transfer Path

The automotive manufacturers will use the A2Mac1 database and internal OEM databases to evaluate competitive material, design and process decisions, assess applicability to current and future automotive designs, and implement viable lightweighting solutions.

Conclusions

The project has successfully negotiated a common methodology between the automotive manufacturers for vehicle selection criteria, conducting teardowns, and reporting teardown results. The project has not progressed sufficiently to provide definitive conclusions, which is subject to vehicle teardown analysis, individual vehicle reports, and a summary report.

Development of Ablation Casting Process for High Volume Production of Structural Aluminum Components (AMD1100)

Principal Investigator: Dr. Jacob Zindel, Ford Motor Company
(313) 845-8559; e-mail: jzindel@ford.com

Principal Investigator: Stephen D. Logan, Chrysler Group LLC
(248) 512-9485; e-mail: sl16@chrysler.com

Principal Investigator: Herb Doty, General Motors Corporation
(603) 673-9720 ext. 2598; e-mail: herb.doty@gm.com

Accomplishments

Critical process steps were defined and process information was collected to enable the development of a cost model for ablation casting. This included:

- An aggregate and water reclamation system.

- Fast cure for molds and cores

- A manufacturing process that produces castings at a rate of approximately one per minute.

- A cost model for OEMs to compare similar parts and processes

- Components (transom bracket) were successfully cast using a wrought alloy with exceptional mechanical properties. Wrought alloys are essentially impossible to cast using conventional industrial processes.

Future Directions

- Each project participant will have to examine their own constraints and needs with respect to the application of this process for their respective businesses.

- The cost model will provide sufficient information on capital equipment and processing details for proper decisions regarding the application of this process for their manufacturing needs.

Technology Assessment

- Target: To provide a cost model based on the Ablation Casting Process that the OEMS can review and quickly decide if this process is technically and financially applicable to a new component that is being considered for vehicular use.

- Gap: Conventional cost models that the OEM's currently use will not work for parts cast by the Ablation Process.

Introduction

The Ablation Casting Process most closely resembles a sand casting process that utilizes a water soluble binder that allows the mold to be washed away by water sprays as the part solidifies (Figure 8). This produces very high temperature gradients and short solidification times which are highly desirable. In two previous USAMP projects (AMD-405 for Al B206 alloy and AMD-601 for Mg alloys), this process produced castings with excellent tensile and fatigue properties.
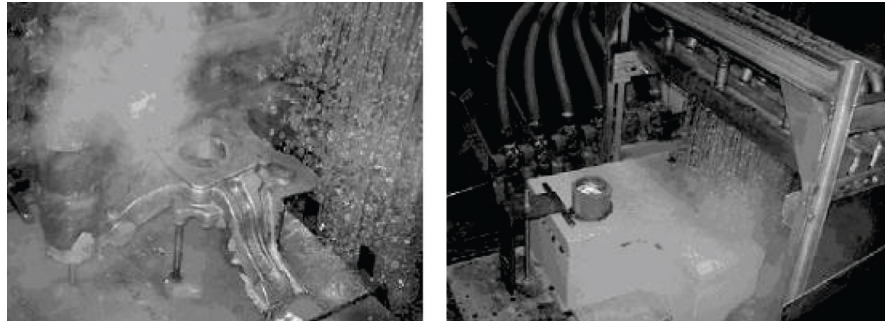
Figure 8. Ablation of Mold in Progress and Ablation complete

A barrier to the implementation of the ablation process for high volume production was the lack of a cost model to show whether the process is: less expensive, more expensive, or equal in cost to competing casting processes. Because the ablation process can also be used to produce high strength wrought alloy castings, the cost of components produced from the process must also be compared to the cost of forged components.

Approach

This project was structured around an existing development project between Mercury Marine and Alotech (ablation process patent holder) for the development of an Al transom bracket for their watercraft shown in Figure 9. Ten additional project participants were enlisted to accomplish the project deliverables. The participants included supplier foundries, other transportation industries and equipment builders which indicates the broad range of interest in the technology.

Figure 9. Mercury Marine Transom Bracket Cast by the Ablation Process

Results and Discussion

Throughout the production runs, the process parameters were finalized for: 100% reclamation of sand (aggregate) and water for continuous use; the fast cure for molds and cores; a manufacturing process to produces castings at a rate of approximately one per minute (depending on size and thickness). The cost model data was collected throughout the production runs and a working cost model was developed for this particular part using the ablation process.

The ablation process demonstrated the capability to cast complex shapes with higher integrity and significantly better mechanical properties than conventional casting process. While the testing procedures and related material properties are still being compiled, preliminary data shown in Figure 10 clearly illustrates the capability of the ablation casting process to produce high integrity components using a difficult to cast alloy (6061) compared to components cast from a conventional casting alloy (A356) using the permanent mold process.
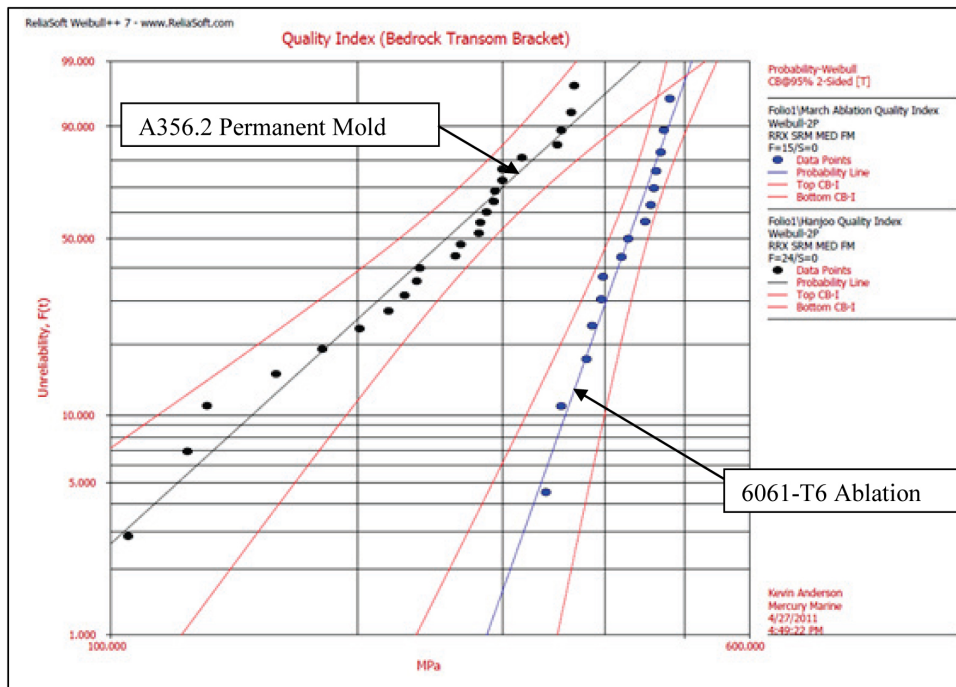
Figure 10. Comparison of 6061-T6 Ablation versus A356.2 Permanent Mold – Quality Index. (This Information was provided courtesy of Mercury Marine. Mercury Marine makes no warranty, express or implied, or assumes any legal liability or responsibility for the accuracy, completeness, or usefulness of this information.)

Technology Transfer Path

On-going detailed results from this project have been provided to all project participants by Mercury Marine on the mechanical property testing results that have been completed to date. Exchange of testing information from all of the project participants will continue as more parts are tested and all results will be correlated in the Final Report. However, it will then be the responsibility of the OEMS and suppliers to review the test results and consider the implementation (and use) of the ablation process for new vehicular components.

Conclusions

All the process steps unique to this process have been defined which enabled a cost model of the process to be created. All of the processing steps appear to be scalable for high volume production. Sufficient process data has been collected to populate the cost model so comparisons can be made between ablative casting and current casting and forging processes.

Mechanical property data collected from the castings tested to date indicate that they have excellent tensile and fatigue properties, consistent with the prior AMD projects

Conclusions

Over the past year, AMD sponsored projects have made significant progress in overcoming (or reducing) technological hurdles to implementation of light metal applications in the automobile industries by 1) generating a cyber-infrastructure and working committee to predict Mg component properties based on their processing history, 2) demonstrating concept feasibility for using multi-layer nano-ceramic coatings to help mitigate galvanic corrosion between steel fasteners and Mg components, 3) production of Mg front-end demo structures, 4) engineering a heated door inner panel die for warm forming evaluations, 5) producing and testing Mg and multi-material joined test samples with cerium and Zr pretreatments, 6) conducting teardowns and reporting results for six competitive automotive body-in-whites, and 7) developing and evaluating high volume production capable ablation casting process for part quality evaluation and cost model development.

Presentations/Publications/Patents

AMD703

Agnew S.R., Raeisinia B., Hector L.G., Wagoner R.H., Piao K., "Twinning and Detwinning in a Mg Alloy," presented at the International Symp. on Plasticity, Puerto Vallarta, Mexico, January 2011.

Agnew S.R., Raeisinia B., Akhtar A., "Incorporating the effect of solute into crystal plasticity models" presented at the International Symp. on Plasticity, Puerto Vallarta, Mexico, January 2011.

Issa, A., Saal, J.E. and Wolverton, C., "First-Principles Coherency Strain in Mg3RE Precipitates," presented at APS March Meeting, Dallas, TX, March 22, 2011.

Issa, A., Saal, J.E. and Wolverton, C., "First-Principles Coherency Strain Energy in Mg-Mg3RE (D019) Systems," Physical Metallurgy Gordon Research Conference, Easton, MA, August 2011.

Raeisinia B., Agnew S.R., Akhtar A., "Incorporation of Solid Solution Alloying Effects into Polycrystal Modeling of Mg Alloys," Metall Mater. Trans. A, 42A (2010) 1418-1430.

Raeisinia B., Agnew S.R., "Using polycrystal plasticity modeling to determine the effects of grain size and solid solution additions on individual deformation mechanisms in cast Mg alloys," Scripta Mater., 63 (2010) 731-736.

Rettberg, L.H., Jordon, J.B., Horstemeyer, M. F., and Jones, J.W., "Low-Cycle Fatigue Behavior of Die-Cast Mg Alloys AZ91 and AM60," Metallurgical and Materials Transactions, (in press), 2011.

Saal, J.E., Issa, A., Ganeshan, S., Shin, D. and Wolverton, C., " First-Principles Investigation into Precipitates and Strengthening of Magnesium-Rare Earth (RE) Alloys," Presented at 10th AlEMI Workshop, Vancouver, BC, June 8, 2011.

Saal, J.E. and Wolverton, C. "Solute-Vacancy Binding of the Rare Earths in HCP Magnesium," Physical Metallurgy Gordon Research Conference, Easton, MA, August 2011.

Wang H., Raeisinia B., Wu P. D., .Agnew S.R., Tomé C.N., "Evaluation of self-consistent polycrystal plasticity models for magnesium alloy AZ31B sheet," Int. J. Sol. Struct., 47 (2010) 2905-2917.

AMD704

Chi Qu, X. Wang: Progress Report on Multiple-Layer Coating for Anti-Corrosion

L. He, R. Stewart and J. Fan, Reports on Testing of Chemo-Mechanical Coupling and Strength of Multiple-Layer Nano-Coatings

L. He, R. Stewart and J. Fan, Multiscale Simulation and FEA Results for Effects of Locating-Layer Thickness and Layup Sequence on Interfacial Strength and Fracture Toughness

V, Brick, R. Nanni, M. Bluy and M., Locus, Preliminary Design and Considerations of Bolt Twisting Tests for Reliability Analysis of Coated-Fasteners in Laboratory and Service Conditions

AMD904

Badarinarayan, H., Behravesh, S., Bhole, S., Chen, D., Grantham, J., Horstemeyer, M., Jahed, H., Jordon, J., Lambert, S., Patel, H., Su, X. and Yang, Y., "Monotonic and Fatigue Behavior of Mg Alloy in Friction Stir Spot Welds: An International Benchmark Test in the Magnesium Front End Research and Development Project, " in Magnesium Technology, 2011, Wim Sillekens, Sean R. Agnew, Suveen N. Mathaudhu, and Neale R. Neelameggham, eds., The Minerals, Metals and Materials Society, Warrendale, PA, 2011, pp 629-634.

Bernard, J. D., Jordon, J.B., Horstemeyer, M.F., Kadiri, H.E., Baird, J., Lamb, D. and Luo, A. A., "Structure-property Relations of Cyclic Damage in a Wrought Magnesium Alloy", Scripta Materialia, (2010), 63, (7), 751-756.

Chen, D.L., Emami, A. R. and Luo, A. A., "Cyclic Deformation of Extruded AM30 Magnesium Alloy in the Transverse Direction", Journal of Physics: Conference Series, (2010) , 240, 012048.

Jordon, J.B.; Horstemeyer, M.F.; Daniewicz, S.R.; Badarinarayan, H.; Grantham, J.; Material Characterization and Modeling of Friction Stir Spot Welds in a Magnesium AZ31 Alloy. J. Eng. Mater. Technol. 2010, 132, pp 041008-1-10.

Jordon, J.B; Gibson, J.; Horstemeyer, M.F.; El Kadiri, H.; Baird, J.; Luo, A.A.; Effect of Twinning, Slip, and Inclusions on the Fatigue Anisotropy of Extrusion-Textured AZ61 Magnesium Alloy. Mat Sci Eng. A. 2011, 528, pp 6860– 6871.

McCune, R. C. , Wang, Y.-M., Gu, H., Schneider, B. and Vartolas, F., "Evaluation of Corrosion Protection Systems for Magnesium-Intensive Automotive Body Structures," Materials Science and Technology, 2010, Houston, TX, ASM International, Oct. 19, 2010.

Quinn, James; "Magnesium Front End Research and Development (MFERD) Joining Activities Overview," Oral Presentation to the International Workshop on Welding and Joining of Magnesium Alloys (University of Waterloo), July 28, 2011

Song, S., McCune, R.C., Shen, W. and Wang, Y.-M., "Use of an AC/DC/AC Electrochemcial Technique to Assess the Durability of Protection Systems for Magnesium Alloys," in Magnesium Technology, 2011, Wim Sillekens, Sean R. Agnew, Suveen N. Mathaudhu, and Neale R. Neelameggham, eds., The Minerals, Metals and Materials Society, Warrendale, PA, 2011,pp 531-535.

AMD1001

Maddela, S.; O'Keefe, M.J.; Wang, Y.M.; Effect of hydrogen peroxide concentration on corrosion resistance of cerium-based conversion coatings on Mg AZ91D alloy. In ECS (The electrochemical society) conference, Boston MA, October 9, 2011.

Castano, C.E.; Maddela, S.; O'Keefe, M.J.; Wang, Y.M.; A comparative study on the corrosion resistance of cerium-based conversion coatings on AZ91D and AZ31B magnesium alloys. In ECS (The electrochemical society) conference, Boston MA, October 9, 2011.

Maddela, S.; O'Keefe, M.J.; Wang, Y.M.; The influence of galvanic current on cerium-based conversion coating on Mg, Al, and galvanized steel couples. In TMS 2012 Symposium: Magnesium Technology 2012, March 11-15, 2012, Orlando, FL.

Castano, C.E.; Maddela, S.; O'Keefe, M.J.; Wang, Y.M.; Effect of thickness on the morphology and corrosion behavior of cerium-based conversion coatings on AZ31B magnesium alloy. In TMS 2012 Symposium: Magnesium Technology 2012, March 11-15, 2012, Orlando, FL.

Maddela, S.; Castano, C.E; O'Keefe, M.J.; Wang, Y.M.; Thor, L.; Chang, S.; Corrosion protection of Mg-Al-galvanized steel assemblies. In Mg 2012: 9th International Conference on Magnesium Alloys and Applications, July 8-12, 2012, Vancouver, BC, CA.

Castano, C.E.; Maddela, S.; O'Keefe, M.J.; Wang, Y.M.; Effect of deposition temperature on the properties of cerium-based conversion coatings on AZ31B magnesium alloys. In Mg 2012: 9th International Conference on Magnesium Alloys and Applications, July 8-12, 2012, Vancouver, BC, CA.

References

AMD704

SAE/USCAR-32 "New Finish Development", SAE International Standard, 2007-03-13

MAGNESIUM VISION 2020: A North American Automotive Strategic Vision for Magnesium, a USAMP Publication, August, 2006.

C. Qu, et al, "Aluminum Oxide and Silicon Nitride Thin Films as Anti-Corrosion Layers", Ceramic Engineering & Science Proceedings, Vol. 31, Issue 3, 2010, p.p. 123-134.

L. Lin, et al., "Multilayer Coatings for Anti-Corrosion Applications," Ceramic Engineering & Science Proceedings, Vol. 32, Issue 3, 2011, p.p. 59-70.

AMD904

Durandet, Y., Song, W., Blacket, S. and Brandt, M., " Spot Joining of Magnesium Using Thermally-Enhanced Self-Piercing Riveting Technology," in Proceedings of the Light Metals Technology Conference, St. Sauveur, Quebec, Canada (2007).

AMD1001

Kulekci, M.K.; Magnesium and its alloys applications in automotive industry. The International Journal of Advanced Manufacturing Technology, Vol. 39 (2008), pp. 851–865.

Gray, J.E.; Luan, B.; Protective coatings on magnesium and its alloys-a critical review. Journal of Alloys and Compounds, 336, 2002, pp. 88-113.

Costa, M.; Klein, C.B.; Toxcity and carcinogenicity of chromium compounds in Humans. Critical Reviews in Toxicology, 36 (2) (2006), 155-63.

Pinc, W.; Geng, S.; O'Keefe, M.J.; Fahrenholtz, M.G.; O'Keefe, T.; Effect of acid and alkaline based surface preparations on spray deposited cerium-based conversion coatings on Al 2024-T3. Applied Surface Science, 255(2009), pp. 4061-4065.

Maddela, S.; O'Keefe, M. J.; Wang, Y.M.; Kuo, H.H.; Influence of surface pretreatment on cerium-based conversion coating on Mg AZ91D alloy. Corrosion, 66(11), 2010, pp. 115008/1-8.

Zheng, R.F.; Liang, C.H.; Conversion coating treatment for AZ91D magnesium alloys by a permanganate-REMS bath. Materials and Corrosion, 58, 2007, pp. 193-197.

C. Auto/Steel Partnership - U.S. Automotive Materials Partnership

Field Technical Monitor: Terry Cullum
Auto/Steel Partnership
2000 Town Center, Suite 320; Southfield, MI 48075
Phone: (248) 945-4770; e-mail:tcullum@steel.org

Field Technical Monitor: Ronald Krupitzer
American Iron and Steel Institute
Steel Market Development Institute
2000 Town Center, Suite 320; Southfield, MI 48075
Phone: (248) 945-4761; e-mail: rkrupitzer@steel.org

Technology Area Development Manager: William Joost
U.S. Department of Energy
1000 Independence Ave., S.W.; Washington, DC 20585
(202) 287-6020; e-mail: william.joost@ee.doe.gov

Technology Area Development Manager: Carol Schutte
U.S. Department of Energy
1000 Independence Ave., S.W.; Washington, DC 20585
(202) 287-5371; e-mail: carol.schutte@ee.doe.gov

Field Project Officer: Joseph Renk
National Energy Technology Laboratory
626 Cochrans Mill Road, P.O. Box 10940; Pittsburgh, PA 15236
Phone: (412) 386-6406; e-mail: joseph.renk@netl.doe.gov

Contractor: Auto/Steel Partnership (A/SP)
Contract No.: DE-EE0003583

Executive Summary

Advanced High Strength Steels (AHSS), because of their unique mechanical properties, have the potential to reduce vehicle mass. AHSS steels differ from conventional mild steel and High Strength Low Alloy (HSLA) steels because they are produced using unique combinations of alloy composition and processing methods to achieve their high strength without compromising formability. There are four unique families of AHSS with sub grades within each: Dual Phase, Complex Phase, TRIP, and Martensitic steels. Each family has unique properties (quasi-static, fatigue, and high strain rate) and manufacturing characteristics (joining, stamping, hydroforming, and precision flow forming), which need to be fully understood if the materials are to be successfully applied to high volume automotive applications. To maximize the mass savings from using these materials, focal design projects have been carried out to better define the manufacturing processing issues and needs to most effectively apply these new materials to reduce vehicle mass. Using design optimization tools, the A/SP also demonstrated the need for even more advanced or next generation steels. Work has focused on developing the critical manufacturing technologies necessary to produce parts using these materials economically (cost parity) on a high volume basis. In addition, work has been done to understand the properties of these materials that are important to product durability and safety. These steels are 100% recyclable and there are no known recyclability issues. The objective is to enable the use of advanced steels to create components and structures with mass reductions of 25% and greater.

Stamping is the most common way of transforming sheet steel into the complex shapes that make up the automobile. To be efficient and timely, the process to develop dies to convert sheet steel into complex shapes needs to incorporate sound product/process decisions with accurate computer based tools. The empirical knowledge base and math tools that have worked so effectively in designing dies for conventional steels are not adequate when used with AHSS. Over the past year, the focus of the A/SP 050 project, AHSS Stamping, has been to improve the springback and fracture predictability of the math based tools used to design dies and to determine potential local softening processes for AHSS to improve formability.

It is recognized that sheet metal follows nonlinear strain paths during forming operations and crash events and the nonlinearity is more important for AHSS steels than lower strength steels. The A/SP 061 project, Nonlinear Strain Path, aims to deliver a comprehensive set of experimental data and predictive models for AHSS under nonlinear strain path deformation. Current product performance simulations using commercial finite element (FE) design packages for formability and crashworthiness generally assume that the vehicle body parts have no prior strain history at the start of the simulation with a uniform thickness for a given part. For more accurate prediction and correlations of design intent to product manufacturing and performance, it is critical to incorporate prior manufacturing effects such as forming and bake-hardening into product performance simulations with more reliable constitutive and fracture models so that the full potential of lightweighting can be realized. The results will enable more efficient vehicle design for more weight reduction opportunities taking advantage of the rapid hardening behavior of AHSS and enable the accelerated usage of AHSS by reducing cost and time for stamping die development

AHSS is very destructive to stamping dies and even more so as the strength of AHSS has progressed from the 590 grades thru the 780 grades and to the 980 grades. The A/SP 360 project, Stamping Tooling Optimization, aims to provide understanding that will lead to improved die designs, die materials, and surface treatments that will allow continued commercial application of AHSS for mass reduction.

Joining is a critical process in the high volume production of automobiles. The A/SP 370 project, Joining Knowledge Management, is designed to improve access to the latest joining information to enable more efficient and effective utilization of AHSS in automotive manufacturing. The current practice to propose, validate, and approve AHSS or other light weight material utilization in vehicle production requires engineers to extract relevant and useful technical information from many logically unrelated sources of data and knowledge related to base material properties, welding process, joint performance, etc. This current practice is inefficient, ineffective, and inhibits rapid knowledge transfer and utilization of new technological development in AHSS joining.

Automotive body structural design and engineering analysis experts report that crash models run with high AHSS content typically under-predict vehicle crash performance, causing them to over-design structures and add more weight than needed to achieve acceptable performance. This under-prediction effect is felt to be caused by not including forming strain, work hardening, and thinning effects in the crash model. The A/SP 390 project, Mapping of Forming Effects to Structural Models, is designed to develop the data to populate computer based design tools to improve the prediction of AHSS in deformation situations.

While running in the electric mode, Advanced Hybrid Electric Vehicles (AHEV) and Extended Range Electric Vehicles (EREV) carbon canisters, used for fuel evaporative emissions control, cannot be purged. Consequently, in current-generation designs, the fuel tanks are sealed which raises the internal pressure of the tank. Current design plastic tanks cannot meet the high internal operating pressures and thick walled (1.4 to 2.0 mm) steel tanks are used which result in high mass. The A/SP 400 project, Lightweight Sealed Steel Fuel Tanks, is designed to enable and demonstrate the manufacturing feasibility of low mass, sealed steel fuel tanks suitable for use in AHEV/EREV while achieving equivalent performance and cost.

Activity and Developments

Advanced High-Strength Steel Stamping—A/SP 050

Principal Investigator: Changqing Du, Chrysler Group LLC
(248) 576-6680; e-mail: CD4@chrysler.com

Principal Investigator: Ching-Kuo Hsuing, General Motors Corporation
(586) 907-1015; e-mail: Ching-Kuo.hsuing@gm.com

Accomplishments

- Provided a series of AHSS edge cracking limits under hole expansion deformation with pierced holes of 20 mm to 80 mm diameter. The results enable the stamping industry to develop AHSS edge cracking criteria for hole expandability of AHSS sheets with pierced hole diameters in this range. The results show that the hole expansion limits of the tested AHSS sheets with 20 mm-80 mm hole sizes are higher than that of cutout radius sizes in the range of 150 mm to 300 mm.

- Provided micro structural analysis results of the sheared effected zone of the test samples that were used for the hole expansion tests. A strain calculation method was developed based on the optical measurement of the metal flow line on the shear-effected zone. The micro structure analysis results indicated that the maximum shear strain on the sectioned surface, which is perpendicular to the cutting edge, decreases with increasing cutting clearance of the sheared edge. The strain calculation method may be used in the near future to quantify the damage of the shear effected zone due to the shear cutting process.

- Evaluated the numerical simulation predictability on a B-Pillar stamping part with DP980 steel. The results suggest that the newly developed material hardening model (Yoshida) provides more accurate springback prediction for this part.

- Conducted stamping trials on two stamping draw dies to evaluate formability, stretch-bend ability, and edge cracking limits on two newly developed 980 MPa AHSS and one 3rd Generation (3G) QP (Quenching & Partitioning) 980 MPa steel. The aggressive geometry of the B-Pillar die was selected to evaluate the formability of these steels. The straight rail draw die was selected to evaluate the stretch-bend ability of AHSS because severe shear fractures occurred in all Dual Phase steels with 780 MPa and above strength in past trials. Three of the nine tested 980 MPa steels were made without fracture on the straight rail draw die.

- Conducted local softening experiments and evaluations on one type of DP980 steel and proved that both induction heating and laser heating approaches can be used to soften the DP980 steel sheet locally to approximately 800 MPa strength.

- Conducted the large size cutout edge cracking die trials on two newly available 980 MPa AHSS and one 3G QP (Quenching & Partitioning) 980 MPa steel. This task provided edge cracking limit criteria for large cutouts with radius between 150 mm and 300 mm. The results indicated that all the newly developed steels showed higher edge stretch ability or thinning limits than that of earlier versions of DP980 steels tested three years ago. The results enable the stamping industry to develop edge cracking criteria to better predict material and process performance when these higher strength grades of AHSS are selected.

- Evaluated the pre-form effects on AHSS edge stretch-ability through the experimental stretch tests on the pre-formed steel samples. The results indicated that the edge cracking limits of the tested Dual Phase steels have limited to no effect from the pre-forming process, while the tested low alloy High-Strength steels showed early edge cracking in the pre-formed zones.

- Conducted an experimental stamping die deflection measurement and provided dynamic experimental data at multiple locations of a DP980 B-Pillar die set during the stamping process for die structural FEA simulation correlation, verification, and enhancement.

Future Direction

The A/SP plans to continue the work in a direct funded (automotive Original Equipment Manufacturers (OEMs) and steel companies) project.

Technology Assesment

- Target: Provide the automotive community with a more accurate empirical knowledge base, validations on computerized simulation models, and enhanced criteria to encourage the use of lighter AHSS and UHSS in auto manufacturing.

- Gap: Current databases don't provide sufficient data on AHSS with tensile strengths of 980 MPa and higher.

- Target: Determine the effectiveness of local softening techniques to improve the stamping of AHSS and UHSS.

- Gap: Stamping of AHSS/UHSS with tensile strengths of 980 MPa and higher with challenging part geometries frequently result in fracture.

Introduction

Stamping is the most common way of transforming sheet steel into the complex shapes that make up the automobile. To be efficient and timely, the process to develop dies to convert sheet to complex shapes needs to incorporate sound product/process decisions with accurate math based tools. The empirical knowledge base, computer simulation models, and the fracture criteria used to predict material and process performance that had worked so effectively in designing dies for steels with tensile strengths of 780MPa or less are not adequate when applied to AHSS with tensile strengths of 980MPa and above because of the lack of understanding of their fracture behaviors, mechanical properties, special micro-structural, and process response. Comprehensive testing data are needed to enhance the simulation models and empirical criteria to support computer simulations on various stamping processes for better prediction on formability and fracture. There is also a need to develop low cost stamping processes that may have the potential for sustainable AHSS manufacturing processes.

Also, there is a need to improve the springback and fracture predictability of the computer based simulation models and criteria for production stamping die designs and to conduct the feasibility study on a potential low cost blanking preparation technology for sustainable AHSS sheet metal manufacturing processes.

Approach

- Perform lab scale experimental studies and micro-structure analysis for the development of AHSS edge cracking criteria in stamping applications to develop a better understanding of the local fracture phenomenon.

- Conduct production scale stamping trials and formability measurements to evaluate the newly received 2G and 3G AHSS and UHSS sheets.

- Conduct computer simulations and material modeling correlations.

- Evaluate the feasibility of blank preparation processes for UHSS stamping – Blank Local Softening.

Results and Discussion

Task 1.1. AHSS Edge Cracking Experiments – 6" Diameter Hole Expansion

The goal of this task is to provide experimental data for the development of edge cracking failure criterion including the effects of part geometry and to identify the causes of failure mode transformation, i.e. from edge cracking to necking/split. The tests evaluated the following:

- Various hole diameters from 10, 20, 40, 60 to 80mm

- Edge test (specimens with sheared straight side) used to simulate the large radius

- Three cutting clearances (0.1 t, 0.2 t and 0.3 t)

- Materials: DP780 and DP980 of 1.0 mm, 1.4 mm and 1.8 mm thicknesses

- Different surface coatings: GA, EG, and CR, 6 lots of steel from 2 sources: Group A and Group B

Both hoop strain, which is the hole expansion ratio (HER), and the thinning limit at the point near the crack of the test sample were measured. The hole expansion ratios and the thinning limits of the tested DP780 samples are shown in Figure 1 and Figure 2, respectively. From the HER and thinning limit results, it can be noted that the HERs and thinning limits of Group A steels are higher than that of Group B steels for holes with diameters of 40 mm and above. The HERs and thinning limits of Group A steels increased as the hole diameter increased, while the HER and thinning limits remained at similar levels regardless of the hole diameter for Group B steels.
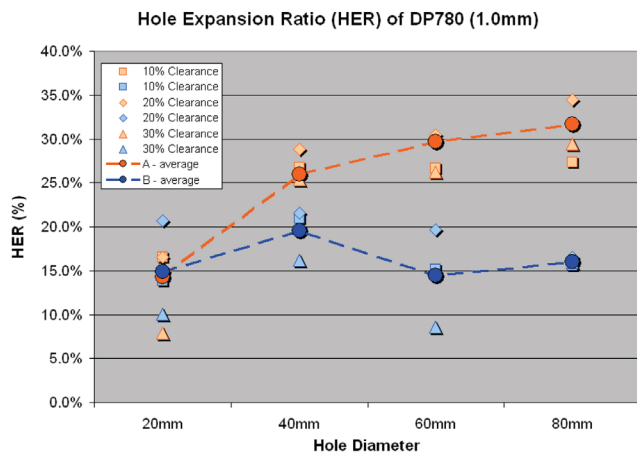
Figure 1. HER vs. Hole Diameter DP780 Samples
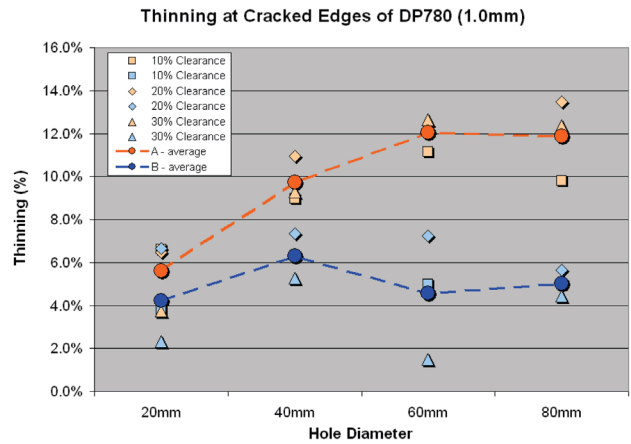
Figure 2. Thinning Limits vs. Hole Diameter DP780 Samples

The thinning limits of the cracks in the rolling direction (RD) and in the transverse direction (TD) are compared for DP780 samples and DP980 samples, as shown in Figure 3 and Figure 4, respectively. The thinning limit for cracks in the transverse direction is about 0.5% to 1% less than that of cracks in the rolling direction for the same steel.
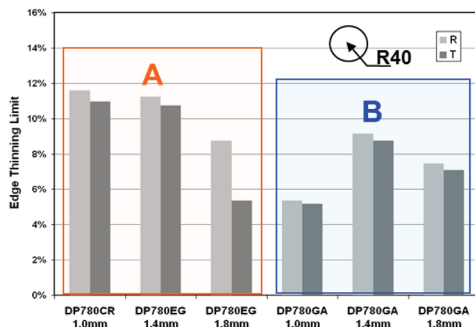
Figure 3. Edge Thinning Limit - DP780
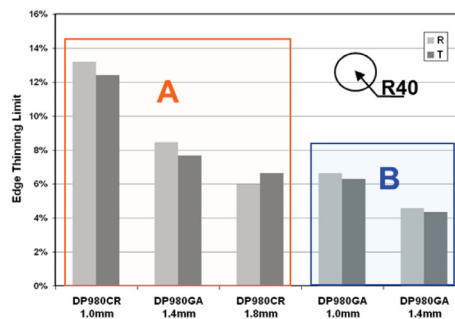
Figure 4. Edge Thinning Limit – DP980

Conclusions

- The edge thinning limit seems to increase with the hole diameters. It seems to be affected by the strain gradient during sample testing.

- No significant differences were observed in edge thinning in the rolling and transverse directions.

- A larger number of cracks in the sheared edge might cause the premature edge cracking of steel B.

- The edge cracking differences in steel A and B might be caused by the microstructures since their tensile properties are similar.

Task 1.2. Microstructure Study on Sheared Edge

The goal of this task is to analyze the root cause for edge fracture and provide physical observations from the sheared edge to final in-plane stretching fracture. The following approaches have been taken:

- Characterization of as-received sheets

- Characterization of sheared edges

- Characterization of stretched edges and cracks

- Provided physical insights and comparison of traditional fracture criteria (FLD) with observed fracture limits.

Analyses were conducted on a total of 280 samples before and after the hole expansion from Task-1.1.

Figure 5 illustrates the newly developed process to determine the metal flow lines of the shear-effected zone from the optical image of a section of the sample sheared edge. All sheared samples were sectioned in the RD & TD, etched, and the metal flow lines were traced.

Based on the metal flow lines of the sheared edge section, the effective strain distribution caused by a cutting process can be calculated. A Matlab computer program has been developed, Figure 6, to automatically calculate the distribution of all strain components. With a mouse click at any point, the strain will be displayed by the software.

MATLAB Image Processing

Tracing the lines

Fitting the lines

Differentiate the fitting curves

Obtaining angle for each point

Converting angle into effective strain

Obtaining the strain field

For small clearance, $u \approx 0$, $\frac{\partial u}{\partial x} = 0$

From volume=const., $\frac{\partial v}{\partial y} = 0$

$\frac{\partial v}{\partial x} = \tan \alpha = k$

by measuring flow line tilt angle Lagrangian strain $\mathbf{L}$ and True Strain $\mathbf{E}$ can be obtained:

$L_{xx} = \frac{1}{2}\left(\frac{\partial v}{\partial x}\right)^2 = 0.5k^2$

$L_{xy} = \frac{1}{2}\left(\frac{\partial v}{\partial x}\right) = 0.5k$
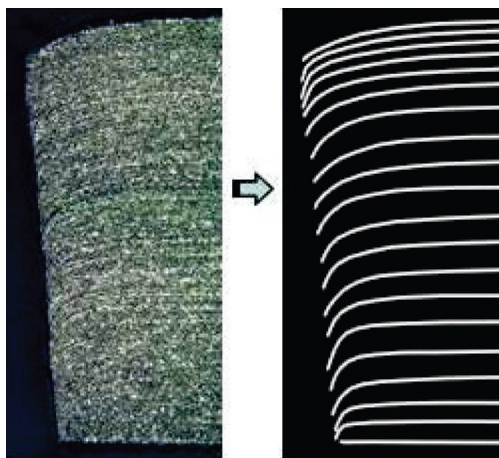
Figure 5. Strain Distribution of Shear-Effected Zone Obtained from the Optical Image
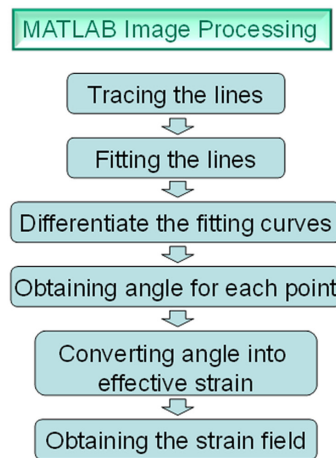
Figure 6. Flow-Chart of Matlab Strain Calculation Program and Mathematic Equations
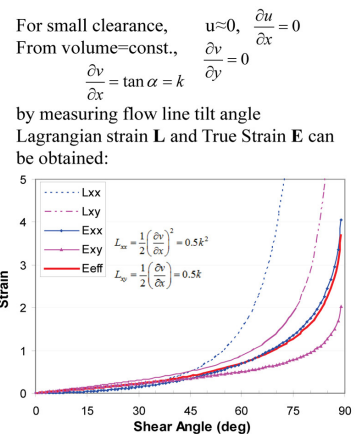
The effective strain distribution maps were generated for all samples. In order to analyze the hole dimension effects, the shear strain distribution maps and the maximum shear strain of the tested samples with different hole diameters were compared when other sample parameters were fixed. Figure 7 and Figure 8 show the effect of hole diameter on shear strain distribution and the maximum shear strain (marked value) of DP780 (GA, 1.4 mm) and DP980 (GA, 1.4 mm), respectively.
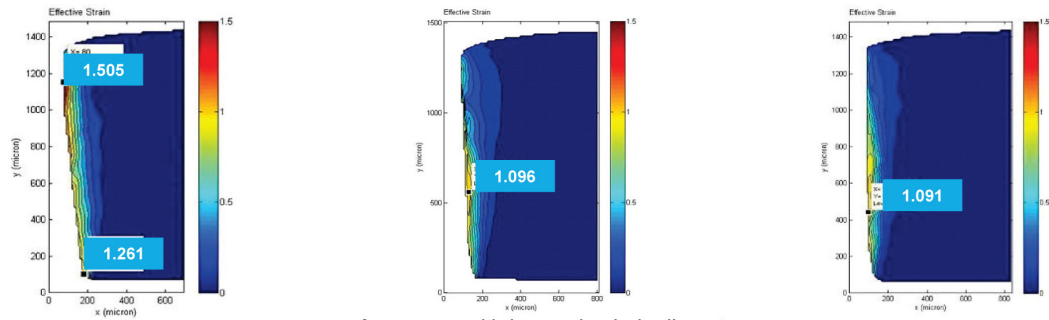
ε_max **decreases** with increasing hole diameter

Figure 7. The effect of hole diameter on shear strain distribution of DP780 Samples
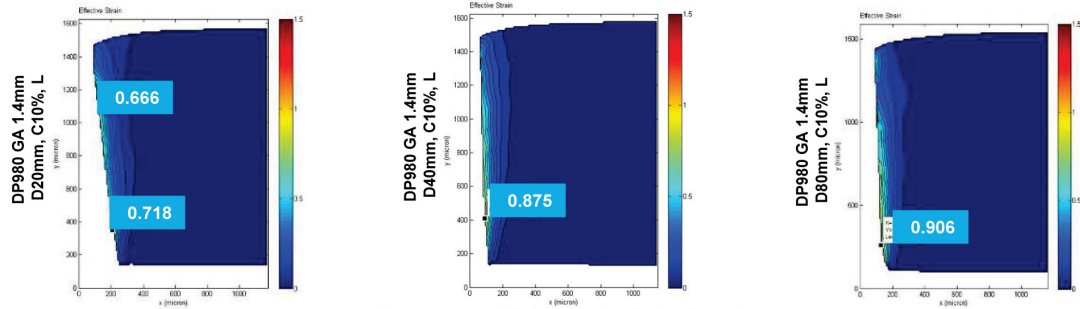
ε_max **increases** with increasing hole diameter

Figure 8. The effect of hole diameter on shear strain distribution of DP980 Samples

It can be noted that as the hole diameter increases, the position of the maximum shear strain moves down from the burnish/fracture area to the fracture/burr area. From the results of DP780 (GA, 1.4 mm) steel (Figure 7), it was found that the maximum shear strain on the section increases with increasing hole diameter; while the opposite was noted in the DP980 (GA 1.4 mm) results (Figure 8).

The effect of cutting clearance and the orientation of the steel samples on shear strain distribution were also evaluated (Figure 9).
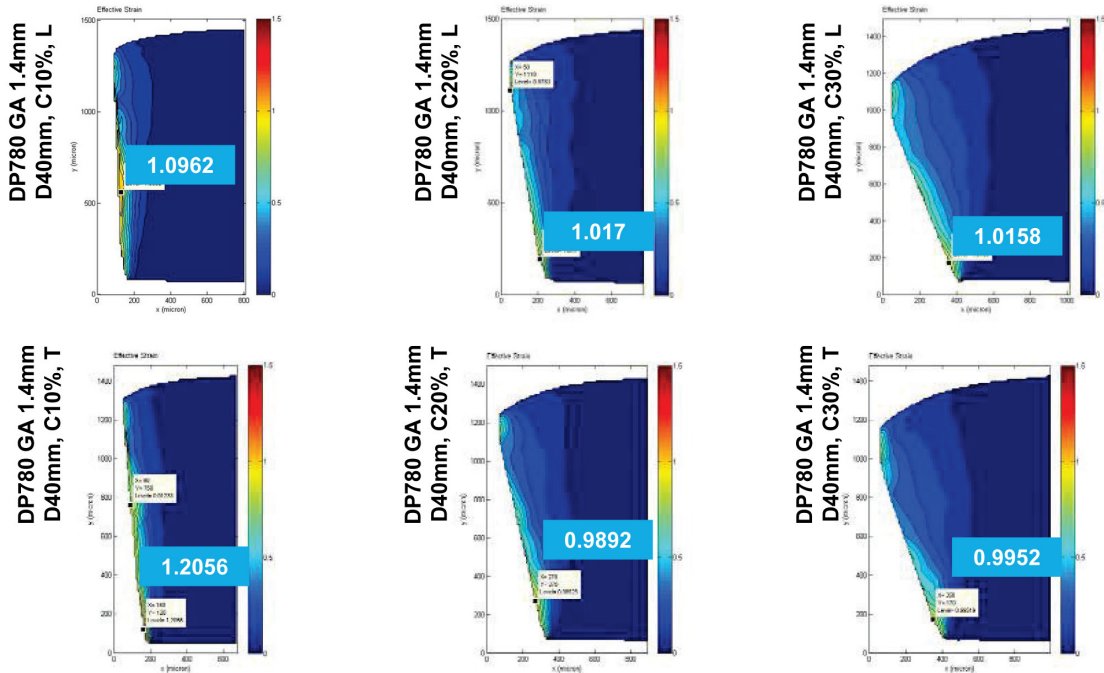
Figure 9. The effects of Cutting Clearance and Orientation on Shear Strain Distribution.

As the cutting clearance increases, the shear effected zone area increases and the maximum shear strain decreases.

No consistent trend is shown between the longitudinal and transverse directions.

Task 2. Numerical Simulation on a B-Pillar

The goal of this task is to evaluate the stamping CAE predictabilities of formability and springback for a B-Pillar and to provide recommendations on material modeling. LSDYNA was selected as the simulation package.

The formability prediction showed that this part can be formed with no splits but with severe wrinkles. The result correlates well with the DP980 tryout panels (Figure 10).
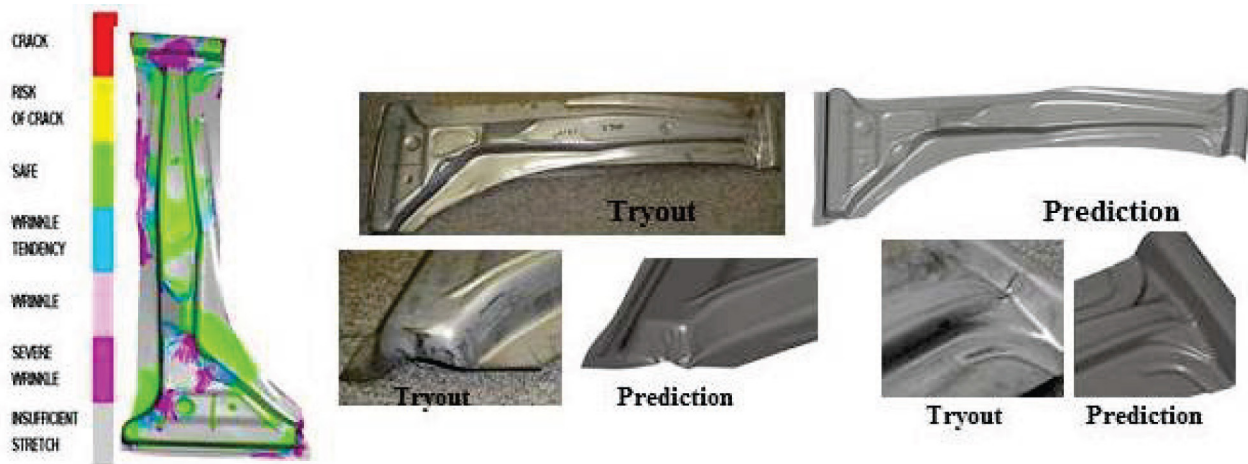
Figure 10. Formability Compression. No split was predicted but several wrinkles were predicted. The prediction agreed with the tryout panel.

The current springback simulation results suggest that the newly developed material hardening model (Yoshida) provides more accurate springback prediction for this part.

Task 3. Stamping Trial on Two Stamping Draw Dies to Evaluate Both Formability and Shear Fracture on the Newly Developed AHSS and 3G UHSS

B-Pillar experiments

The goal of this task is to evaluate both formability and edge cracking limits on two newly developed 980 MPa AHSS from different sources and one 3G, QP 980 MPa steel. The task was designed to evaluate the formability of each material, galling (sheet powder deposition) on the surface of the die from each material and the springback of each material.

The springback measurements were conducted on four panels of each tested steel type. The average deviations of the measured parts are shown in Figure 11. The average deviation for each part is the average deviation of all 45 measurement points of the part. There are 5 points for each section and 9 sections in each part, as illustrated in the right-upper corner of Figure 11.

The average deviations of all measured panels are in the range of 1.8 mm to 2.2 mm. The maximum deviation, 8.3 mm, was found in part M3#2 which is the 2nd trial panel of the steel provided by the #3 steel source. The results showed that:

- As expected, forming results varied from one material to another (three sources of materials)

- Springback results indicate that, with these materials, there are challenges in retaining the part shape.

- The overall magnitude of spring-back between materials is similar.

- The amount of spring-back on the same material varies from part to part. However, in some areas of the part, it is the same.

- The largest deviations in the part are due to side wall curl.

- Twist is also significant in the part.

- Although most coated materials had little or no galling (sheet powder deposition) galling, uncoated material performed well only in one case.

- Some steel makers provide DP980 sheet with favorable properties for draw forming.

- With proper geometry, complex parts can be made out of these newly developed 980 MPa steels.

Stamping Trial #2

Supplier	Material
M1	QP1000
M2	DP980/700Y
M3	DP980/700Y

Max = 8.3mm
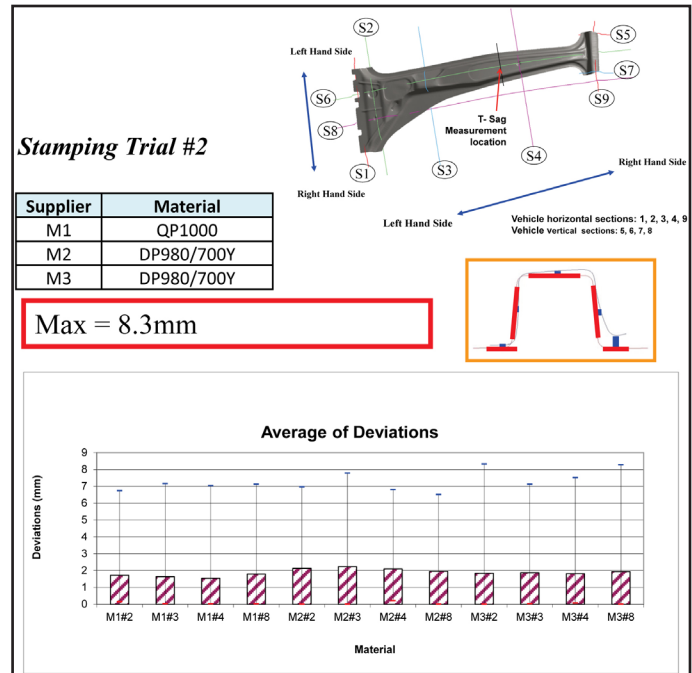
Figure 11. Springback Measurement Results – Average of Deviations

Straight Rail Experiments

A straight rail, from the straight portion of a channel (Figure 12), was selected to evaluate the stretch-bend-ability on the newly developed dual phase steels and one 3G Q&P 980 MPa steel. In past trials, no steel part with 980 MPa tensile strength was made from this die due to shear fracture along the beads on two sides of the part that was designed to reduce springback. The stamping trials were conducted with nine types of 980 MPa steels from 5 sources.

The results indicated that the rails with three of the nine steels were able to be formed without shear fracture.

Figure 13 shows one of the parts made of QP 980 MPa steel.

Figure 12. Straight Rail – Portion of a Channel

Mat	R-total	R-good	good ratio	T-total	T-good	good ratio
BQP	4	4	1.00	3	3	1.00

Figure 13. Straight Rail – QP 980

Task 4. Local Softening Technique Experiments and Evaluations on DP980 Steel

This project is seeking a low cost (vs. hot stamping) blank preparation process for cold stamping of parts with 1000MPa or higher tensile strength. Both Induction Heating and Laser Heating methods have been investigated.

• Results of Induction Heating: Local heating can be used to reduce the tensile strength and increase the elongation for the tested DP980 sheet steel. Both peak-temperature and cooling rate affect the grain coarsening with reduced elongation.

• Results of Laser Heating: Achieved 20% reduction in yield and tensile strength (Figure 14) and a 10% increase in total elongation. It was successfully demonstrated that a laser softening process can be applied locally to DP980 steel blanks in order to locally improve the material properties for stamping.

• The technology was successfully applied to the B-Pillar DP980 blanks for further production scale B-Pillar draw die trials (Figure 15).

• The computer simulation was conducted with the softened B-Pillar blank and the results show that the B-pillar can be made with the softened DP980 blank without formability issues (Figure 16).

• The B-Pillar draw die trials have been scheduled in early 2012.
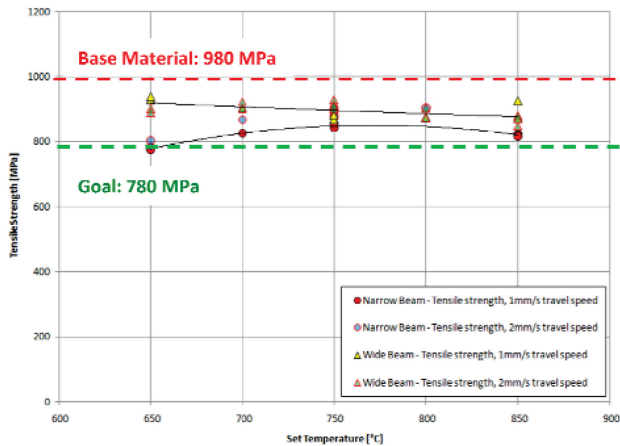
Figure 14. Strength of Softened DP980
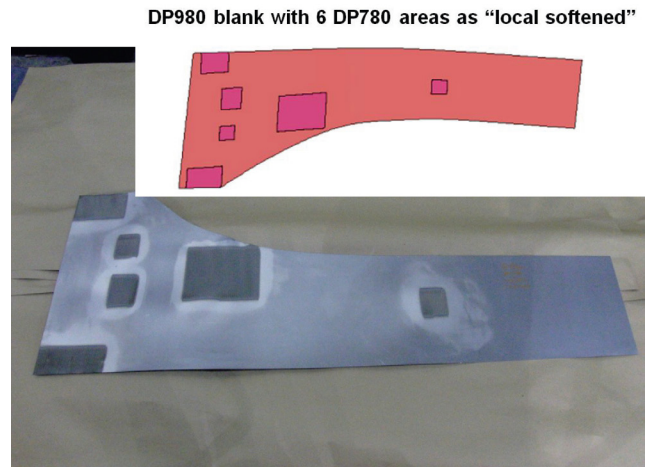
Figure 15. B-Pillar DP980 Blank with Local Softened Patches
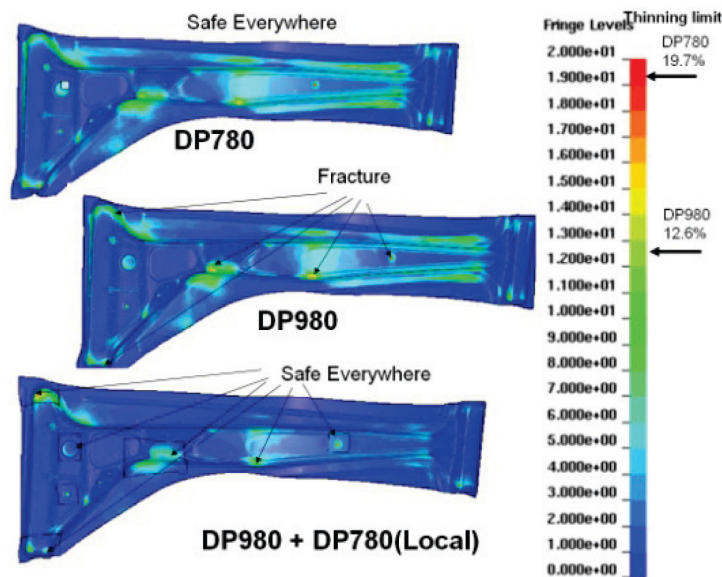
Figure 16. FE Prediction

Task 5. Large Size Cutout Edge Cracking Die Trial and Hole Expansion Test

The objective of this task is to develop AHSS sheet edge fracture criterion for stampings with large radius stretched features. Sets of Chrysler LLC, Edge-Cracking Experimental Dies were used (Figure 17).

Three newly developed 980 MPa steels, including 1 QP steel, 2 DP980 steels and one mild steel were selected for the experimental tasks; Mechanical properties of the 980 MPa steels were tested by GM and Chrysler Material Labs. Mild steels were tested by the steel maker; 34 panels were made; the edge thinning measurements were conducted.

Conclusions

- The experimental results indicated that the edge stretch thinning limit of these newly developed 980 MPa grade steels are about 2% to 3% higher than that of DP980 MPa steels tested two years ago.

- The edge stretch thinning limits were found in the range of 6% to 8.5%.

- There was no significant cutting clearance effect observed on the edge stretch thinning limit from the tested samples with cutting clearances from 5% to 15%.

- The edge cracking criteria for the tested materials will be developed by individual Automotive OEMs.

Forming Die Design:
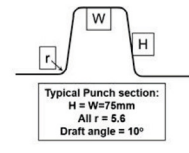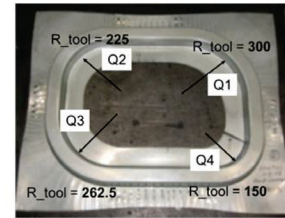
Baseline sheet thickness T_0=1.47mm
Draw die binder force: 1200psi, 16cylinders
Cutting clearance 5%, 10%, 15%, 20% & 25%

Blanking Die Design:
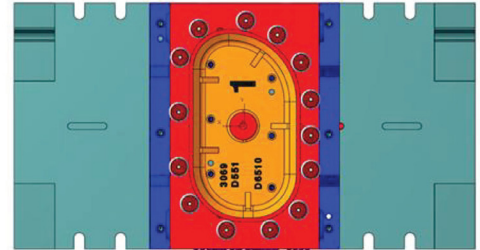
14 Polyurethane Spring:
OD = 60 mm, ID = 14 mm, Compress 20 mm, Total holding force = 22.4 ton

Figure 17. Edge Cracking Draw Panel and Blanking Die Design

Task 6. Stretch Test with Digital Image Correlation (DIC) Strain History Measurement Method on the Pre-Formed Coupons

The purpose of this task is to evaluate the pre-form effects on edge stretch ability. The following approaches were taken: 1) Build Lab tool to create preform shape on steel coupons; 2) Tension test to simulate edge stretching (Figure 18); 3) DIC measure strain (Figure 19); and 4) FEA simulations.
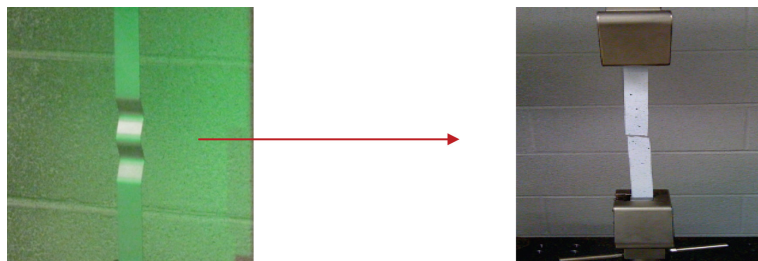
Figure 18. From pre-formed strip until fracture
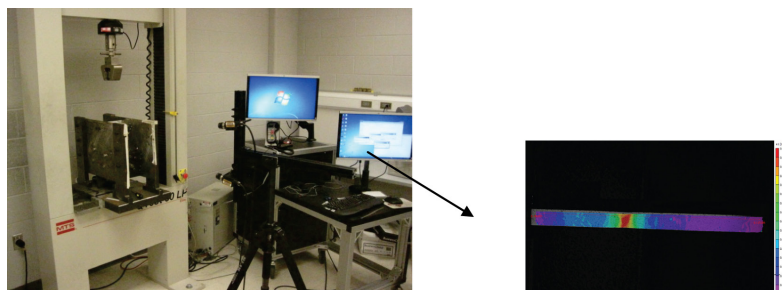
Figure 19. DIC strain measurement equipment and results

Five grades of AHSS with three different scallop profiles were tensile tested from the pre-forming stage until fracture. The summary of fracture location and critical passing profile are defined in Table 1.

Table 1. Fracture location (inside – outside pre-form zone) for each material and orientation from 3 defined pre-form profiles

Material (+ direction)	Profile 1: Fracture Outside preform Inside preform	Profile 2: Fracture Outside preform Inside preform	Profile 3: Fracture Outside preform Inside preform
590 R (Rolling)	Inside	Inside	Inside
590 R (Transverse)	Outside	Inside	Inside
DP 780 (Rolling)	Outside	Outside	Inside
DP 780 (Transverse)	Outside	Outside	Outside
DP 980 (Rolling)	Outside	Outside	Outside
DP 980 (Transverse)	Outside	Outside	Outside
HSLA 50 (Rolling)	Inside	Inside	Inside
HSLA 50 (Transverse)	Outside	Outside	Outside
Q&P 980 (Rolling)	Outside	Outside	Outside
Q&P 980 (Transverse)	Outside	Outside	Outside

From Table 1, it can be noted that:

- Fracture inside the pre-formed area for at least 2 of the 3 scallop profiles were observed in the 590R (rolling), 590R (transverse) and HSLA 50 (rolling) samples.

- The fracture outside the pre-formed area was observed in most tests of DP780, DP980, and Q&P 980 steels, except Profile 3 DP780 (rolling).

The following conclusions were reached during the first three approaches.

- The pre-form process induces the reduction of the edge stretch-ability of 590 and HSLA 50 steels.

- The pre-form process does not affect the edge stretch-ability of DP980 and Q&P 980 steels.

- The pre-form process has minimum effect on the edge stretch-ability of DP780 steels.

FEA simulation

FEA simulations on the pre-forming followed by stretching were conducted to validate the modeling techniques for more accurate prediction.

Figure 20 shows the comparisons of tensile strain distributions along the center line of the sample by DIC measurement and FEA simulation with different solution methods and material models.
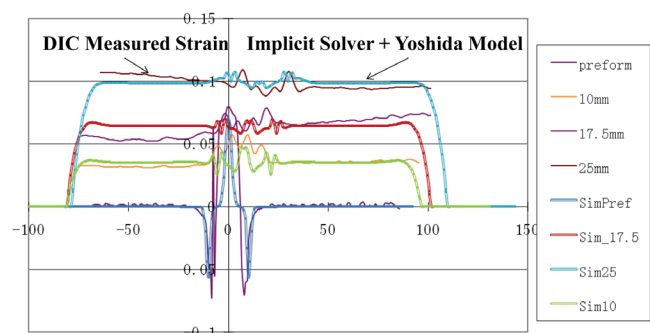
Figure 20. FEA Simulation Results vs. DIC Measurements – Surface Tensile Strain

It was found that only the implicit method with the modified Yoshida model (isotropic/kinematic hardening model) can predict the bending/unbending strains well. Isotropic hardening and the explicit method under-predict the bending strains.

Task 7. An experimental stamping die deflection measurement

The objective of this task was to measure DP980 die deflection during the stamping process to provide real experimental data for FEA simulation verification, correlation, and enhancement.

The approach was to conduct DP980 B-Pillar stamping trials at a die shop and perform the Dynamic Die Deflection measurements with High-speed 3D Photogrammetry (PONTOS) as shown in Figure 21a and Figure 21b.

Figure 21a. Measurement System – Pontos

Figure 21b. Pontos with High speed cameras

Using the PONTOS system with high speed cameras, coordinate points (targets on die surfaces), as shown in Figure 22, throughout the full cycle of the press were tracked. This enabled the system to measure the deflection of various die components - lower shoe, upper shoe, and binder. When the PONTOS system is used, the images can be gathered to isolate the movement of each component in relation to other components.

Figure 23 shows the dynamic motion of three points on the lower die shoe (red lines in Figure 22) during the full cycle of the press. The point of interest is at the bottom of the stroke, as indicated by the arrow in Figure 23 where the majority of deflection occurs. The locations of the three points (left, center, and right) at the bottom of the stroke and a static base line were used to calculate the maximum deflection of this component, Figure 24.

Figure 22. Targets on Die Surfaces

Figure 23. Measured dynamic motions of three points on the lower die shoe
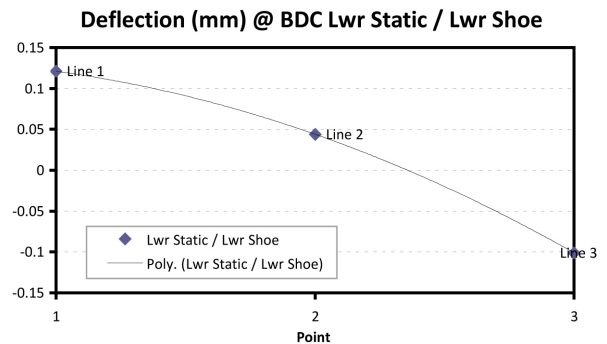
Figure 24. Lower Die Shoe Deflection

Conclusions

- The die behaves similarly from front to back, but differently internally and on the side of the press.

- The maximum die deflection is almost 2.0mm.

- The stamping trial process and the measurements are consistent throughout the entire test.

- The measurement data will be used as references for FEA correlation – Future work.

Technology Transfer Path

- Project Technical Review Meetings will be held at all member companies.

- The experimental results, findings, empirical criterion, case study data sets, and computer modeling, have been received by all member companies.

- The applicable criteria have been developed upon OEMs' needs.

- As planned, the results of this project will be documented in CDs, and presented in Great Designs in Steel (Spring 2012), SAE and NADDRG.

Nonlinear Strain Paths (A/SP-061)

Principal Investigator: Z. Cedric Xia, Ph.D.; Ford Motor Company
(313) 845-2322; e-mail: zxia@ford.com

Principal Investigator: Thomas B. Stoughton, Ph.D.; General Motors Company
(586) 986-0630; e-mail: thomas.b.stoughton@gm.com

Principal Investigator: Changqing Du, Ph.D.; Chrysler Group LLC
(248) 576-5197; e-mail: CD4@chrysler.com

Accomplishments

- Developed a comprehensive database of orientation-dependent uni-axial tension behavior for yield, transient hardening and fracture with uni-axial and equi-biaxial pre-straining.

- Developed a comprehensive database of orientation-dependent bake-hardening behavior for yield, transient hardening and fracture with uni-axial and equi-biaxial pre-straining.

- Developed a limited database of forming limits with uniaxial, equi-biaxial, and general bi-axial pre-straining under continuous loading and unloading conditions.

- Produced a preliminary evaluation of advanced material models for transient hardening, forming limits and fracture.

- Developed a guideline for industrial applications and a recommendation of future model development for AHSS.

Future Direction

The A/SP plans to continue this work in a direct funded (automotive OEMs and steel companies) project.

- Target: Develop the ability to precisely identify, quantify and simulate the cumulative effects of the forming, heat treatment and coating processes on material properties and component performance experienced in the automotive stamping and manufacturing processes and to add to existing databases to improve computer modeling and simulation software for AHSS.

- Gap: Current product performance simulations using commercial FE design packages for formability and crashworthiness generally assume that the vehicle body parts have no prior strain history at the start of the simulation with a uniform thickness for a given part. For more accurate prediction and correlations of design intent to product manufacturing and performance, it is critical to incorporate prior manufacturing effects such as forming and bake-hardening into product performance simulations with more reliable constitutive and fracture models so that the full potential of lightweighting can be realized.

Introduction

The Nonlinear Strain Paths (NSP) project aims to increase fundamental understanding and deliver a comprehensive set of experimental data and associated predictive models for Advanced High Strength Steels (AHSS) under nonlinear strain path deformations. The models include constitutive behavior, forming limit and fracture criteria for stamping/hydroforming simulations and vehicle crashworthiness simulations. The materials of focus are Dual Phase (DP) DP600 and DP780 grades, with Deep Drawing Quality (DDQ) and Bake Hardenable (BH) BH210 grades as baseline comparisons. Exploratory work will also be done on DP980 and TRansformation Induced Plasticity (TRIP) TRIP780 grades. The developed and validated models will (1) enable efficient vehicle design for more weight reduction opportunities to take advantage of the rapid hardening behavior of AHSS; and (2) enable the acceleration of AHSS usage by reducing the cost and time for AHSS manufacturing engineering.

Approach

The collaborating partners include Chrysler Group LLC, Ford Motor Company, General Motors Company, AK Steel, ArcelorMittal, Severstal NA, ThyssenKrupp, and US Steel. The partners were supported by up to a dozen test laboratories, finite element modeling (FEM) software vendors, and stamping technology vendors. The project team also includes experimental researchers and metallurgists at the National Institute of Standards and Technology (NIST).

The approach was to conduct experiments under nonlinear deformation conditions to characterize the strain phenomena in AHSS sheet and to identify the gaps between prediction and experiment. The team then quantified the effect under representative experimental variations of deformation conditions encountered through the life of automotive sheet metal products from the stamping plant to the vehicle service. Experimental data collection tasks took advantage of recent advances in Digital Image Correlation (DIC) technology, an optical method that employs tracking and image registration techniques for accurate 2D and 3D measurements of deformations, displacement, and strain from the digital images. Based on the correlation results, the project identified the best available advanced constitutive, forming limits and fracture models applicable to nonlinear deformation of sheet steels. The best models from the validation will be implemented in production software for stamping and crashworthiness.

Results and Discussion

The two year project was kicked off on September 29, 2009 and completed all technical work on September 30, 2011. The team developed a consensus test matrix addressing the boundaries encompassing both crash and formability applications of the strain data and drafted a consensus technical specification for tensile testing of six grades of AHSS using the DIC apparatus. Specifications were also developed using consensus best practices for DIC data acquisition and detailed data analysis. A second supporting experimental plan was developed for temperature-dependent strain testing.

Task 1. Transient Strain Hardening under Nonlinear Strain Paths

The objective of this task was to deliver a comprehensive set of experimental data and identify predictive models for the AHSS under nonlinear strain path deformations. The models include constitutive behavior, localized necking and fracture criteria for stamping and vehicle crashworthiness simulations. The task evaluated the following:

- 6 Advanced High Strength Steel Grades: DDQ, BH210, DP600, DP780, DP980, and TRIP780.

- 3 Pre-strain Orientations: Rolling, Transverse, Diagonal directions.

- 7 Pre-strain Levels:

    - uni-axial: 0%, 5%, 10%, 15%, 20%

    - Equi-biaxial: 5%, 10%.

- 7 Subsequent Tensile Orientations (relative to pre-straining orientation): 00, 150, 300, 450, 600, 750, 900 (Figure 25).
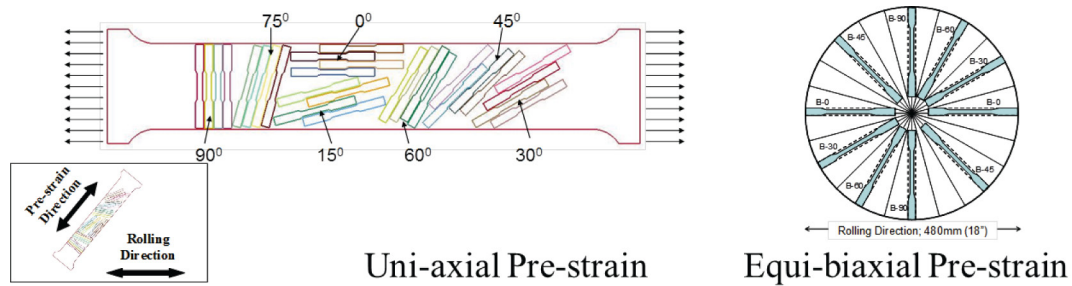
Figure 25. Cut patterns used to obtain desired orientations of tensile specimens in 15 degree increments after prestrain of the metal in uniaxial tension or equal-biaxial tension. These specimens provided information on the nature of transient hardening behavior under discontinuous strain paths.

Task 2. Forming Limits under Nonlinear Strain Paths

The objective of this task was to conduct experimental laboratory draw die trials to evaluate the impact of nonlinear strain paths on forming limits. This was done by first conducting forming simulations to prove the selected draw die process, evaluate the required forming tonnage, and confirm the die face geometry for achieving nonlinear strain path at the fracture zones. Secondly a draw die (see Figure 26) was constructed based on the forming simulations and die trials conducted using TRIP 780 steel with Digital Image Correlation (DIC). Lastly, the results from the die trial were compared against the simulation and the simulation modified to reflect observed behavior.
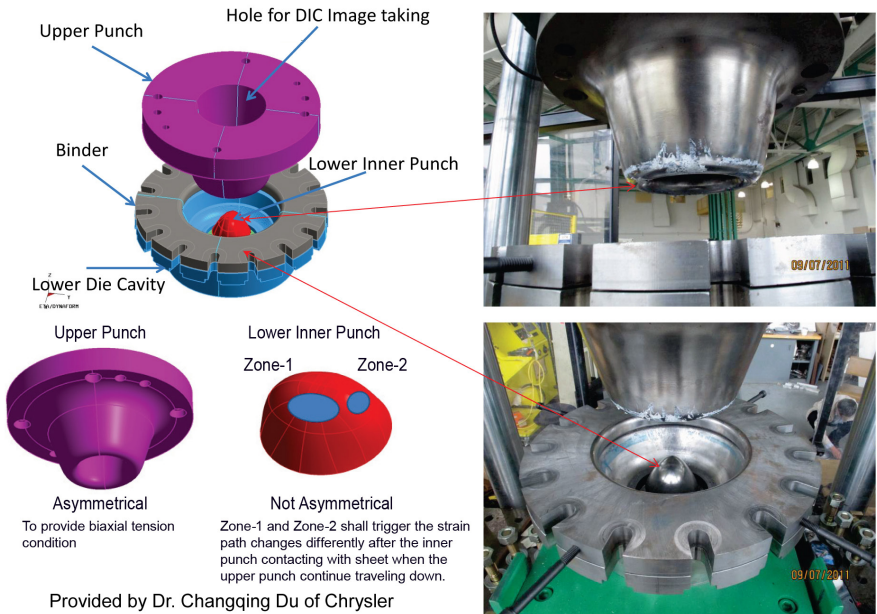
Provided by Dr. Changqing Du of Chrysler

Figure 26. Experimental Die with Digital Image Correlation to Evaluate Nonlinear Strain Path Deformation

Task 3 Bake Hardening under Nonlinear Strain Paths

The objective of this activity was to better understand material bake-hardening behavior when the deformation path is not aligned with the prior path before bake-hardening through lab-controlled testing. Sheet steels are subject to biaxial deformation during stamping and BH, DP, and TRIP grades get bake-hardened in the paint shop. The deformation paths during crash or denting will be different from the ones experienced in forming. The team plans to develop anisotropic bake-hardening models (to be done in 2012), which will be correlated with experimental data using the test matrix outlined below, and then implemented in simulation software.

- 3 Steel Grades: BH210, DP600, TRIP780

- 3 Pre-strain Orientations: Rolling, Transverse, Diagonal directions.

- Pre-strain Levels:

  - uni-axial: 2%, 5%

  - Equi-biaxial: 2% each direction

- 7 Subsequent Tensile Orientation (relative to pre-straining orientation): 00, 150, 300, 450, 600, 750, 900.

Task 4. Advanced Fracture Modes Under Nonlinear Strain Paths

The objective of this task was to develop, validate, and implement a physics-based Fracture Model applicable to FEA simulation that can predict the effect of the trim process on the trim edge condition and predict the subsequent formability of the trimmed edge. Working with the Massachusetts Institute of Technology, the team significantly advanced this work laying the foundation for development of more advanced fracture model(s) to include consideration of material anisotropy, strain-rate, temperature, and more complex deformation histories, including combined manufacturing and product performance.

Technology Transfer Path

Computer modeling and simulation software used by the OEMs has already adopted some of the results of this project. Analysis of the results will continue for some time after project completion and will be implemented as appropriate. Automotive OEMs will implement the findings from this project by importing applicable data into OEM material and process standards, which will guide material and process selection for the designing and engineering of advanced high strength steels.

Conclusions

The project has completed all technical work and is currently preparing the final report. The work conducted during the course of this project has improved comprehensive databases and material models for transient hardening, bake-hardening, forming limits, and fracture.

Mapping of Forming Effects to Structural Models (A/SP-390)

Principal Investigator: Raj Sohmshetty, Ford Motor Company
(313)317-9035; email: rsohmshe@ford.com

Accomplishments

- A baseline vehicle model from the A/SP Light Weight Front End project was selected to study the forming effects on structural analysis. Major components in the vehicle model were selected for consideration of forming effects based on strain energy absorptions in frontal impact and forming severities.

- Forming strain and thickness distributions of the selected components were obtained using the approaches of one step forming analysis, incremental forming analysis and rule-of-thumb.

- A systematic approach was developed to map the forming results to the vehicle structural model.

- Frontal impact analyses were conducted on the vehicle model incorporated with various forming strains.

- The impact analysis results indicate that there exists the potential for weight reductions if the forming effect is taken into account when the impact performances are considered.

Future Directions

- Optimization study to assess weight saving opportunities when forming effects are included in the impact analysis

- Identification of the most appropriate approach for consideration of the forming effects in the structural models

- Investigation of forming effects on the impact analysis accuracy as compared with the test data.

Technology Assessment

- Target

  - Define the minimum accuracy required for mapping the forming effects to structural models to provide good accuracy in dynamic deformation during the crash modeling phase.

  - Provide specifications to develop automotive product development cycle compatible software tools and processes to incorporate forming effects into structural crash models.

- Gap

  - The structural design and analysis community requires a robust and simple software tool to rapidly perform forming analyses and map the strains and thickness distribution to product attribute models.

  - Some forming effects mapping software tools are available, but are too cumbersome to be practical in routine design and structural analysis activities.

  - Generating forming simulation data takes too much time and expertise.

  - Often detailed manufacturing process data is not available during the early design phase.

Introduction

Automotive body structural design and engineering analysis experts report that crash models run with high AHSS content typically under-predict vehicle crash performance, causing them to over-design structures and add more weight than needed to achieve acceptable performance. This under-prediction effect is assumed to be caused by not including forming strain, work hardening, and thinning effects in the crash model.

While methods are available to perform forming simulations prior to running crash models and map the resulting thicknesses and flow stresses into the crash model, the process is not automated and is too time consuming to be used practically in the crashworthiness design and modeling phase. This project defines a minimum requirement for forming model accuracy and direct and validate subsequent efforts by the commercial software development community to develop automatic forming strain assessment and mapping tools to permit rapid treatment of forming effects in crash models. This approach has the potential to save up to 10% weight in some cases.

Approach

The vehicle model from the A/SP Light Weight Front End project was used in the study. No physical testing is planned for the project. Due to the limited availability of the vehicle test data, comparisons are conducted among the results in the following scenarios to determine the forming effects on the crash analysis:

- Analysis with the virgin materials

- Analysis with mapped incremental forming analysis

- Analysis with mapped one step forming analysis

- Analysis with one step forming strains mapped and incremental strains mapped for limited   components not suited for one step analysis

- Analysis with uniform forming strains

Results and Discussions

A total of 36 components (55% high strength steels) were selected from the vehicle model for inclusion of forming effects based on the rankings of strain energy absorptions (about 60% of the total plastic strain energy of the vehicle) and strain energy densities from frontal impact analysis, and also forming severities.

One step forming analysis for each selected component was conducted assuming various forming scenarios including zero, low, high, optimal and combined binder forces.

Draw developments were conducted for each of the selected components for incremental forming analysis. The forming effects only due to the first drawing process are considered. Forming results due to the secondary processes, such as preforming, flanging, piercing, re-striking, and cam forming are ignored.

Comparisons between the incremental and the one step forming analysis results indicate that the one step forming analysis captures the forming modes very well. Comparisons between the incremental and the mapped incremental forming results indicate the mapping procedure from the forming model to the structural model works well with high accuracy.

A rule of thumb approach was also employed to specify the uniform strains for the selected components. The impact mode is similar to the ones with forming effects by one step and incremental forming analysis approaches.

Front impact results of B-pillar acceleration pulses, steering column, and A-pillar intrusion with forming strains obtained by various forming analysis approaches indicate that:

- The inclusion of the forming effects may increase the B-Pillar accelerations by about 7G (20%) and reduce the steering column intrusion by about 80mm (13%).

- There is potential for weight reductions if the forming effect is taken into account when the impact performances are in considered.

- A simple rule of thumb uniform strain specification may provide a direction on the effect of forming at an early design stage.

- There is potential for weight reductions if the forming effect is taken into account when the impact performances are considered.

- There are large discrepancies between the impact analysis and the test data.

Technology Transfer Path

Detailed results from this project were provided to the project participants. Forming strain analysis guidelines to be transferred to willing Commercial Software Development partners. Enhanced forming strain analysis and mapping software to be developed at the Commercial Software Vendors own cost and distributed to interested OEM and Steel companies through their existing software marketing channels.

Conclusions

The A/SP Light Weight Front End vehicle model was employed to study the forming effects on front impact analysis. A total of 36 major components, 55% of which are high strength steels, were selected for inclusion of forming effects based on the rankings of the strain energy absorptions and energy densities from the baseline frontal impact analysis and forming severity. The thickness and plastic strains of each component are estimated based on the one step and the incremental forming analyses, and a rule of thumb uniform strain approach. A procedure was developed to incorporate the material thickness and plastic strains in the structural model. The results indicate that there is potential for weight reductions if the forming effect is taken into account when the impact performances are considered.

Stamping Tooling Optimization (A/SP-360)

Principal Investigator: Don Adamski, General Motors Company
(586) 596-2533; e-mail: Donald.j.adamski@gm.com

Accomplishments

- The Coating Fatigue task, which tested five insert steels, with and without ion nitriding, and coated with physical vapor deposited (PVD) CrN coatings, is complete. The project completed the 100,000 hit die trial on DP-980 with no insert failures.

- The completed coating fatigue study provided improved understanding of the complex relationship between the coating, steel substrate, and interface under applied impact and sliding forces. The results contribute to a growing database, which will eventually serve as a basis for computer modeling and simulation, but in the short term guides OEMs in appropriate insert steel and coating selection for stamping Advanced High Strength Steel (AHSS.)

- This coating fatigue testing revealed that duplex coatings (physical vapor deposition on top of ion nitriding) have equivalent durability as coatings deposited via chemical vapor deposition (CVD). Duplex coatings can be applied to tool steels at lower cost and induce less distortion than CVD coatings thereby improving tool life and enabling the forming of AHSS in high volume automotive applications.

- The die trial is complete with analysis on-going. Although designed to be aggressive and induce insert failure, all inserts lasted the full 100,000 hit trial, which exceeded expectations. This experience has increased OEM confidence in their ability to form, pierce and trim AHSS and in selecting durable insert steels and coatings.

Future Direction

The Auto/Steel Partnership (A/SP) plans to fund Phase 2 of this project.

Technology Assessment

- Target: Identify and define tests that provide a quantitative assessment of die inserts and coating technologies to enable the optimized selection of the appropriate insert steel, heat treatment and coatings for AHSS.

- Gap: Implementation of AHSS has been impeded by the high cost of tooling and the lack of knowledge on the performance of insert steel, surface treatment, and coatings for high volume stamping.

Introduction

The ability to fully realize the benefits of AHSS depends upon the ability to aggressively form, trim, and pierce these steels into challenging parts. Earlier work from the A/SP-230 Tribology Project developed a coating fatigue test that showed promising results. This test is now being adopted by the coating industry as a means of assessing insert surface treatment and coating performance. This project builds upon this work to evaluate whether surface treatment could extend the performance of PVD coatings.

The Tribology project also revealed that edge chipping, and not wear, was a dominant failure mode of trim inserts at uphill angles above 20°. This project utilized this information to develop a new test to quantify insert performance with respect to the edge chipping and to design a new die for subsequent die trials. The objective of the die trials is to 1) compare insert performance of the same design under the same loading conditions by stamping 100,000 parts and 2) provide samples for analysis and validate the edge chipping test.

Approach

Task 1. Coating Fatigue

The coating fatigue test was developed during the A/SP-230 Tribology project (Figure 27) and used to test and evaluate the cyclical impact and sliding fatigue performance of the coated specimens. Prior to this test, there was no effective means of assessing supplier and insert performance without expensive component manufacturing trials where poor performance could result in significant cost. The complex relationship between the substrate, coating and interface under typical stamping loading conditions is well captured by this test where specific variables can be evaluated for their effect on insert durability. In this study, the effect of surface treatment, specifically nitriding, on PVD and CVD coatings was emphasized.
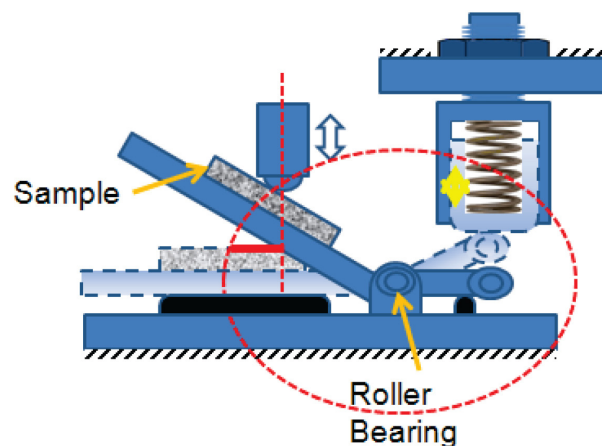
Figure 27. Coating Impact-Sliding Fatigue Test Phase II Apparatus.

The Coating Fatigue Test matrix consists of five substrates, two surface treatments and five coating suppliers (see list below). Each sample was evaluated for coating fatigue cracks, cohesive failures (chipping and peeling), and adhesive failures (sheet material transfer). The results of this study are expected to guide future AHSS stamping part/die design, die material, heat treat, and coating selection for stamping of AHSS.

- Substrates

  - Carmo

  - AISI-D2

  - AISI-4140

  - Cast Cut #1

  - NAAMS-D6510

- Substrate Treatments

  - Plasma Nitride

  - Philos Titanium Diffusion

- PVD CrN Coating

Coating Suppliers: Phygen, IonBond, Richter, Oerlikon, and Eifeler-Lafer (randomly assigned letters A, B, C, D, and E)

Task 2. A/SP-360 Die Trial

The objective of the die trial is to determine the optimal die materials, surface treatments, and designs for stamping AHSS, in this case DP980 steel, with regards to durability and cost effectiveness. To provide an effective comparison between the different conditions, the tool geometry had to be sufficiently aggressive to generate early failures. The progressive die use in the A/SP-230 Tribology project was modified to include an aggressive 20° uphill angle trim inserts with the purpose of generating insert failures within 100,000 hits, which would enable a quantifiable comparison of insert performance based on the number of hits. The project developed a test matrix, which lists the substrate steel, heat treatment, coating, tool geometry, and expected failure mode for trim, flange, and pierce inserts to be evaluated.

For trim steels, the expected failure mode depended upon tool geometry and could be wear, edge chipping or a combination of both. The A/SP-230 Tribology project demonstrated that edge chipping was the dominant failure mode when the angle of the tool exceeded 20° and wear was dominant under 20°. The Stamping Tooling Optimization matrix includes uncoated 0° and 20° paired inserts (where the material and heat treatment are the same) to capture both failure modes. Surface wear is the expected failure mode for the flange and pierce inserts. To capture the wear information, the 0° trim and flange inserts were measured using a hand held profilometer and impression records of each tool insert were made. However, due to project timing and funding, only qualitative wear measurements will be performed.

A study was initiated on edge chipping using digital image processing. The team postulated that tool durability could be quantitatively assessed by measuring the volume of material lost as a function of the number of hits. Figure 28 depicts how mass loss could be estimated from digital imaging.
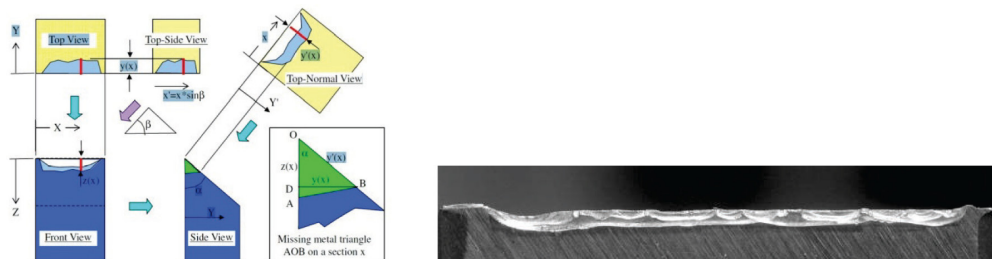
Figure 28. Edge Chipping Study (left) as applied to a chipped tool insert (right)

Results and Discussion

Task 1. Coating Fatigue

The study concluded the following:

Non-nitrided substrates except AISI-D2 were not strong enough to support the CrN coatings for applications in very high impact-sliding contact stress conditions.

1. AISI-D2 is the best substrate for CrN coatings if the nitriding process is not included in die materials preparation.

2. Plasma nitriding significantly increased the coating performance for all the substrates.

3. Plasma nitriding can make Carmo steel even better than D2 as the substrate for CrN coatings to resist impact and sliding forces.

4. The nitrided Cast Cut #1 also performed well. AISI-4140 and NAAMS-D6510 steels did not perform well with and without plasma nitriding process treatments.

Of particular benefit was the finding that duplex CrN coatings (nitriding coupled with PVD) can perform as well as CrN CVD coatings. Since PVD coatings are applied at lower temperature than CVD, the duplex coatings distort less, which improves insert life thereby yielding a lower cost more durable coating system.

Task 2. A/SP-360 Die Trial

- *Edge Chipping Study*
  Trim inserts from the A/SP-230 Tribology project that exhibited edge chipping were given to Wayne State University to perform optical measurements. Digital image processing was employed to estimate the volume of mass lost on the tool inserts. Figure 29 shows the results for the tool inserts provided, which were sufficiently credible to justify future work. The project had insufficient funds and time to include this work as part of the current die trial and has deferred this work to future programs.

- *Die Trial*
  The die trial was completed in October with results pending analysis. All inserts lasted the full 100,000 hit trial, which was unexpected considering that this trial tested DP980 steel whereas the A/SP-230 Tribology trial tested lower strength DP-780. Preliminary observations are listed below.

Figure 29. Edge Chipping Study Results

1. In the absence of trim insert failure, an edge chipping study will be the only means of quantifying insert performance.

2. Duplex coatings performed very well and a more aggressive die design and set up is necessary to evaluate performance.

Technology Transfer Path

The automotive OEMs will implement the findings from the coating fatigue and die trial studies by importing applicable data into OEM material and process standards, which will guide material, heat treat, and coating selection for the forming of advanced high strength steels.

Conclusions

1. The Coating Fatigue Test is a cost effective test tool from which part/die standards can be continuously improved. The results from these tests are already being implemented at automotive OEMs and their continuous improvements are critical to the successful application of AHSS.

2. The die chipping study was sufficiently credible to justify inclusion in a future A/SP project. This work is expected to drive more fundamental research into the root cause of die chipping as a function of steel substrate material and heat treatment and greatly improve our manufacturing knowledge on how to build a successful stamping die.

Joining Knowledge Management Phase 1 (A/SP-370)

Principal Investigator: Joe Beckham, Chrysler LLC
(248) 512-6498; email: joe.beckham@chrysler.com

Accomplishments

- Delivered phase I system with adequate user functions (FY 2011).

- Populated phase I system with data from A/SP Joint Efficiency project (FY 2011).

Future Directions

- A Phase II Joining Knowledge Management project has been approved for 2012 funding by the A/SP.

- Populate the database with all previous A/SP welding data

- Enhance user functions to accommodate a wide range of data and knowledge rules

- Develop and upgrade to web-based system

Technology Assessment

- Target: Demonstrate adequate user functions for managing material joining data and knowledge. Provide users with easy access to welding knowledge so that new steel grades can be used in designs more effectively and in a timely manner.

Introduction

In pursuing opportunities to utilize lightweight materials in vehicle production, engineers at OEMs and suppliers are constantly searching for technical data, knowledge, and related tools that help them understand the design criteria, welding/joining process technologies, and performance of components welded with AHSS or other lightweight materials.

Presently, in order to propose, validate, and approve AHSS or other light weight material utilization in vehicle production, engineers need to extract relevant and useful technical information from many logically unrelated sources of data and knowledge related to base material properties, welding process, joint performance, etc. The current practice is inefficient, ineffective, inhibits rapid knowledge transfer, and utilization of new technological development in AHSS joining.

Approach

This project is the first phase of a two-phase project that develops and implements a Joining Knowledge Management system to:

- Accumulate and organize existing welding data

- Accelerate knowledge transfer through efficient and effective use of data

- Build and grow welding knowledge rule base

Since the phase I system focuses on developing and reviewing user functions, a desktop based application was developed. With the intention to migrate the system to a web based system, a separated SQL CE database was also developed to work with the front end of the application. The phase II project will include work to deploy the system to a web-based architecture. The application is written with Microsoft Visual Studio Visual Basic.

Results and Discussion

Only key user functions delivered in phase I system are illustrated in the following discussions and screenshots. Complete user function details can be found in detailed project report.

- Joining data search interface allows users to search data by category, component name, joint configuration, process name, steel grade, steel gauge, and coating conditions.

- Retrieved data records are organized and presented in a tab control structure. These details include project information, base metal grade/gauge/coating, component images, welding process image and welding process details, static properties of joints, and cross-section photos of joints, fatigue performance of joints, specifications, and reports. A screenshot of this function is shown in Figure 30.
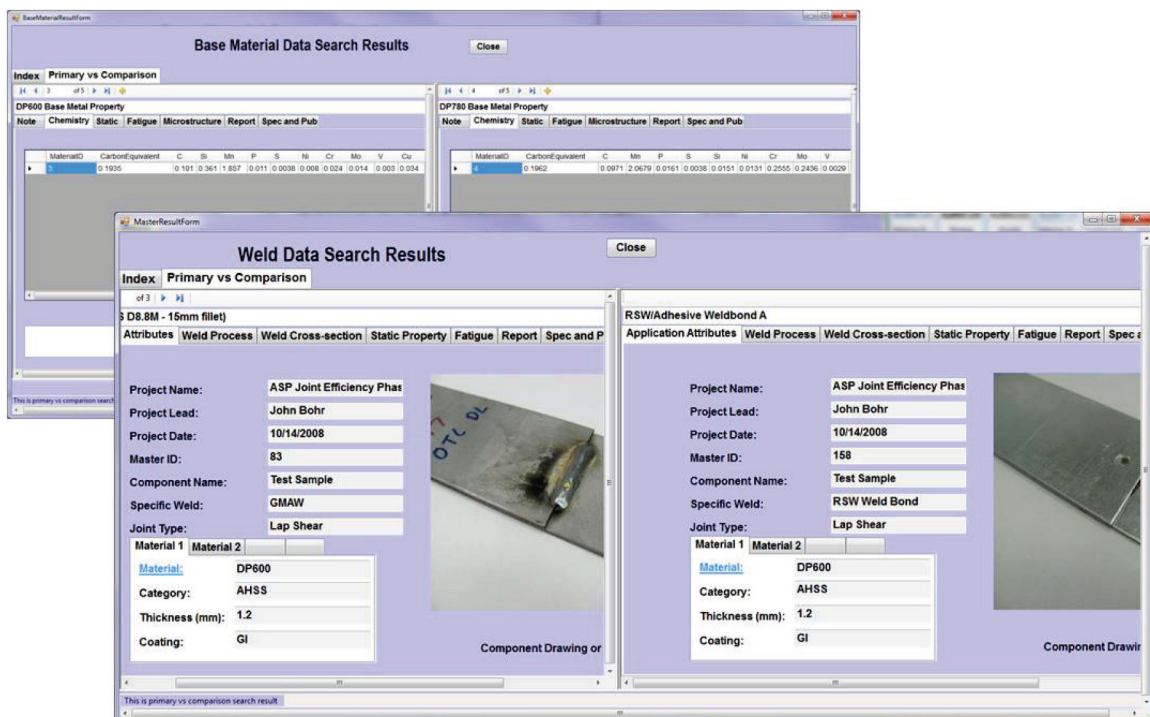
Figure 30. Data Presentation for Retrieved Records

- The data density map function allows users to visualize the landscape of existing data. It highlights areas where high concentration of data exists and areas where there is lack of data. Attributes of the data records can be viewed using the two axis on the map as well as fields on the selection summary tab. Users can click on a cell on the map or select multiple cells and retrieve the details for the selected cells. A screenshot of this function is shown in Figure 31.
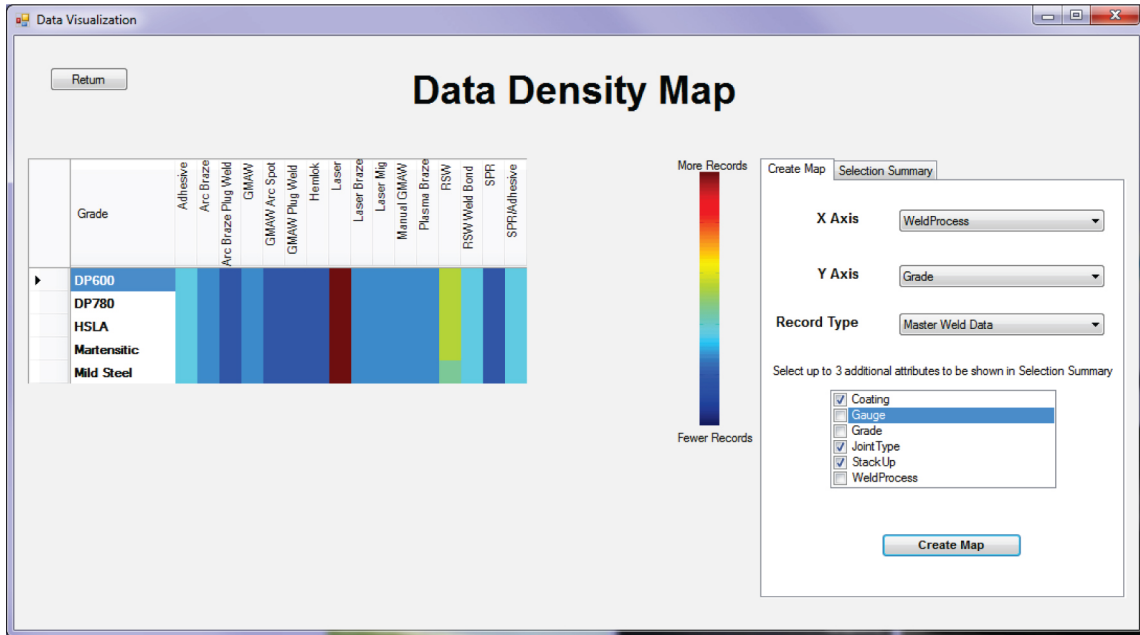
Figure 31. Data Density Map

- A comprehensive data input interface is developed for this application. Authorized users can add, edit, and delete records from either the weld record table or the base material record table. Minimal training is required to use this interface.

- The reporting function allows users to select multiple data records and gather all related technical information in a well-structured report. This function is very useful when users need to compare/analyze multiple past studies.

- As shown in Figure 32, knowledge rule function is broken down into three sub-functions: Recommend Weld Schedule, Recommendation from Past Studies, and Issue Resolution. There is also an overarching Solution Visualization option that presents all recommendations in a visual perspective.
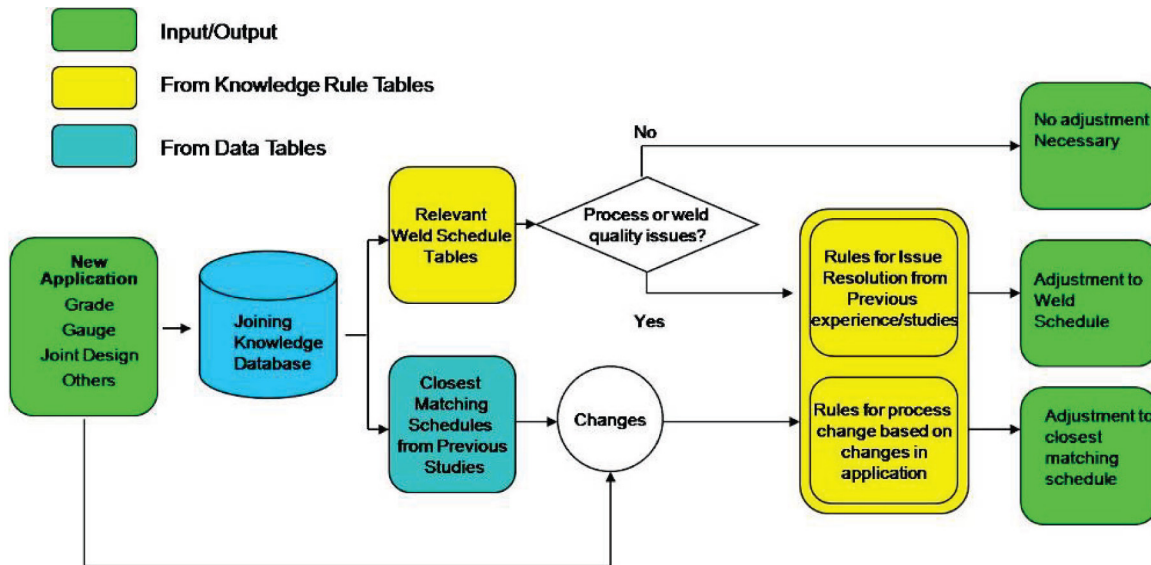
Figure 32. Flow Chart for Knowledge Rule Function

- Data from the following A/SP projects are entered into the phase I system:

  - Joint Efficiency Project

  - A/SP RSW Starting Weld Schedules

Technology Transfer Path

Installation CDs for the system were made and distributed to representatives from automotive OEMs and steel companies. Group and individual demonstration sessions were also conducted. Feedback for future enhancements was documented.

Conclusions

The delivered system demonstrated adequate user functions to:

- Organize and structure welding data

- Easily search/retrieve/compare/report data

- Identify future development needs

- Assist engineers to make technical decisions for new welding applications

- Populate database with joining technology project data (A/SP Joint Efficiency project)

To implement the Joining Knowledge Management system, phase II work needs to focus on:

- Populate the database with all previous A/SP welding/joining data

- Enhance user functions to accommodate a wide range of data and knowledge rules

- Develop web-based system

Lightweight Sealed Steel Fuel Tanks (A/SP-400)

Principal Investigator: Phil Yaccarino, General Motors Company
(586) 201-1329; e-mail: phil.yaccarino@gm.com

Principal Investigator: Peter Mould, Automotive Steel Technologies, Inc.
(810) 225-8250; e-mail: prmould@comcast.net

Accomplishments

- Mass reductions of 22% to 41%, compared with initial benchmark tanks of two advanced hybrid electric vehicles, have been demonstrated by using thinner AHSS TRIP carbon steel and austenitic stainless grades (such as AISI 304L and AISI 201 LN) in conjunction with designs encompassing stiffening ribs and structural baffles. For one of the benchmark tanks, the possible use of weld-bonded reinforcements was also demonstrated as an effective structural enhancer.

- The manufacturability of the low mass fuel tanks was demonstrated by computer FE analysis.

- The low mass tanks have structural stiffness equivalent to the benchmark tanks, and superior fatigue life. Equivalent corrosion durability is expected but needs to be confirmed by follow up validation testing.

- Cost analyses of the low-mass tank options showed that when thin carbon steels (such as AHSS TRIP) are substituted for the thick low carbon, low strength steel of the benchmark tank, only small increases in production cost occur, i.e., +5.6% and +2.1% for low production volumes (50K units/year) and high production volumes (150K units/year), respectively. When thin austenitic stainless steel (AISI 301 LN) is substituted for the thick carbon steel, cost increases of 35.0% to 37.7% (depending on production volume) can be expected even though the stainless steel option may allow the avoidance of post painting the tank assembly.

Future Directions

- The analytical computer studies were completed on September 30, 2011 and no further work is planned.

- It is recommended that a confirmation of fatigue and corrosion durability study be conducted.

- It is recommended that a post-study validation phase be conducted by manufacturing prototype tanks.

Technology Assessment

- Target: Current-generation sealed steel fuel tanks for AHEV and EREV are able to resist the high internal pressures that result from the sealing of the fuel tanks, but increase the mass of the fuel tanks compared with unsealed tanks. Hence, a technology target exists to reduce the mass of the sealed tanks while meeting the performance requirements and without significantly increasing production costs.

- Gap: The use of advanced high strength steels and/or stainless steels have not been investigated for potential weight saving opportunities for optimized designed sealed steel fuel tanks for AHEVs and EREVs.

Introduction

While running in the electric mode, AHEV and EREV carbon canisters, used for fuel evaporative emissions control, cannot be purged. Consequently, in current-generation designs, the fuel tanks are sealed which raises the internal pressure of the tank. Current designs of plastic tanks cannot meet the high internal operating pressures, and thick walled (1.4 to 2.0 mm) steel tanks are used which result in high mass. Thus, the purpose of this nine month project was to enable and demonstrate the manufacturing feasibility of low mass, sealed steel fuel tanks suitable for use in AHEV/EREV while achieving equivalent performance and cost.

Approach

Steel tanks from two current 2010 AHEV were acquired and used as initial benchmarks. The tanks were re-engineered, without significant shape change, to allow the use of thinner AHSS carbon steels or stainless steels. The identification and characteristics of the benchmark tanks are shown in Table 2.

Table 2. Characteristics of benchmark steel tanks

| 2010 Model | Tank | | | | Steel | |
	Vehicle Type	Capacity gal (l)	Mass* pounds (kg)	Weld Method	Thickness inch (mm)	Type
Lexus Rx450h	CUV	16 (60.6)	65.6 (29.83)	Electric Resistance Seam	0.079 (2.0)	Low carbon, mild steel
Mercedes M450 H	SUV	25 (94.7)	67.5 (30.68)	Plasma	0.059 (1.5)	301 LN[+] Stainless

* Includes post-paint for both tanks and fuel reservoirs in the Mercedes tank.
[+] For AISI 301 LN austenitic steel, L denotes low C (0.03% max) and N denotes high N (about 0.1%)

For each of the benchmark tanks, a 5-step computer engineering process (shown in Figure 33) was used to develop a low mass alternative.

Because the engineering space was not available for each benchmark tank, the shape of the low mass tank could not be changed. Without this constraint, higher mass reductions than obtained in this study likely would have been achieved.

Stress reduction options (such as stiffening ribs and structural baffles) were applied to the baseline structure in Step III. This allowed substitution of thinner AHSS or stainless steels in Step IV to provide lower mass alternatives. The ability to form the tanks was verified in Step V; but to limit the scope and time of the project, only single step forming was evaluated. (A multi-stage forming approach may well have enabled additional steels and/or thicknesses to be considered.) As part of Step V the fatigue and rigidity of the low mass tanks was also verified. For the Mercedes tank, weld-bonded reinforcements were studied, as an alternative to baffles, for reducing the baseline stress.
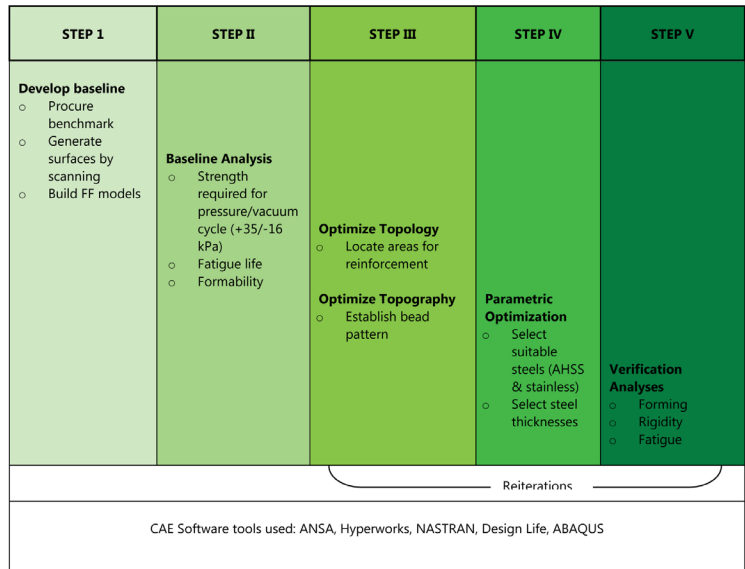
Figure 33. Stepwise procedure used to develop low mass alternatives to the benchmark fuel tanks

Due to the engineering alternatives that were defined in Step V, cost analyses were conducted using in-house modeling techniques of the CAE contractor EDAG. Additionally, assessments were made of corrosion durability and the commercial availability of the substitute steels.

Results and Discussion

For the carbon steel Lexus tank, stress reductions, compared with the baseline, were achieved by using stiffening ribs on the outer surfaces of the upper and lower shells and by extending existing internal baffles (designed for anti-slosh) or incorporating new baffles as structural elements. Forming analyses showed that only a ductile AHSS carbon steel (TRIP 450/800) could be used at thinner gages. Similarly, a 301 LN (1/4 hard) steel allowed the forming of the tank shells at thin gages. Combination of steel and thickness options are shown in Figure 34 and indicate a mass reduction of 33.8% for TRIP 450/800 upper and lower shells (Case 22) and 40.7% for the stainless steel (Case 23). It should be noted that pairing of different steels for the upper and lower tank shells was avoided because of concern regarding possible galvanic corrosion.

Case Study Number	Tank Shell Thickness (mm)	Mass (kg)	Mass Savings (%)	Von Mises Max. Stress (MPa)	Von Mises High Stress at Fatigue Limit (MPa)	Steel Grade Candidates (Satisfactory Forming)	
18	1.4 Upper	22.8	22.3	341	590	TRIP 350/600	
	1.4 Lower			338		TRIP 350/600	
19	1.3 Upper	20.1	31.4	398	529	TRIP 400/700	TRIP 450/800
	1.1 Lower			529		TRIP 450/600	301 LN-1/4 Hard
20	1.0 Upper	17.4	40.6	579	631	301 LN-1/4 Hard	
	1.0 Lower			631		301 LN-1/4 Hard	
21	1.0 Upper	18.7	36.2	671	571	301 LN-1/4 Hard	
	1.2 Lower			450		TRIP 450/800	301 LN-1/4 Hard
22	1.1 Upper	19.4	33.8	500	531	TRIP 450/800	301 LN-1/4 Hard
	1.2 Lower			450		TRIP 450/800	301 LN-1/4 Hard
23	0.9 Upper	17.4	40.7	667	676	301 LN-1/4 Hard	
	1.1 Lower			529		TRIP 450/800	301 LN-1/4 Hard

Figure 34. Combinations of steels and thicknesses having satisfactory formability and stress requirements for the Lexus tank.

For the low mass carbon steel option (Case 22) and stainless steel option (Case 23) shown in Figure 34, cost analyses of the Lexus tank were conducted using standard material, stamping and assembly costs assuming a 'brownfield' site (existing plant). Because carbon steel tanks are usually post-painted after assembly for added corrosion protection, the cost of post-painting was included for the low mass carbon steel (AHSS TRIP) option, but not for the austenitic stainless steel (301 LN ¼ Hard) option because of its high corrosion resistance. Costs were determined for two production volumes – low volumes (50K units/year) and high volumes (150K units / year). The costs, together with masses and mass reductions, are shown in Figure 35. It should be noted that the costs/kg saved are low for the carbon AHSS steel options (+0.45/+0.14) but significant for the stainless steel option (+2.33/+2.10).

Tank	Steel Type	Shell thickness (mm)		Mass kg	Mass Reduction		Normalized costs, $		Cost change %		$ / kg saved	
		Upper	Lower		kg	%	Low Volume	High Volume	Low Volume	High Volume	Low Volume	High Volume
Lexus RX 450h	Low Carbon	2.0	2.0	29.3	--	--	10.00		--	--	--	--
New design - AHSS	TRIP 450/800	1.1	1.2	19.4	9.9	33.8	10.56	10.21	+5.6	+2.1	+0.45	+0.14
New design - Stainless	301 LN ¼ Hard	0.9	1.1	17.4	11.9	40.7	13.50	13.77	+35.0	+37.7	+2.33	+2.10

Figure 35. Mass reductions and cost changes for the low mass options of the Lexus tank

For the stainless steel Mercedes tank, thinner shell thicknesses could only be formed by using 201 LN or 301 LN stainless steels. Thinner carbon AHSS lacked the formability to make the parts.

Mass reductions ranging from 24.8% to 38.4% were obtained for the thinner stainless steels depending on whether baffles or weld bonded reinforcements were needed as structural enhancements (Figure 36).

Iteration #	Description	Shell Thickness (mm)	Baffle/Reinf Thickness (mm)	Total Mass (kg)	Mass Change (kg)	Mass Change (%)	Von-Mises Max Stress (Mpa)
B	Baseline	1.5	---	24.2	---	---	282
O	Topography Optimized	1.5	---	24.2	---	---	252
B1	Topography + Baffles	0.8	0.7	14.9	9.3	-38.4%	262
WB1	Topography + WB Reinf	0.8	0.3	15.1	9.1	-37.6%	272
WB2	Topography + WB Reinf	1.1	0.3	18.2	6.0	-24.8%	275

Figure 36. Mass reductions obtained for the Mercedes tank

In estimating the production costs of the low mass Mercedes tank options shown in Figure 36, low production volumes (50k units/year) and high production volumes (150K units/year) were considered. Post painting of the assembled tanks was not included in the cost estimation because it was believed that the tanks have sufficient corrosion durability without post painting. The production costs together with the mass reductions for the low-mass Mercedes tank options are shown in Figure 37. The lower material costs for 201 LN* steel enabled a cost decrease for the low-mass Mercedes tank (Figure 37). The optimum cost and mass reduction is most likely a combination of structural baffles and weld-bonded reinforcements.

---

*AISI 201 LN grade has a lower Ni content (3.5% to 5.0%) than AISI 301 LN (6% to 8%) and hence has a lower cost.

Tank	Steel Type	Shell thickness (mm)		Mass kg	Mass Reduction		Normalized costs, $		Cost change %		$ / kg saved	
		Upper	Lower		kg	%	Low Volume	High Volume	Low Volume	High Volume	Low Volume	High Volume
Mercedes M 450H	301 LN	1.5	1.5	24.2	--	--	10.00		--	--	--	--
Topography + baffles	201 LN Annealed	0.8	0.8	14.9	9.3	38.4	7.80	6.76	-22.0	-32.4	-3.40	-4.69
Topography + WB Reinf-1*	201 LN Annealed	0.8	0.8	15.1	9.1	37.6	--	--	--	--	--	--
Topography + WB Reinf-2*	201 LN Annealed	1.1	1.1	18.2	6.0	24.8	7.93	7.15	-20.7	-28.5	-4.95	-6.37

* – WB Reinf-1 0.8mm thick shell with 0.3mm thick reinforcements (6 on upper, 5 on lower)
-- WB Reinf-2 1.1mm thick shell with 0.3 mm thick reinforcements (2 on upper, 2 on lower)
– No cost analysis was conducted on WB Reinf-1 because the high number of patches was viewed as impractical

Figure 37. Cost comparisons for the original and low-mass versions of the stainless steel Mercedes tank

Technology Transfer Path

The results from the present study are being shared with product design and manufacturing functions within Chrysler, Ford and General Motors and within the steel community. Additionally, presentations of the findings and recommendations for additional work are planned at the Automotive Fuels Conference (Novi, MI March 2012) and Great Designs in Steel (Livonia, MI May 2012). Furthermore, a technical paper for publication in SAE Proceedings (or similar) is planned.

Conclusions

CAE studies have shown that thinner AHSS carbon (TRIP) steel or stainless steels coupled with structural enhancing techniques such as stiffening ribs, structural baffles and weld-bonded reinforcements can be used to significantly reduce the mass of current- generation sealed steel fuel tanks. In this study of two benchmark tanks (Lexus Rx450h and Mercedes M450H) mass reductions of 20.7% to 40.7% were obtained depending on the steels selected and the structural options used.

Additionally, fatigue performance requirements were exceeded and equivalent structural rigidities were obtained for all low-mass options. Various corrosion-durable systems are available for the AHSS carbon steels. The stress corrosion cracking sensitivity of stainless steel options and the need for post painting needs to be assessed.

All of the steels identified for the low-mass options in this study are commercially available.

Conclusions

Project specific conclusions are included in each project section of the report.

The body of work on AHSS included in this report has focused on developing enabling technologies that allow greater use of AHSS in automotive manufacturing. This increased use of AHSS in light duty vehicles has resulted in a lower cost lightweighting option for auto makers. The use of AHSS has continued to increase each year since the beginning of this cooperative agreement in part due to the technologies developed during this period. The net result are vehicles that are safer and more fuel efficient than ever.

Increased fuel economy and safety standards continue to challenge the auto industry to produce safer and more fuel efficient vehicles. The Auto Steel Partnership is committed to addressing these challenges with continued research on AHSS to enable low cost lightweighting options for auto makers. Several of the projects described in this report will continue to be funded in 2012 by the Auto/Steel Partnership to continue this vital work.

Presentations/Publications/Patents

Young, D.; "Coating Impact – Sliding Fatigue Wear Tests", Presented at the 2011 Great Designs of Steel Seminar, May 19, 2011, Livonia, Michigan

Hall, J. N.; Mulholland, T.; et. al. Investigation of Stamping Tooling Durability for Dual Phase Steels, SAE World Congress Proceedings; SAE, Warrendale, PA, April 2011.

Zhou, D.J.; "AHSS Edge Cracking Criteria Development from Large Stamping with a Big Cutout", Presented at the 2011 Great Designs of Steel Seminar, May 19, 2011, Livonia, Michigan

D. Nondestructive Evaluation Steering Committee
U.S. Automotive Materials Partnership

Field Technical Monitor: Martin Jones
Ford Motor Company - NDE Lab
35750 Plymouth Road; Livonia, MI 48150-146
(313) 805-9184; e-mail: mjone147@ford.com

Field Technical Monitor: George Harmon
Chrysler Group LLC
Materials Characterization Laboratories
Mail Code 482-00-11; 800 Chrysler Drive; Auburn Hills, MI 48326-2757
(248)512-4840; e-mail: gjh8@chrysler.com

Field Technical Monitor: Leonid Lev
General Motors Company LLC
GM R&D and Planning
Mail Code 480-106-21; 30500 Mound Road; Warren, MI 48090-9055
(586) 986-7450; e-mail: leo.lev@gm.com

Technology Area Development Manager: William Joost
U.S. Department of Energy
1000 Independence Ave., S.W.; Washington, DC 20585
(202) 287-6020; e-mail: william.joost@ee.doe.gov

Technology Area Development Manager: Carol Schutte
U.S. Department of Energy
1000 Independence Ave., S.W.; Washington, DC 20585
(202) 287-5371; e-mail: carol.schutte@ee.doe.gov

Field Project Officer: Joseph Renk
National Energy Technology Laboratory
626 Cochrans Mill Road; P.O. Box 10940; Pittsburgh, PA 15236
(412)386-6406; e-mail: joseph.renk@netl.doe.gov

Contractor: U.S. Automotive Materials Partnership (USAMP)
Contract No.: DE-FC26-02OR22910

Executive Summary

Many new materials and joining methods are being explored and evaluated in the quest for lighter weight passenger and commercial vehicles. Often these materials and processes introduce new challenges to the quality of automotive structures and components due to their chemical reactivity, lower volumetric strengths, and "newness" in the automotive production environment. Nondestructive evaluations (NDEs) can often ensure the quality of these materials and also reduce their cost by replacing destructive tests with nondestructive ones. The Nondestructive Evaluation Steering Committee has worked with the other USAMP divisions to identify opportunities for using nondestructive testing (Harmon et al., 2006). The focus of these has been high-value, high-need, fast in-line inspections. In addition to collaboration on other projects, the Nondestructive Evaluation Steering Committee is currently sponsoring two focused projects.

The following sections outline the two current projects which target high-integrity light metal castings and resistance spot welding (RSW) respectively. High-integrity light metal castings currently require 100% inspections and use methods that are expensive and may not detect all significant discrepancies. RSW currently relies on spot sampling and destructive tests which have relatively low confidence levels and incur high costs. These are both areas where NDE success can significantly improve vehicle quality and reduce costs, which are among the goals of the Lightweight Materials program.

The Reliability Tools for Resonance Inspection of Light Metal Castings Project (NDE 901) has completed an experimental program of casting tensile bars, inspected with multiple NDE methods including radiographic testing (RT), fluorescent penetrant inspection (FPI), and resonance inspection (RI). The resonance shifts noted in the RI were correlated to the discrepancy types and material strength. The team has written an ASTM style standard to insure reliability and reproducibility. Several software tools were developed in this project which, when used together, can generate a resonant inspection algorithm based only on finite element (FE) based simulations. Future work has been identified which includes the refinement of the FE discrepancy library and development of software tools to predict the probability of detection (POD) of RI to performance-critical casting discrepancies.

The Shearographic Nondestructive Evaluation of Spot Welds for Lightweighting of the Vehicle Project (NDE 1002) has produced and inspected with digital shearography a large number of RSW coupons. A number of loading schemes were examined and substantial progress was made in the project by using the images produced by heating the coupons. It was possible to sort the weld nuggets into large, medium, and small categories using the processed shearographic image. A numerical algorithm was developed which appears to be able to predict the weld nugget size based on simulated test data. The algorithm was successfully tested for sensitivity to errors in the experimental data. Several next steps have been identified including continuing the strategy of determining the actual weld nugget size directly from the shearographic image and integrating the experimental with the numerical techniques to develop a robust spot weld inspection tool.

Activity and Developments

NDE901—Reliability Tools for Resonance Inspection of Light Metal Castings

Principal Investigator: Martin Jones, Ford Motor Company - NDE Lab
Phone: (313) 805-9184; e-mail: mjone147@ford.com

Accomplishments

- Created novel FE models for shrink porosity in aluminum (Al) from experimental measurements: CT images of density and resonance measurements of stiffness. (FY2011)

- An industry first, software tools were developed that generate a database of RI frequencies for discrepant parts entirely using FE models. (FY2011)

- Also an industry first, a software tool was developed that can generate a database of RI frequencies for acceptable parts. (FY2011)

- A third software tool was built that optimizes combinations of resonance frequencies to build an algorithm that can sort good parts from discrepant ones, based only on FE-based simulations. The performance is very good on the two tested castings. (FY2011)

- "A Proposed Standard for Production Resonance Inspections", written in ASTM style, was approved by representatives of the OEMS, casters, and RI vendors. (FY2011)

- Completed an experimental program of casting tensile bars, inspecting with multiple NDE methods including RI, and correlating resonance shifts to discrepancy types and material strength. (FY2011).

Future Directions

- Development of integrated (software) tools to predict the POD of RI to performance-critical casting discrepancies.

- Generate and characterize, utilizing RI, transverse cracks in 10 sample bars.

- Include these effects into additional FE models or refine current FE for the FE discrepancy library developed by this project.

Technology Assessment

- Target: Develop an industry-wide RI standard that is reproducible and traceable. "A Proposed Standard for Production Resonance Inspections" is ready for publication.

- Target: Generate an RI sort algorithm based only on FE-based simulations. The tensile bar and knuckle FE-based sort algorithms were able to sort >99% of the good components correctly and >90% of the discrepant parts.

- Gap: Software tools are needed to predict the POD of RI to performance-critical casting discrepancies.

Introduction

There are many automotive castings that are either safety or performance critical to the vehicle and require 100% inspection with extremely high requirements for the confidence of reliability. Usually these have complex shapes and present extremely difficult inspection problems. RI has unique capabilities for these inspections. Sound in the range of 100 to 200,000 Hz can readily penetrate these castings and is sensitive to heat treatment, porosity, cracks, and oxide inclusions. RI also has significantly lower capital and piece costs than either RT or FPI. In fact, RI is already used for 100% inspection of many castings such as knuckles, rockers, master cylinders, and calipers. Despite these advantages, RI has not achieved full acceptance because the sensitivity and robustness cannot be ensured with current implementations.

Approach

Working with RI system vendors and casting vendors, we are developing new tools to improve the robustness of RI in production. Working with RI system vendors, we have a large pool of experience on current implementation processes and recurring issues. Working with casting vendors, we are generating three sets of castings that allow quantitative assessments of resonance frequency shift sensitivities and correlation to casting strength.

The first toolset establishes standard RI processes for the production facility. This includes both a process work flow procedure to create the RI plan for a new part and a standardized procedure to ensure reliability and traceability of RI inspected parts when the RI plan is in production.

The second toolset is a FE software program that uses the CAD model and the engineering performance requirements for a part and generates the inspection parameters and expected performance. The inspection parameters include the small set of inspection frequencies and a sort module that processes the measured frequency shifts to pass or fail a particular casting. This FE model uses FE sub-models for the discrepancies to accurately predict frequency shifts.

Results and Discussion

Standardized Processes

In FY2011, "A Proposed Standard for Production Resonance Inspections" was written to quantify RI performance and ensure performance over the life time of the test. The objective was "to establish a reproducible and traceable procedure that quantifies the inspection performance and is supplier independent." A key element of the standard is the use of "primary quality tests" to assemble reference sets of "reference-accept" and "reference-reject" parts that perform as part-specific

reference gages. The standard quantifies the performance of both the inspection hardware and the sort algorithm using gage repeatability and reproducibility (R&R) studies. The standard specifies the documentation and information retention needed to ensure traceability. It is written in ASTM format and is ready for ASTM review.

Integrated Tools for POD to Critical Defects

There are three essential ingredients for predicting POD: 1) the sensitivity of the response to the size of the discrepancy (for RI, the response is the frequency shift of a resonance due to the discrepancy), 2) the noise in the frequency shifts due to all sources including measurement error and resonance variability due to acceptable material and geometry variations, and 3) the sort module selected. The discrepancies to be included are shrink porosity, oxide inclusions, and cracks. Previously the resonance properties of two Al production knuckles were measured. This year, laboratory-cast cylinders were used to generate discrepancies in tensile bars.

Three cylinders ranging from 0.8" to 2" diameter were sand cast together using A356 Al and given a T-6 heat treatment. These included specimens with a full range of shrink porosity and oxide inclusions. The tensile bars were non-destructively evaluated with RI, FPI, computed tomography (CT), surface profiling, and weighing before they were pulled to determine ultimate tensile strength, fracture location, and failure mode. In order to generate tight cracks, some tensile bars were also fatigued using 3-pt bending using an ultrasonic welder, but cracks could not be reliably generated.

The resonance shifts seen with different discrepancy types were similar to those seen in the knuckles. The porosity shifted the resonances to lower frequencies. A quantitative analysis of the frequency shifts with mass loss indicates that the relative change of stiffness is several times the relative change of density. The integration and development of the software tools for the POD remains the subject of future work.

Finite Element Sort Modules

A complete FE-based tool bench to predict resonance frequencies of Al castings and create an RI sort module was built. There are three major components: 1) FE-based database of good parts, 2) FE-based database of discrepant parts, and 3) a sort module optimization tool that uses either experimental or FE-based resonance databases to select a small set of inspection frequencies. These tools were built using MATLAB® for rapid development, portability, and include a rich set of built-in utilities. MATLAB® is used in different three ways. 1) To combine discrepancy and good part FE models into discrepant part FE models; 2) To process the results of FE resonance calculations performed in Nastran and 3) to create the sort modules.

The good parts are generated using a few FE calculations to determine the sensitivity of resonance frequencies to material (density, shear modulus, Young's modulus) and geometry changes (e.g. degate-height). The frequency shifts are then calculated for the combined effects of randomly distributed properties within the known distributions of values. The linear responses were tested for all variables.

For the discrepant parts, a series of discrepancy FE- models were created from experimental measurements. A tool was created that can map these discrepancy FE-models into a target component model and then generate a Nastran calculation of the resonances of the discrepant part. This tool can handle a variety of discrepancy and target mesh types. The discrepancy locations are determined either from CAE analysis or by distributing the discrepancies over the entire part.

The sort optimization tool first selects a set of analysis frequencies and determines the frequency separation of discrepant parts from good parts. The sort is scored by an objective function that weighs the number of misclassified parts and the number of inspection frequencies. The selection of frequencies is then optimized using a genetic optimization algorithm. This tool has a graphical user interface for selecting input databases and managing the sort switches, objective function weights, and the genetic algorithm behavior. The user interface also graphs the convergence process, the sort distribution, and sort error rates. Typically the optimization only requires a few minutes to converge even when working on a component with over a hundred resolved resonances. The FE-based sorts for the tensile bar and knuckle were able to sort >99% of the good components correctly and >90% of the discrepant parts.

Technology Transfer Path

Discussions are underway with a major software supplier to commercialize the FE-based tools which have been developed. "A Proposed Standard for Production Resonance Inspections" to establish a reproducible and traceable procedure that quantifies the inspection performance and is supplier independent, will be submitted to ASTM for possible publication.

Conclusions

The project has successfully concluded on schedule and delivered the project objectives of two major new tools to improve resonance inspection for automotive light-weight castings. An industry-first FE based tool bench that can generate an RI frequency database for good and discrepant parts has been delivered and tested. Protocols based on production experience have been written to implement a quantitative, reliable, and traceable RI and insure its performance in production.

NDE1002—Shearographic Nondestructive Evaluation of Spot Welds for Lightweighting of the Vehicle

Principal Investigator: Lianxiang Yang, Oakland University
 (248) 370-2284; email: yang2@oakland.edu

Principal Investigator: Randy Gu, Oakland University
 (248) 370-2235; email: gu@oakland.edu

Principal Investigator: Leonid C. Lev, General Motors Research and Planning
(586) 986-7450; e-mail: leo.lev@gm.com

Accomplishments

- A large number of mild steel weld coupons (350+) containing examples of good and poor weld quality were produced for the test in the project. (FY2011)

- Several methods of loading the weld coupons were investigated, including mechanical vibration, thermal loading from a heat gun and a flash lamp, and magnetic mechanical loading. (FY2011)

- The optical images were studied and compared with torn weld samples. A preliminary method was used to determine the size of the weld nugget from the optical images. (FY2011)

- The problem of determining the weld nugget size was formulated as an inverse problem in which optical measurement was added to the well-posed mathematical problem. A numerical algorithm was identified to solve the inverse problem. (FY2011)

- To determine the efficiency of the numerical algorithm in predicting the weld nugget sizes, noise was added to the simulated experimental data for the optical surface measurements. The numerical algorithm was very accurate in calculating the weld nugget sizes. (FY2011)

Future Directions

- Prepare weld coupons in AHSSs, Al, and Mg.

- Finalize a strategy to determine the weld nugget size from the optical images.

- Investigate the performance of the numerical algorithm for the thermal loading case.

- Integrate the experimental and numerical technique together to develop an inspection tool for detecting quality welds in the production environment.

Technology Assessment

- Target: Identify the preferred loading method for the shearographic image of RSW's. Thermal loading with the heat gun has produced the most consistent results.

- Target: Identify the weld nugget size using only shearography. The current research has developed techniques that allow the sorting of the welds into large, medium, and small categories.

- Gap: A rapid, non-contact, full field method to quantify the quality of RSW's. No proven correlation between the weld nugget size and the shearographic image.

Introduction

RSW is the conventional joining method for body structures. When optimized, it produces strong, robust joints in mild steel at low cost. RSW has been adapted to newer lightweight metals ranging from the AHSSs to Al and Mg. Because of the difficulties of keeping the weld process in control (weld-tip wear, weld-gun control, corrosion, etc.), RSW requires frequent weld inspections, typically by tear downs (destructive testing). This is very expensive and has low sampling rates. RSW of lightweight materials is more critically needed because of increased weld brittleness and because of the high, variable conductivity of Al and Mg.

Approach

The project is to investigate the feasibility of a hybrid approach which combines the shearographic optical measuring technique and a numerical algorithm for determining the weld nugget size of RSW coupons. In the numerical-experimental scheme, a suitable optical technique is first identified to obtain an image of a distorted weld sample representing its surface displacement. The determination of the nugget size from the experimental measurement is formulated mathematically as an inverse problem. A FE method is developed to solve the ill-posed inverse problem. The project is carried out on two different fronts – experimental investigation and numerical study of the inverse problem.

Results and Discussion

Experimental Investigation

Digital shearography is a laser measuring technology based on digital data processing, phase-shifting techniques, and interferometry. A distinguishing feature of shearography is the use of a self-reference interference system. Instead of using a reference beam, shearography utilizes a shearing device to bring the light waves from two points on the object surface into one point on the image plane, which results in an interference phenomenon, i.e. so-called shearing speckle interferogram, without using an additional reference beam.

Shearography is a nondestructive testing (NDT) technology that can provide the first derivative of the deformation along its shearing direction. In applications, the samples have to be loaded in a certain way and, under this loading, the to-be detected defect or feature will deform differently along the shearing direction than the other area, so that the first derivative will reveal desired information. In this project, the most reliable and repeatable shearographic images were obtained with thermal loading from a heat gun.

A matrix of over 350 RSW coupons was fabricated for this project. The coupons were assembled from mild steel plates 6"×6" RSW in the center to a second mild steel plate 4"×4". The thickness of the various coupons were combinations of plates from 0.8 mm to 1.3 mm. The weld nuggets varied from 2 mm to 6 mm in diameter. These coupons were secured in a load frame and subjected to a "standardized" six second exposure to an industrial heat gun. The applied heat distorts the material

surrounding the weld nugget and the shearographic imaging system records the resulting interferogram. An analysis of the image is made to estimate the weld nugget diameter. Because the weld nugget is not necessarily symmetrical the coupon is rotated 90° in the load frame and tested again, obtaining a second weld nugget diameter estimate. The test was conducted three times in each orientation to verify repeatability.

Numerical Study of the Inverse Problem

There have been numerous studies in predicting the weld nugget size during the spot weld process. In a forward problem, we are provided with known material model, specific loading conditions – mechanical as well as thermal, and well-defined boundary conditions. In the current project, there is an additional set of optical measurements on the surface available causing the problem to become ill-posed with more boundary conditions than needed in a forward problem. A numerical algorithm has been identified to solve the ill-posed inverse problem by minimizing the deviation between the theoretical prediction and the experimental measurements. The algorithm was tested using several examples in which the experimental measurements are simulated data from a separate finite element analysis.

To determine the feasibility of the proposed hybrid approach, a two-dimensional model is employed in the development. The model is the weld assembly with two concentric plates. The stress as well as the deformation near the weld nugget on the actual test specimen would display very analogous patterns to those of the true axisymmetric model used in this analysis.

To use the hybrid approach algorithm to determine the weld nugget size, we need the following items of information: material properties, boundary conditions, applied loads, geometry of the weld assembly, and the surface measurements of displacement. In the current hybrid approach, the geometry of the model needs to incorporate an initial guess of the weld nugget size. To determine the sensitivity of the involved parameters on the algorithm, several examples are run with various initial guesses for the weld nugget size. As in many inverse problems, noise imbedded in the experimental data could pose a great challenge. To determine the performance of the algorithm when noise is present in the optical measurements, several more examples are tested. In these examples, noise of various magnitudes is generated randomly in the simulated experimental data.

Technology Transfer Path

This project was ultimately funded as a one year feasibility study. The results of the project will be recorded in the final report. An informational seminar is planned for 2012 to be hosted by Oakland University and USAMP NDE Steering Committee.

Conclusions

The nugget size of the RSW is difficult to precisely measure. Using the shearography technique on the heated spot weld enables the welds to be categorized as small, medium, and large. The fringe patterns of the interferogram of the spot weld will have a distinguishable difference according to the nugget size. The thickness of the weld coupons did not appear to have a detrimental effect on the development of the fringe patterns. Hundreds of experiments were conducted on these RSW coupons and the repeatability of this testing was verified. The inverse problem of determining the weld nugget size from known conditions and additional optical surface measurement is formulated as a minimization problem which can be solved using a genetic algorithm. The proposed algorithm was tested using a number of examples with simulated experimental data. From the current study, it demonstrated that it has great potential to integrate the shearographic technique and the numerical method to form a powerful tool for determining weld quality.

Conclusions

The two projects directed by the NDE Steering Committee have made notable contributions to the NDE knowledge base. The integration of FE modeling with NDE technologies is on the path to successful implementation lightweighting strategies. NDE is an enabling methodology for the lightweighting of the vehicle. The successful RI of lightweight automotive castings will ensure the safety of consumers and improve the quality, integrity, and reliability of the vehicle. Digital shearography may provide a full field method for verifying the structural integrity of RSW in a wide variety of lightweighting materials.

The NDE 901project has successfully concluded on schedule and delivered the project objectives of two major new tools to improve RI for automotive light-weight castings. Protocols based on production experience have been written to implement a quantitative, reliable, and traceable RI and insure its performance in production. The documentation requirements in this "standard" insure the reliability and repeatability of the RI. A FE based tool bench that can generate an RI frequency database for good and discrepant parts has been delivered and tested. This FE-based tool bench will allow part designers to determine the efficacy of the RI prior to the production of even a prototype part. It will also replace the heuristic approach to RI development with a physics-based methodology. The future effort to develop POD tools for RI will complement the current suite of software tools and allow the expanded implementation of RI as a production ready method for verifying the quality of light metal automotive castings.

The NDE 1002 project has had a very successful start at solving a long standing problem in the automotive industry; the noncontact inspection of RSW. The hybrid approach of this project produced encouraging results in both the experimental and numerical arenas. The experimental side of the project completed a study of loading methods and concluded that thermal loading with a heat gun produced superior results. The analysis of the experimental images allows the sorting of the weld nuggets into three size categories. Improvements in the image analysis hold promise for the development of a more accurate sizing system. The numerical part of the hybrid approach also had several encouraging developments. In addition to the development of the two-dimensional model, a numerical algorithm has been identified to solve the ill-posed inverse problem. It is found that the initial guess of the weld nugget size has little influence on the proposed numerical algorithm. Analogous to other numerical schemes for ill-posed inverse problems, the use of excessive experimental measurements would hamper the performance of the numerical algorithm. For an evenly inflated experimental data (Type I Error), the proposed algorithm predicts the correct trend for the weld nugget size – larger deflection with smaller weld nugget size. For the experimental data containing random noise (Type II Error), the algorithm correctly predicts the trend. When the experimental data contains mild level of random noise (Type II Error) centered on the theoretical experimental measurements, the algorithm accurately predicts the weld nugget size. Future efforts will investigate the performance of the numerical algorithm for the thermal loading case. Digital shearography provides an opportunity to inspect a much larger population of spot welds than current methods at a lower cost and improved ergonomics. As the industry moves to new, lightweight materials, the reliability of the welded joint becomes ever more critical and will result in far greater requirements for inspection. Digital shearography holds the promise of a full field, noncontact inspection method that will enable RSW in advanced lightweight materials.

Presentations/Publications/Patents

Lai, C.; Sun, X.; Dasch, C.; Harmon, G.; Jones, M. 2011. Quantify Resonance Inspection with Finite Element-Based Modal Analyses, J. Vibration and Acoustics 133(3): Article No. 031004. doi:10.1115/1.4002955

Dasch, C.; Jones, M.; Harmon, G.; Brady, M.; Waters, J.; Saxton, J.; Stultz, G.; Palombo, G.; Farkas, L.; Lai, C.; Sun, X. "Towards Quantitative Resonance Inspection: Measurements and Modeling for an Automotive Aluminum Casting", paper presented at ASNT Spring Research Meeting, San Francisco, April 2011.

Harmon, G. NDE 901—Reliability Tools for Resonance Inspection of Light Metal Castings, DoE Merit Review, May 2011.

One manuscript has been submitted to 2012 SAE World Congress for review for possible publication.

Nan Xu, Xin Xie, Lianxiang Yang, Randy Gu, Nugget Size Measurement In Spot Weld Using Shearography, submitted to SAE World Congress, 2012.

References

Harmon, G.; Dasch, C.; Mozurkewich, G.; Hopkins, D. Strategic Plan for Nondestructive Evaluation Development in the North American Automotive Industry, USCAR Website, 2006.

ASTM B557M, Standard Test Methods for Tension Testing Wrought and Cast Aluminum- and Magnesium-Alloy Products; ASTM International, West Conshohocken, Pennsylvania, 2008.

Hopkins, D.; Mozurkewich, G.; Dasch, C. NDE Inspection of Resistance Spot Welds in Automotive Structures Using an Ultrasonic Phased Array, AMD409 Final Report; USAMP Report, 2010.

Steinchen, W.; Yang, L. Digital Shearography: Theory and Application of Digital Speckle Pattern Shearing Interferometry; SPIE Press, Bellingham, Washington, 2003.

Robert H. Todd, Dell K. Allen and Leo Alting Manufacturing Processes Reference Guide, 1994, Industrial Press Inc.

J.D. Cullen, N. Athi, M. Al-Jader, P. Johnson, A.I. Al-Shamma'a, A. Shaw and A.M.A. El-Rasheed, Multisensor fusion for online monitoring of the quality of spot welding in automotive industry, Measurement, V 41(4), May 2008, pp. 412-423.

K. Deb, Multi-Objective Optimization using Evolutionary Algorithms, John Wiley & Sons, 2001.

R.E. Steuer, Multiple Criteria Optimization: Theory, Computations, and Application. New York: John Wiley & Sons, Inc., 1986.

A.N. Tikhonov, and A.V.Arsenin, Solutions of Ill-Posed Problems, Winston, Washington, D.C., 1977.

J. V. Beck, B. Blackwell, and C. R. St. Clair, Jr., Inverse Heat Conduction—Ill-Posed Problems, Wiley-Interscience, New York, 1985.